Interpretation of Potential Fields by Modern Data Processing and 3-dimensional gravity Modeling of the Dead Sea Pull-Apart Basin / Jordan Rift Valley (JRV)

Dissertation zur Erlangung des
naturwissenschaftlichen Doktorgrades
der Bayerischen Julius-Maximilians-Universität Würzburg

Vorgelegt von

Eng. Mohammed H. Hassouneh

aus
Jordanien

Würzburg 2003

ABSTRACT

This work presents the analysis, 3D modeling and interpretation of gravity and aeromagnetic data of Jordan and Middle East. The potential field data delineate the location of the major faults, basins, swells, anticlines, synclines and domes in Jordan. The surface geology of Jordan and the immediate area east of the Rift is dominated by two large basins, the Al-Jafr basin in the south and the Al-Azraq-Wadi as Sirhan basin to the northeast. These two basins strike southeast-northwest and are separated by an anticlinal axis, the Kilwah-Bayir swell. The Karak Wadi El Fayha fault system occurs along the western flank of the swell. The Swaqa fault occurs on the southwest hinge of Al-Azraq basin and the Fuluq fault occurs on its northeast hinge. In the south west of Jordan, Wadi Utm-Quwaira and Disi-Mudawara fault zones are shown clearly in the aeromagnetic and gravity maps. The previous major faults are well correlated with the structural map of Jordan published by Bender (1968).

3D modeling of gravity data in the Dead Sea basin (DSB) was used together with existing geological and geophysical information to give a complete structural picture of the basin. The 3D models of the DSB show that the internal structure of the Dead Sea basin (DSB) is controlled by longitudinal faults and the basin is developed as a full graben bounded by sub-vertical faults along its long sides. In the northern planes of the 3D model, the accumulation of Quaternary (salt and marl) and Mesozoic (pre-rift) sediments are thinner than in the central and southern planes of the model. In the northern planes, the thickness of the Quaternary sediments is about 4 km, 5 km in the southern planes and it exceeds 8 km in the central planes of the DSR. The thickness of the pre-rift sediments reaches 10-12 km in the northern and southern planes and exceeds 15 km in the central planes of the DSR. The planes of the 3D models show that the depth to the crystalline basement under the eastern shoulders of the DSR is shallower than those beneath the western shoulders. It is about 3-5 km beneath the eastern shoulders and 7-9 km under the western shoulder of the DSR.

The gravity anomaly maps of residual and first derivative gravity delineate the subsurface basins of widely varying size, shape, and depth along the Rift Valley. The basins are created by the combination of the lateral motion along a right-tending step over and normal faulting along the opposite sides. Al Bakura basin occupies the upper Jordanian River valley and extends into the southern Tiberias Lake. Bet Shean basin to the south of Al Bakura basin plunges asymmetrically toward the east. The Damia basin, comprising the central Jordan Valley and Jericho areas to the north of the Dead Sea is shallow basin (~600-800m deep). The Lisan basin is the deepest basin in the Rift. The 3D gravity models indicate a maximum of ~12 km of basin fill. Three basins are found in Wadi Araba area, Gharandal, Timna (Qa'-Taba) and Aqaba (Elat) basin. The three basins become successively wider and deeper to the south.

The three regional gravity long E-W profiles (225 km) from the Mediterranean Sea crossing the Rift Valley to the east to the Saudi Arabia borders, show the positive correlation between topography and free air anomaly and strong negative Bouguer anomaly under the central part of the Dead Sea Basin (DSB) and normal regional Bouguer anomaly outside of the DSB in the transform valley.

Depth to the top of the bedrock in the under ground of Jordan was calculated from potential field data. The basement crops out in the south west of Jordan and becomes deeper to northwards and eastwards to be about ~ 8 km below ground surface in the Risha area.

Kurzfassung

In der vorliegenden Arbeit wird die Analyse gravimetrischer und aeromagnetischer Daten aus dem Gebiet Jordaniens und des umgebenden Teils des mittleren Ostens mittels 3D Modellierung vorgestellt. Die Variationen der Potentialfelder folgen systematisch den Hauptstörungen, Becken, Schwellen, Faltenstrukturen und Dome in Jordanien. Die Oberflächengeologie Jordaniens und der Gebiete unmittelbar östlich der Riftzone werden von zwei großen Beckenstrukturen dominiert: Das Al-Jafr Becken im Süden und das Al-Azraq-Wadi (auch Sirhan Becken) im Nordosten. Diese Becken streichen SE-NW und sind durch eine Antiklinalstruktur, die Kilwah-Bayir Schwelle separiert. Das Karak Wadi El Fayha Störungssystem liegt im Bereich der westlichen Flanke der Schwelle. Im Südwesten grenzt die Swaqa Störung, im Nordosten die Fuluq Störung das Al al-Azraq Becken ab. Im Südwesten Jordaniens können auf den erstellten aeromagnetischen und gravimetrischen Plänen klar die prominenten Störungszonen Wadi Utm-Quwaira und Disi-Mudwara nachgewiesen werden. Alle diese geophysikalisch indizierten tektonischen Elemente korrelieren gut mit den geologischen Aufnahmen von Bender (1968).

3D Modellierung der gravimetrischen Anomalie des Toten Meer Beckens (DSB) im GIS mit geologischer, seismischer und (Bohrloch) geophysikalischer Information wurde eingesetzt, um eine komplette Darstellung der Strukturen des Beckens zu erzielen. Die 3D-Modelle des DSB zeigen, dass die interne Beckenstruktur von Längsstörungen kontrolliert werden und das Becken als Vollgraben ausgebildet ist. Beide Grabenflanken werden von subvertikalen Randbrüchen begrenzt. In den Nord-Schnitten des Modells ergeben sich für die Akkumulation der Quartären Grabenfüllung (Salz und Mergel) mit etwa 4 km ebenso wie der der Mesozoischen (prä-Rift) Sedimente mit etwa 10 km geringere Mächtigkeiten als in den südlichen Schnitten. Hier liegen die Mächtigkeiten der Quartären Grabenfüllung bei etwa 5 km und die des Mesozoikums bei über 12 km. Die maximale Mächtigkeiten werden allerdings in zentralen Schnittlagen des Modells errechnet, wo das Quartär mit über 8 km und das mesozoikum mit über 15 km modelliert wurde. Im Modell des DSB liegt das kristalline Basement in der östlichen Grabenschulter mit 3-5 km deutlich flacher als mit 7-9 km unter der westlichen Grabenschulter.

Die Anomaliepläne der Schwere, sowie die der ersten Ableitung weisen auf viele, oberflächlich nicht erkennbare Teilbeckenstrukturen im Verlauf des Riftes hin. Diese Becken werden durch die Kombination der Blattverschiebung mit dextralem „Stepp over“ und Abschiebungen erklärt. Das Al Bakura Becken nimmt den oberen Bereich des Jordan Tales ein und dehnt sich bis in den Bereich des Tiberias See aus. Das südlich anschließende Bet Shean Becken taucht assymetrisch nach Ost ab. Das Damia Becken, im zentralen Jordan Tal und im Gebiet von Jericho, oberhalb des Toten Meeres gelegen, ist mit einer Tiefe von 600-800m eine sehr flache Struktur. Im nach Süden anschließenden Lisan Becken kann nach der Modellierung eine Sedimentfüllung von etwa 12 km angenommen werden. Im Bereich des Wadi Araba konnten drei

weitere Becken wurden aus der Modellierung abgeleitet werden (Gharandal, Timna (Qa-Taba) und Aqaba (Elat), die alle zum Süden hin weiter und tiefer werden.

Die drei regionalen E-W Schwereprofile (225 km Gesamtlänge) vom Mittelmeer über das Tote Meer bis zur Grenze von Saudi Arabien zeigen eine positive Korrelation zwischen der Topographie und der Freiluftanomalie sowie eine starker negative Bougueranomalie im Bereich des zentralen DSB. Außerhalb des DSB im Rifttal ist die Bouguerschwere normal.

Die Tiefenlage der Kristallinbasis im Untergrund von Jordanien wurde aus den Daten der Aeromagnetik berechnet. Das Basement ist im Südwesten Jordanien aufgeschlossen und seine Tiefenlage nimmt sukzessive nach Norden und Osten auf etwa 8 km im Raum von Risha zu.

Acknowledgments

The author is very much indebted to the thesis supervisors, **Prof. Dr. B. Zimanowski** and **Prof. Dr. H. J. Goetze**, who initiated and accompanied this project with continued interest. I wish to thank them for their guidance and assistance throughout the field- and office work, they have always had an open door for problems, questions, and discussions. Prof. Dr. B. Zimanowski guided me through the thesis step by step and his warm encouragement throughout the research and his relevant advice and discussions.
Prof. Dr. H. J. Goetze shared his wide knowledge of gravity method with me and showed me how to trace the major structural features from potential field data. Their crucial comments, valuable assistance and reading of the manuscript and enthusiasm were always inspiring and motivating to this thesis.

The author wishes to thank **the Minister of Energy and Mineral Resources**, and the **Director General, staff and colleagues of NRA**, for their continuous support and help during the several gravity field camps.

Particular thanks are due to **Dr. Sabine Schmidt** from the working gravity group of the Institute of geology, geophysics and geoinformatics of the Free University, Berlin for her fruitful lectures about IGMAS and DBGRAV softwares.

I wish to express my sincere gratitude's to **Dr. L. Diele** of the same University for her suggesting the input data of the initial geological model to fit the format of the modeling program IGMAS.

I am very grateful to **Dr. M. Rybakov** from GII and **Dr. U. tenBrink** from USGS for their valuable suggestions and compilation of the Jordanian and Israeli potential field data during the preparation of this work.

The author would like to express thanks **to Dr. Ahmad Al-Malabeh** from Hashemite University and to **Prof. Elias Salameh** from Jordan University for their fruitful discussion and encouragement.

The author expresses deep gratitude to my brother **Dr. Ahmad Hassouneh** from King Hussein Medical City and to my Cousin **Eng. A. Kareem Hassona,** the director general of Hassouna Foerdertechnik und Metallbau GmbH (HFM), Bremen for the financial support that made this work easier. I am obliged to them.

Particular thanks goes to my brother **Ali Hassouneh**, for his valuable notebook computer which facilitates my field and office work during writing the final copy of my thesis.
Particular thanks are due to **Eng. Abd Alwadood Al Kurdi**, the director of Al Masar Technical Company for Engineering production and industrial services, and to **Mr. U'baida Al Kurdi,** the director general of Al Kurdi Investment Company and A'bdoun Mall for their financial support.
Particular thanks are due to **Dr. M. Farajat** for his warm hospitality during my first visit to Germany and his help in one way or another during my stay in Wuerzburg.

Last but not least, my warmest thanks are extended to my **wife and my children** for their patience and support.

TABLE OF CONTENTS

1 INTRODUCTION

1.1 Geographic setting

Jordan is a Middle Eastern country centered approximately at 36^{o}, longitude E and 31^{o}, latitude N. It covers an area of approximately 89.5 sq. km and has a population of about 5.2 million. The topography is marked by the Ghor area along the Jordan River, the Dead Sea and Wadi Araba. The Dead Sea is actually the lowest point on earth at 415 m below sea level (2001). From north to south the heights extend toward the east varying between 600m and 1,500m, with the highest peak, Jibal Rum, reaching the altitude of 1754 m above sea level. The maximum width of the heights, which are traversed by streams and valleys, is 50 km. The land to the east is mostly flat, arid and forms a part of the Ash Sham Desert.
Jordan has developed its economic infrastructure during the last decade through the construction of a modern road network, airports and the Aqaba seaport, all of which connect Jordan with neighboring countries.

1.2 Major tectonic structural features in Jordan

There are several major tectonic structural features in Jordan. The major and complex one is the Dead Sea Rift (DSR) in which both strike-slip and extensional motion has occurred. The DSR is the largest strike-slip faults in the world and it is one of the best examples of deep continental strike-slip basins. The Dead Sea Rift, which extends for thousands of kilometers from the southern part of the Red Sea to the Taurus Mountains in Turkey, constitutes a boundary between the Arabian plate and the African plate. Along the length of this rift there is a horizontal sliding movement between the plates, as the Arabian plate, situated east of the Rift (i.e. Saudi Arabia, Jordan and Syria), moves northward of an order of 105-107 km at a faster rate than the African plate, situated west of the Rift (i.e. Sinai, Israel and Lebanon). The Rift ends in the immediate area of the Taurus Mountains at the meeting points of three plates, the Arabian, the African and the Euro-Asian plate, known locally as the Anatolian plate (Figure 1). These so-called "triple junctions" are a rare phenomenon on land, since most of them are situated at sea. They are very active from a seismic point of view.
The Dead Sea Rift (DSR) crosses the Gulf of Aqaba, Wadi Araba, the Dead Sea Basin (DSB), Jordan valley and Lake of Tiberias. The western sector of Jordan is structurally dominated by the Dead Sea Rift where older Precambrian rocks in the rift in southern part are complicatedly deformed and intruded by younger rocks. Paleozoic rocks overlying the Precambrian dip gently north easterly direction. The overlying Mesozoic and younger rocks have dips of less than 5° toward the northeast into the Al-Jafr Basin.

1.3 The objectives of the study

The main primary scientific objectives of the present study can be summarized as follows:

- To homogenize potential field data and to evaluate them.
- To improve the knowledge of the structural tectonic features occurring in the vicinity of the large fault systems using gravity and aeromagnetic analyses.
- Analyze the 3-dimensional gravity structural modeling of the Dead Sea Basin to investigate the shallow and deep structure of the Dead Sea Basin, to

investigate the mechanism of active faulting along the transform and their implications to seismic risk, to understand the cause for subsidence of the Dead Sea rift and the uplift of the surrounding areas and to seek tectonic indications about the origin of the Dead Sea fault system.

- To map from gravity anomaly the shallow subsurface geologic basins in the Dead Sea rift for future water exploration.
- To provide, for the first time, upgraded depth to gravity and magnetic basement map beneath Jordan from potential field data, well logs and previous published papers.

1.4 Methods and software

The analysis of the Bouguer gravity and aeromagnetic anomaly maps provides the new tectonic structural map of Jordan.
For gravity surveys, LaCoste Romberg D & G gravity meters and Scintrix Automated Gravity Meter (CG3) have been used. Geometrics Model G803 proton precession magnetometer was used for airborne magnetic survey. Gred3d and HBHTC software was used for gravity reduction and terrain calculations. This program computes all necessary corrections to the ideal earth model gravity. In addition, it makes the conversion from gravimeter readings to observed gravity and applies the earth tide and instrument drift corrections. The program consists of four files: the raw data file, conversion table for the gravimeter, the base station file, and a fourth file with digital elevation data for the region (DTM). Surfer7 software was used for gridding and contouring the data. Grapher and Corel draw programs were used for data analysis. The IGMAS modeling program was used for 3D models.

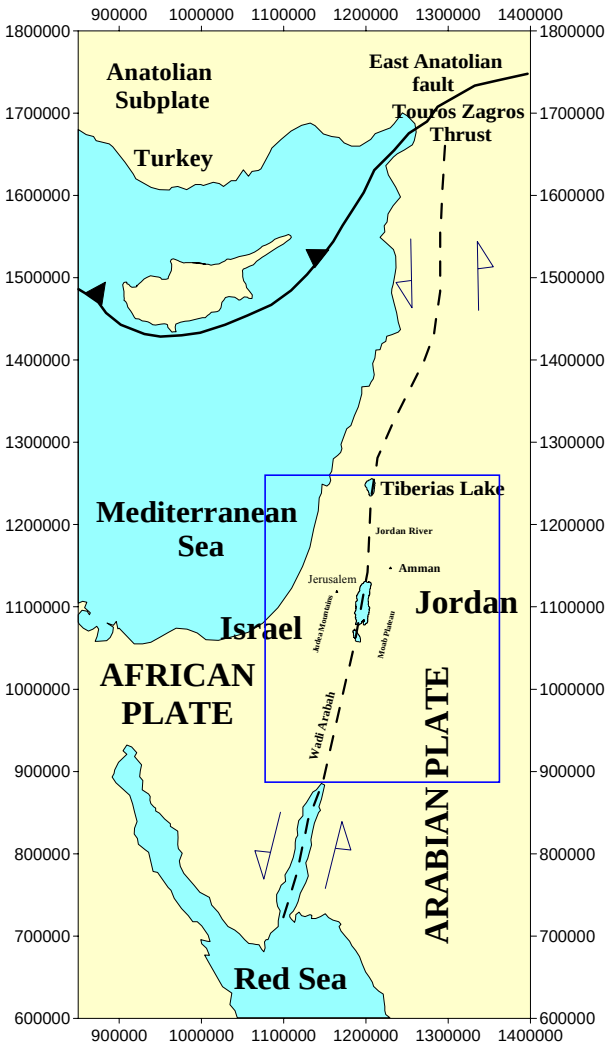

Figure 1: Location map of the study area (blue rectangle) showing the major tectonic structural setting of the Middle East.(after Rybakov, 1999).

2 GEOLOGIC SETTING

2.1 Geology and Stratigraphy of Jordan

The Hashemite Kingdom of Jordan is located at the northwestern part of the Nubian-Arabian shield. In southwestern Jordan, parts of the Arabian shield are exposed. It consists of Precambrian plutonic, metamorphic and minor occurrences of upper Proterozoic sedimentary rocks.

The Precambrian rocks are unconformably overlain by unmetamorphosed Cambrian to Silurian sedimentary rocks, which are predominantly of marine-continental origin, though continental sediments occur within the Cambrian, Lower Ordovician and Upper Silurian sequences, dipping gently north and northeastward.

Upper Paleozoic rocks are not shown at the surface but speculations have been made about the existence of such rocks in the deep sedimentary basins (Bender, 1974). Lower to middle Triassic rocks represent the first stage in Jordan of the Mesozoic transgression of the Tethys from the north. Uppermost Triassic rocks are apparently not represented everywhere. Jurassic rocks of predominately marine carbonates and clastics unconformably overlie these but with limited exposed extent. Extensive uplifting and erosion during Triassic and Jurassic are indicated by the fact that while Lower Cretaceous rocks overlie Triassic rocks, in Zarqa Mai'n, further south they overlie the Paleozoic rocks sequences.

Widespread carbonate deposits of Upper Cretaceous including a variety of marls, limestones and dolomitic limestones represent the most extensive northwest-southeast transgression of the Tethys that continued up to the Oligocene. However, widespread deposition of clastics occurred in central eastern and southern Jordan until the Cenomanian. This pattern of northwest-southeast transgression-regression of the Tethys has been repeated several times during the Mesozoic. The uppermost Cretaceous-lowermost Tertiary thins southeastwards. Local thickening, however, occurs in north to northwest elongated basins.

Coarse linticular unsorted conglomerates of Upper Oligocene to lower Miocene overlaying Upper Cretaceous and Tertiary units occur in the eastern Wadi Araba area. These are of significance as they indicate uplift and probably tectonic activity nearby. A similar conglomerate unit unconformably overlies either the lower unit or the older Cretaceous units occur in the same area with uncertain Miocene-Middle Pleistocene age. (Bender, 1974). Both sets of deposits could be related to initial subsidence and block faulting along the Dead Sea Rift.

Considerable thicknesses of marine sediments were deposited throughout the Tertiary age. However, lacustrine and fluviatile sediments were deposited in areas and uplifted above sea level. More than 3.5 km of evaporates were deposited during late Miocene to early Pleistocene (Bender 1974).

Quaternary deposits are mostly of lacustrine and fluviatile origin thus indicating continuous uplift and retreat of marine environment. Considerable thicknesses of conglomerates were deposited in and near the rift during this time.

The general surface geology of Jordan, Palestine and Israel is shown on Figure 2 and a stratigraphic-geologic time table shown on Figure 3.

2.2 Geological setting of the Dead Sea Transform System

The Dead Sea Transform fault system (DSTFS) is a plate boundary between the Arabian plate on the east and the Sinai-Palestinian sub-plate on the west (Figure 1). It forms the northern most part of the East African Rift system which comprises the East African Rift, the Red Sea Constructive regimes, the Gulf of Sues Extensional fault system and the Gulf of Aqaba and the Dead Sea Transform fault system. The rift system is recognizable for a distance of over 6,000 km. In Jordan, only 360 km of this system is known as the Dead Sea System and it accommodates part of the northwards motion of the Arabian plate against the African plate.
The DSTFS consists of three main structural segments; from south to north they are:

Wadi Araba fault which extends from the northern part of the Gulf of Aqaba to the southern boundary of the Dead Sea basin. It is diagonally cross the Wadi Araba floor and strikes N 15^{o}-20^{o} E. It extends for approximately 180 km with a noticeable straight trace deforming the Quaternary fluvial, aeolin and lacustrine sediments which cover Wadi Araba floor.

The Dead Sea structure is a pull-apart basin, which has been formed due to the steps to the left of the transform (Wadi Araba fault in the south and Jordan Valley fault in the north) around the Dead Sea.

The Jordan Valley fault is essentially the northern extension of the Wadi Araba fault and defines the northern segment of the Dead Sea transform north of the Dead Sea basin up to the Lake Tiberias. It has a roughly N-S trend, forming a major kink in the transform system from roughly N20E to N-S (Galli, 1999)

The block east of Wadi Araba regionally dips more steeply northward than does the Palestine block (west of Wadi Araba), but the sedimentary column on the northern Palestine block is thicker than that on the Jordan block; therefore, the surface structural position of the Cretaceous-Tertiary sedimentary sequences gradually attains the same level on both sides of the Rift Valley between the Dead Sea and Lake Tiberias (Bender, 1975).

Neogene left lateral displacement along the Dead Sea transform is approximately 107 km (Quennell, 1959, 1983, Freund et al. 1970, Garfunkel et al. 1981, Hatcher et al. 1981), (Hassouneh and Rybakov, 1998). The displacement is accompanied with a counterclockwise rotation of 5.5 to 6 degrees of Arabian plate with respect to Africa plate (Quennell, 1959, Joffe and Garfunkel, 1987, Klinger et al. 2000).
The shear along this rift is believed to be responsible of the current structural tectonic pattern in Jordan.

Post Pan-African Orogenic calc-alkaline granitoids, andesitic and rhyolitic rocks, composing part of the Late Proterozoic Aqaba and Araba complexes (Rashdan, 1988) are unconformably overlain by Phanerozoic sedimentary rocks, which have been deformed by tectonic activity, largely associated with the Dead Sea, transform fault system.

The Precambrian tectonomagmatic evolution, structural pattern, and geometry of dike system within the basement rocks suggest that a major rift boundary or zone of

extension (geosuture, hinge line) already existed during the deposition and emplacement of the Late Precambrian complex (Ibrahim, 1993, Stern et al. 1984, Clark, 1985, Bender, 1967). Additional evidence is the morphology of the surface of the Precambrian basement complex (Bender, 1976, Barjous, 1992).

During the Neogene tectonic phases of uplifting of the landmass and/or after the corresponding negative shifts of base-level, either through tectonic events or by ecstatic change in sea-level, the Sinai and the Arabia surfaces were formed by erosion during a prolonged period of stability in the Oligocene (Quennell, 1956). Oblique-slip movement on the Dead Sea system compounded the result of the left lateral faulting and caused local uplifting and/or subsidence of the rift margins (Barjous, 1992).

2.3 Volcanic Activity:

Volcanic activity occurred in the western part of Jordan between middle Jurassic and early Cretaceous time with six major periods of emissions.
This includes tuffs, agglomerates and mafic to intermediate intrusives. Mafic to felsic sills and dykes of probably of younger age (Bender, 1974) are cutting the Mesozoic sedimentary rocks of Wadi Araba.
Quaternary mafic volcanism and shallow intrusive activity are extensive. There are four principal modes occurrence for these mafic rocks with their locus in the Dead Sea rift. They occur as localized flows and plugs, some tuffs and as plateau flood basalts. An extensive plateau crosses northeast Jordan from Syria to Saudi Arabia. (Barberi, et. al., 1979) reported that basalts, which may be directly, associated with the rift, are chemically primitive and appear to reflect rapid propagation of fractures into the mantle then rapid extrusion.
The weathering of this volcanic rock in the extreme temperatures of the desert climate (hot days and cold nights) has formed the extensive boulder field found there today. Silt-filled depressions between low basalt hills are common.

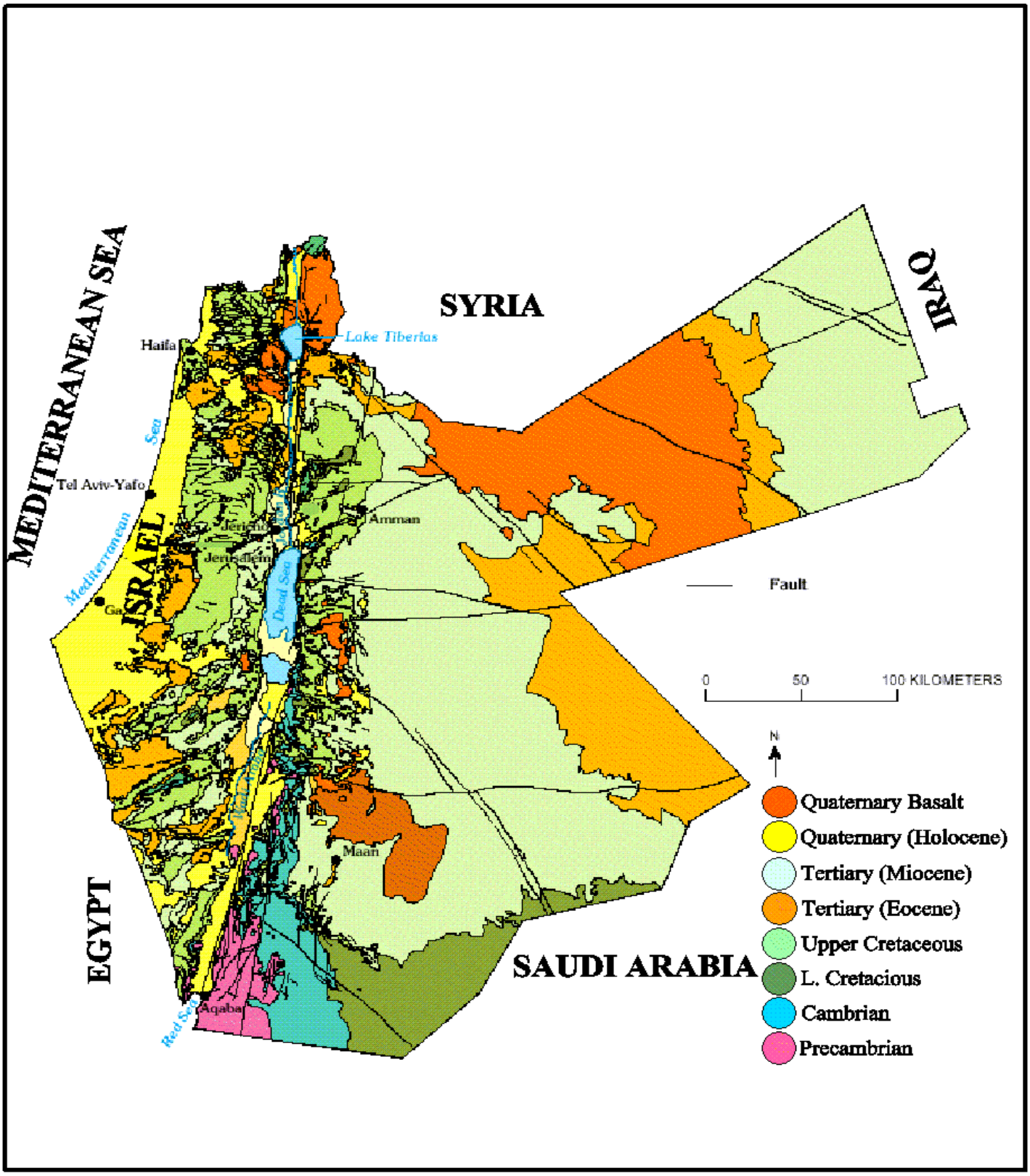

Figure 2: Geology map of Jordan, Israel and Palestinian National Authority (PNA).
(USGS Open report, overview of Middle East water resources, 1998)

AGE	FORMATION	FM. CODE
Q	**Samra**	**SMR**
Tertiary		
	Sara	SAR
	Taqiyeh	TQY
Cretaceous	Ghareb	GRB
	Amman	**AMN**
	Wadi Essir	**SIR**
	Shueib,Hummar,Fuheis,Na'ur	**SHB,HMR,FHS,NAR**
	Kurnub	KRB
Jurassic	Muaddi	MUA
	Arda	ARD
	Umm Maghara	MGR
	Dhahab	DHB
	Zarqa	ZRQ
	Deir Alla	ALA
Triassic		
	Abu Ruweis	RWS
	Umm Tina	TIN
	Iraq Al Amir,Mukharis,Hisban	AMR,MKS
	Ain Musa	HSB,MSA
	Dardun	DRD
	Ma'in	MAN
Devonian, Permian	Umm Irna	IRN
Silurian	Khush-sha Sandstone	KSH
	Mudawwara Sandstone	MDW
Ordovician	Dubaydib Sandstone	DBD
	Hiswa Sandstone	HSW
	Umm Sahm Sandstone	SHM
Cambrian	**Disi Sandstone**	**DSI**
	Umm I'shrin Ss	ISH
	Burj Dolomite/Shale	**BRJ**
	Salib Arkosic Ss	SLB
Precambrian	**Saramuj Conglomerates**	**SMJ**
	Aqaba complex (Granite)	**AC**

Figure 3: Stratigraphic-geologic time table. It is very useful for building real gravity models based on identification of significant density contrasts with specific units of the

stratigraphic succession (more details in chap. 3, sec. 3.3.3). (Compiled by A. Sabbah, 1990).

3 GRAVITY DATA ACQUISITION, PROCESSING AND COMPILATION

3.1 Introduction

From 1976 until 2000, a total of 49,696 land gravity stations were collected in Jordan. In addition, 300 km of marine gravity data were collected in the submerged part of the Dead Sea basin from a small utility vessel using the Bell Aerospace BGM-3 marine gravity system.
In 1998/99, the author collected 2185 detailed high-resolution gravity data on the central and on the southern part of the Dead Sea basin in conjunction with a 3-D reflection seismic survey. These data were integrated with 514 marine gravity observations and 1313 gravity data from the Geophysical Institute of Israel.
From March 20 to April 30, 2002, new 800 gravity stations were measured by the author under the supervision of Prof. H. Götze from Free University, Berlin, in Wadi Araba.
The Jordanian gravity data, Israeli gravity data and the marine data were merged to compile one unified file consisting of 97,711 gravity station, used for this study (Figure 4).

3.2 Data acquisition

The new gravity surveys, which covered (85-90) % of Jordan, were conducted at different times for different purposes (Figure 5). A total of 49,696 gravity stations were measured from November 1976 until January 2000.

The gravity measurements were carried out utilizing Lacoste and Romberg G & D type model gravimeters, Scintrix Automated gravity meter (CG3) and old Worden gravity meter. Each day of data collection began and ended with a measurement taken at the gravity base station which belongs to the Jordan Gravity Standardization Network (JGSN90), established in 1990 (Boyed, et. al., 1990).
Differential GPS techniques, utilizing ASHTEC survey equipments, are applied at a fixed location in order to increase the accuracy of the position of the gravity station.

In 1977, 5783 gravity stations were collected in the Risha area (RH) in the Northeast of Jordan by the Natural Resources Authority (NRA) to locate the subsurface structures before conducting seismic surveys for oil & gas exploration. This was the first start of gravity surveys in Jordan by Jordanian geophysicists after the random surveys conducted by different oil companies like TPC (1947), Pawley (1957), Mecom (1965), Lerici (1966) and INA (1968).

In 1988, Fina Oil Company measured 2591 gravity stations along the seismic lines in the basaltic plateau (BP) in the northeastern part of Jordan. The oil company provided the NRA with a hard copy of the data set. The data were processed and added to the NRA database by the author. In the second half of 1988, 508 gravity stations were collected by the author and Dr. Gordon Andreasen from USGS along six E-W profiles crossing the Dead Sea rift.

In 1989, 4232 gravity stations were measured by a Japanese gravity group along the seismic lines surveyed by the Japan National Oil Company (JNOC); NRA had received the hardcopies of the raw field data. The author together with Mr. Zaid Al Kaysi from NRA prepared the data for processing.

In 1989, 3647 gravity stations were measured along the seismic reflection lines (surveyed by the Austrian Oil Company OMV) by Mr. A. Al A'mre from NRA under the supervision of the author in the Sirhan area (very dry desert) south-eastern part of Jordan near to Saudi Arabia borders.

In 1989, 2015 gravity stations were measured on square nets with a size of 4×4 km (1 point per km2) in Qatrana area (QT) in the central part of Jordan by the NRA gravity group.

In 1989, 1200 gravity stations were measured by the author at the Jordan-Iraqi border along the seismic lines surveyed by Petro-Canada International Assistance Corporation (PCIAC).

In 1990, 5963 gravity stations were measured in Al Jafr area (JF) in the south east of Jordan by the gravity group of NRA along the seismic lines surveyed by PCIAC and GSI.

In 1991, 1612 gravity stations were measured on random survey because of the topography by NRA gravity group in A'jloun area (AJ) in the north of Jordan.

In 1992, 2010 gravity stations were measured on square nets with a size of 4×4 km in Khaldieh area (KH) in the north east of Amman by the gravity group of NRA.

In 1992, 459 gravity stations were measured along narrow Bedwins roads by the author in the Basaltic Plateau (BP), (Harrat Ash Shaam) in northeast Jordan.

From May 1992 until November 1994, 4144 gravity stations were measured by NRA gravity group in Al Azraq area (AZ) east of Jordan.

In 1993, 925 high resolution gravity stations were measured by the author in the Lisan Peninsula (LP) of the Dead Sea rift along 3D seismic survey by the French Seismograph Service Limited (SSL).

In 1993, 461 gravity stations were measured by the author in the Wisad area (WD) in the southeast of Jordan along the seismic lines surveyed by PCIAC.

In 1994, 407 gravity stations were measured by the gravity group of NRA in Al Karamah area in the rift.

From December 1995 until May 1996, 1157 gravity stations were measured in a random survey by the author in Wadi Rum area (WR) in southernmost of Jordan.

From January until September 1995, 999 gravity stations were measured randomly (1 point per km) by the NRA gravity group in Wadi Araba (WA) and Aqaba (AQ).

From September1997 until January of 1999, 1852 gravity stations were measured on square nets with a size of 4×4 km by the NRA gravity group in Muwaqar area (MQ) 30 km east of Amman.

From January 1997 until October 1998, 3531 gravity stations were measured on square nets with a size of 4×4 km by the NRA gravity group in the Ma'an area (MN) 220 km south of Amman.

From June 1998 until September 1998, 400 gravity stations were measured by the author in the cities of Amman and Zarqa large cities using the Ashtec GPS instrument for the first time in Jordan.

From April 1997 until August 1999, 4200 gravity stations were measured by the author in the Dead Sea rift.
From September 1999 until December 1999, 902 gravity stations were measured by the author on the shoulders of the Dead Sea basin.

From March until May 2002, 800 high resolution gravity stations were collected in Bir Madhkour (Wadi Araba) by the international DESERT gravity team under supervision of Prof. H. Götze from Free University, Berlin.

In 1988, 300 km of marine gravity data were measured by Israel National Oceanographic and Limnological Institute and Dr. Uri tenBrink from the USGS in the submerged part of the Dead Sea basin using a small utility vessel using the Bell Aerospace BGM-3 marine gravity system. Gravity was continuously measured during 3 days and 1 night at an average speed of 5 knots. Gravity was recorded at a 1-sec. interval and monitored in the field using two COMPAQ 386 computers. Navigation has been done every 1 sec, by a portable radar ranging system (Mini-Ranger). The water depth was measured using an analog 3.5 KHZ DFS-6000 echo sound with an accuracy of 0.5 m in seawater.

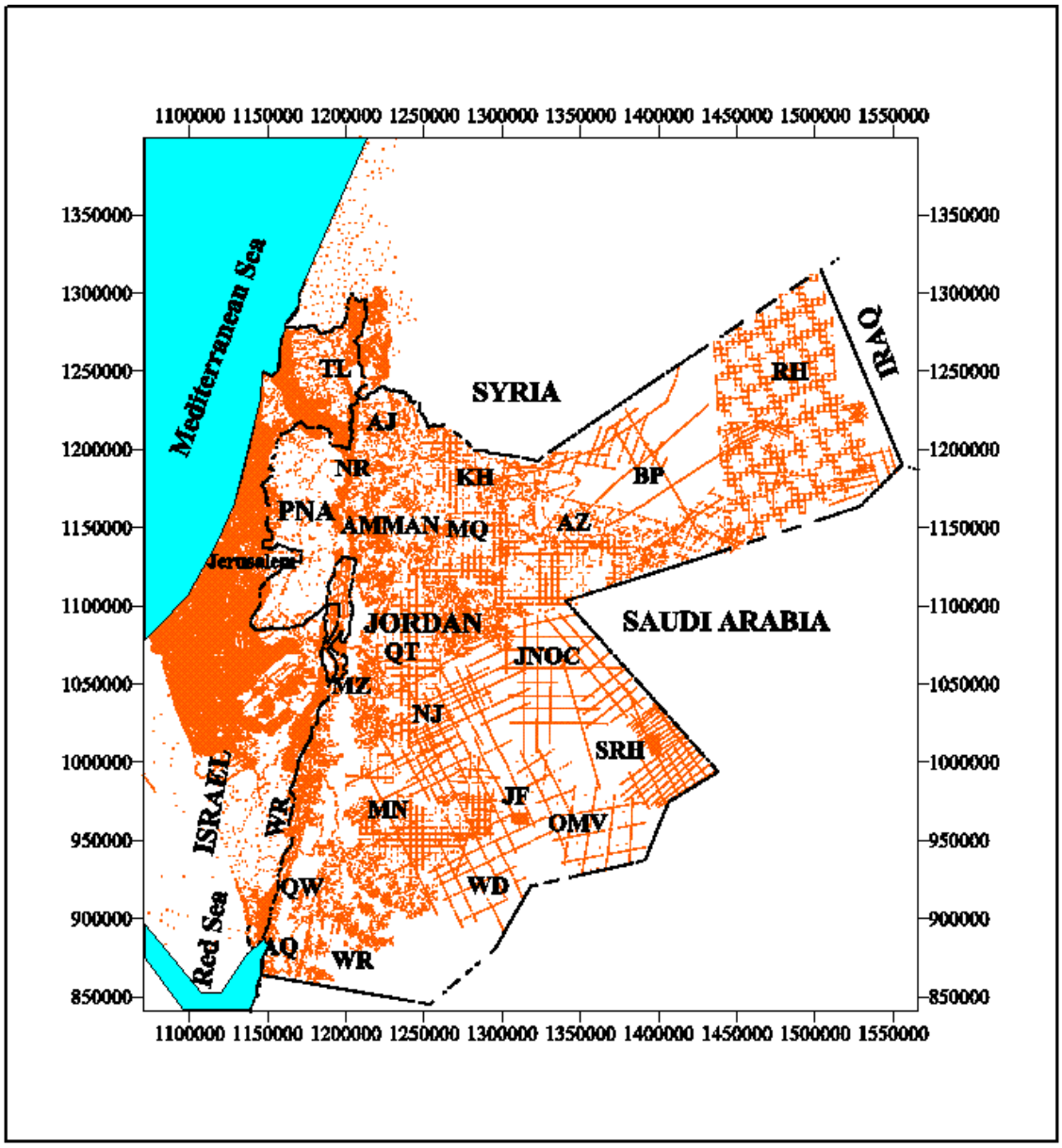

Figure 4: Location map of gravity stations in Jordan, Palestinian National Authority areas (PNA) and Israel. Coordinates in Palestine grid + 1000000 m (Cassini-Soldner Projection). The abbreviations are: RH = Risha area, BP = Basaltic Plateau, AZ = Azraq area, TL = Tiberias Lake, AJ = A'jlun, KH = Khaldieh area, NR = North rift, MQ = Muwaqar area, QT = Qatrana area, MZ = Mazar area, JNOC = Japan national oil company area, OMV = Austria oil company area, SRH = Sirhan area, NJ = North Jafr area, JF = Jafr area, MN = Ma'an area, WD = Wisad area, QW = Quwaira area, WR = Wadi Rum area, WA = Wadi Araba area, AQ = Aqaba area.

3.3 Data processing

All data processing of the previously mentioned field campaigns of the different gravity groups of NRA and other oil companies have been done by the author.

3.3.1 Gravity reduction

Gravity raw data processing and the processing for station complete Bouguer anomalies were computed on UNIX/SUN work station and personal computers.
The software used for data reduction is called *GRED3D* and was developed by USGS (Gettings et. al. 1982). The software computes necessary corrections and the ideal earth model gravity. In addition, it converts the gravimeter readings into gravity and applies both Earth tide and instrument drift corrections. Raw data files contain a station identification, latitude, longitude, elevation, observational time and date of the reading, the gravimeter reading, and inner zone terrain correction (Hayford-Bowie zones A and B within a radius of 68 m from the station) The program consists of 4 subroutines: the raw data file, conversion table for the gravimeter, the base station file, and a fourth file with digital elevation data for the region. The program calculated the gravity reduction of a homogeneous layered spinning earth, the free air, spherical Bouguer slab, and the terrain corrections to generate the gravity effect of the ideal earth model. Finally, the program subtracted the earth model gravity from the observed gravity to give the complete Bouguer gravity anomaly for each station. Observed gravity relative to the IGSN-71 datum was reduced to the Bouguer anomaly using the 1967 gravity formula and a reduction by a density of 2670 kg/m^3. A gravity profile over part of the study area (according to Nettelton's method), was carried out to estimate the suitable bulk density. As a result, it was found that the density of 2670 kg/m^3 has the minimum correlation coefficient with topography (Hassouneh, 1995).

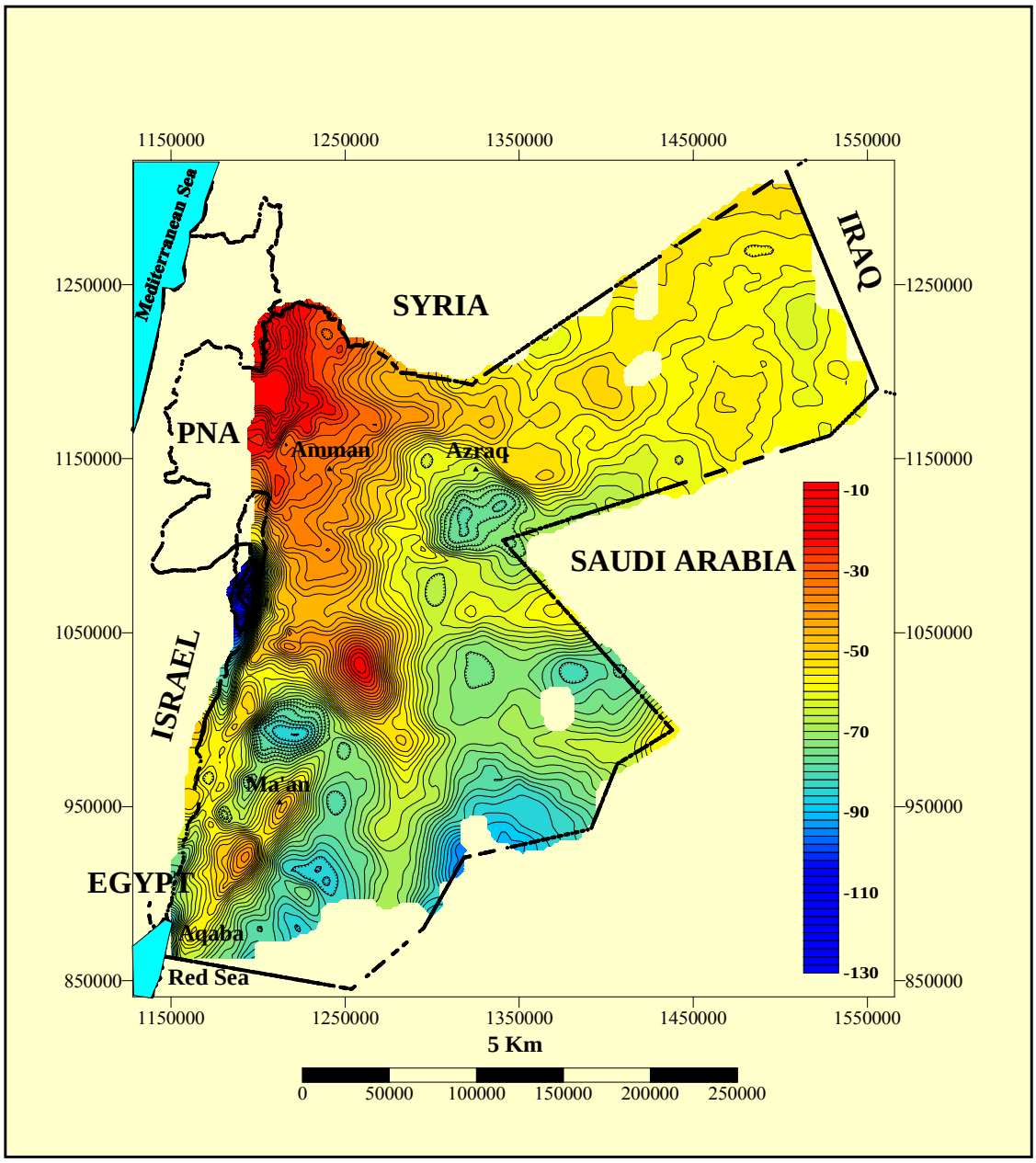

Figure 5: Bouguer gravity anomaly map of Jordan. Coordinates in Palestine-Israeli Cassini grid. Density used for Bouguer reduction is 2670 kg/m^3. Contour intervals 2×10^{-5} m/s^2.

3.3.2 Determination of density characteristics in Jordan

A gravity anomaly is caused by a change in rock density in the surrounding of an observational point. To be able to calculate and interpret observed gravity data, we have to know the densities of the geological formations of the investigated area. The Natural Resources Authority (NRA) made a large number of density determinations on recovered core samples from several oil exploration wells. The following observations can be made about density changes associated with the stratigraphy succession in Jordan (Figure 3) beginning with the oldest rocks:

- Granite is the main constituent of outcropping Precambrian rocks in the Aqaba complex. The density of granites in Jordan is typically 2650 +/- 50 kg/m^3.
- Sarmuj conglomerate from drill hole NH1 has a measured density of 2690 kg/m^3 which is not significantly different from Precambrian granite.
- Cambrian Period, Disi and Salib sandstones having a density of 2750 kg/m^3. With depth they increase in density from 2550 kg/m^3 to 2650 kg/m^3. The Burj dolomite has a notably higher density of 2750 kg/m^3-2800 kg/m^3.
- Ordovician Period, Dubaydib sandstone is observed to generally have a higher density than overlying Silurian rocks (Mudawwara shale). Dubaydib consists of a density of 2720 kg/m^3.
- Silurian Period, which is consists of Al Khush-sha and Mudawwara sandstones, has a density of 2450-2600 kg/m^3.
- Triassic Period, the Ma'in and Abu Ruweiss Formations are mainly carbonates of high density of 2680-2700 kg/m^3.
- Jurassic Period, which consists of Mua'ddi, Arda, Umm Maghara, Dhahab, Zarqa and Deir A'lla Formations, has a density of 2550 kg/m^3.
- Cretaceous Period, which is consists of Ghareb, Amman, Wadi Essir and kurnub sandstones, has a density of 2400-2630 kg/m^3. Amman and Wadi Essir carbonates are higher density units of 10 to 20 kg/m ^{3} than the Kurnub and Ghareb sandstones.
- Tertiary Period, which is consists of Taqieh, Sarah and Samra Formations, has a density of 2000-2200 kg/m^3.

To avoid the ambiguities inherent to the modeling of the gravity data, the available density information will support the construction of a 3D model of the study area.
The following logs of density depth observations were obtained from well logs data for oil exploration wells drilled in Jordan: (Appendix 1, shown the rest of the logs).

Thickness in meters	Period	Formation	Density in kg/m3
0-124 m	Cretaceous	Ghareb Amman,Wadi Essir , Shueib,Hummar Fuheis Na'ur Kurnub	1800 2000 2200 2400 2600 2800 3000
124-306 m	Jurassic	Muadi Arda,Umm Mughara Dhahab,Zarqa Deir Alla	
	Triassic	Abu Ruweis,Um Tina Iraq Al Amir,Mukharis Hisban Ain Musa, Dardoun Ma'in	
306-514m	Permian Silurian	Umm Irna Kush sha,Mudawwara	
514-1785m	Ordovician	Dubaydib, Hiswa Um Sahm Disi	
1785-3336m	Cambrian	Umm Ishrin Burj Dolomite Abu Khushiba Salib Arkosic	
3336-4048m	Precambrian	Saramuj Conglomerates	

Table 1: Density depth observations in Jaf1 oil exploration well located in Al Jafr area. (A. Sabbah and Hassouneh 1989, 1999).

3.3.3 Co-ordinates system (Geo-reference)

In this work, gravity, magnetics, topography, geology, and location maps are based on the new Israel Cassini-Soldner projection. It is linked to the old Palestine system adding 1000,000 m to the origin. The Palestine grid of 1928 is originated at:

$\phi_\circ = 31^\circ 18' 06.27'' $ North
$\lambda_\circ = 34^\circ 31' 42.02''$ East of Greenwich

It is defined at a Clark reference ellipsoid (Clark 1880) which is defined by:

a = 6,378,300.789m
1/f = 293.466004983713280
H= 98.9m.

The other system established in 1933 is based on Cassini-Soldner coordinates. Its origin is located in Jerusalem at:

$\phi_\circ = 31^\circ 44' 02.749''$ North
$\lambda_\circ = 35^\circ 12' 39.29''$ East of Greenwich + $4.200''$ E = $35^\circ 12' 43.490''$.

According to Mugnier (2000) an addition of $4.200''$ to the longitude is in accordance with the decision in 1928 to adopt values from the French grid, founded in Egypt, to correct all Palestine longitudes accordingly. The false easting is 170,251.555m, false northing is 126,867.909m.

3.3.4 Digital terrain model (DTM)

The DTM presented here, Figure 6 and Figure 7, were prepared from different sources:

- Digitizing and laser scanning 1:50,000 topographic maps of the region, Jordan, Israel, Palestine, Syria, Saudi Arabia and Iraq (Gettings and Hassouneh 1988).
- Aerial Stereo Photography (Royal Jordanian Geographic Centre).
- Traditional surveying method and Global Positioning System (GPS).
- Bathymetric surveys.
- Published data of Geological Survey of Israel (GSI), (Hall, 1993, 1994, 1995, 1996) through the joint earth science projects between NRA (Natural Resources Authority, Jordan), GSI (Geological Survey of Israel) and GII (Geophysical Institute of Israel).

The DTM used here is an ASCII file and contains only spatial elevation data at a regularly gridded pattern in raster format.
The spacing of the regional DTM, Figure 6, is 500 m grid and for the DTM of the Dead Sea Rift, Figure 7, is 200 m grid.

Both DTMs provide a digital representation of the region's terrain over a two dimensional surface.
The DTM gives elevations to centimetres resolution at a grid with 200 m spacing, and 1 meter at a grid with 500 m which is based on the Cassini-Soldner (Israel Grid) projection. Both DTMs is among the highest resolution DTM datasets available for the region.

DEM shows various other features of interest. Going from south to north, we note the following:

- On the eastern shoulders of the Rift, in southern Jordan, Figure 6 and Figure 7, show numerous small to large lineaments trending north to northeast and approximately southeast-northwest which are Wadi Araba (WA), Quwaira (QW) and Disi-Mudawara (DM) faults.
- On the eastern shoulders of the Rift, in the central part of Figures 6 and 7, there are 3 large lineaments trending NW-SE which are Wadi Al Hasa (WH), Karak-Wadi Al Fayha (KWF), and Wadi Al Mujib (WMJ) faults.
- On the eastern shoulders of the Rift, in northern Jordan, Figure 6 and 7 show numerous small to large lineaments like A'jlun anticline, Zarqa River and basalt flows.
- On the western of the Rift, in northern Palestine and Israel, Figure 6 and 7, show numerous small to large lineaments trending NW-SE, NE-SW, interpreted as faults, arcs, folds and anticlines.

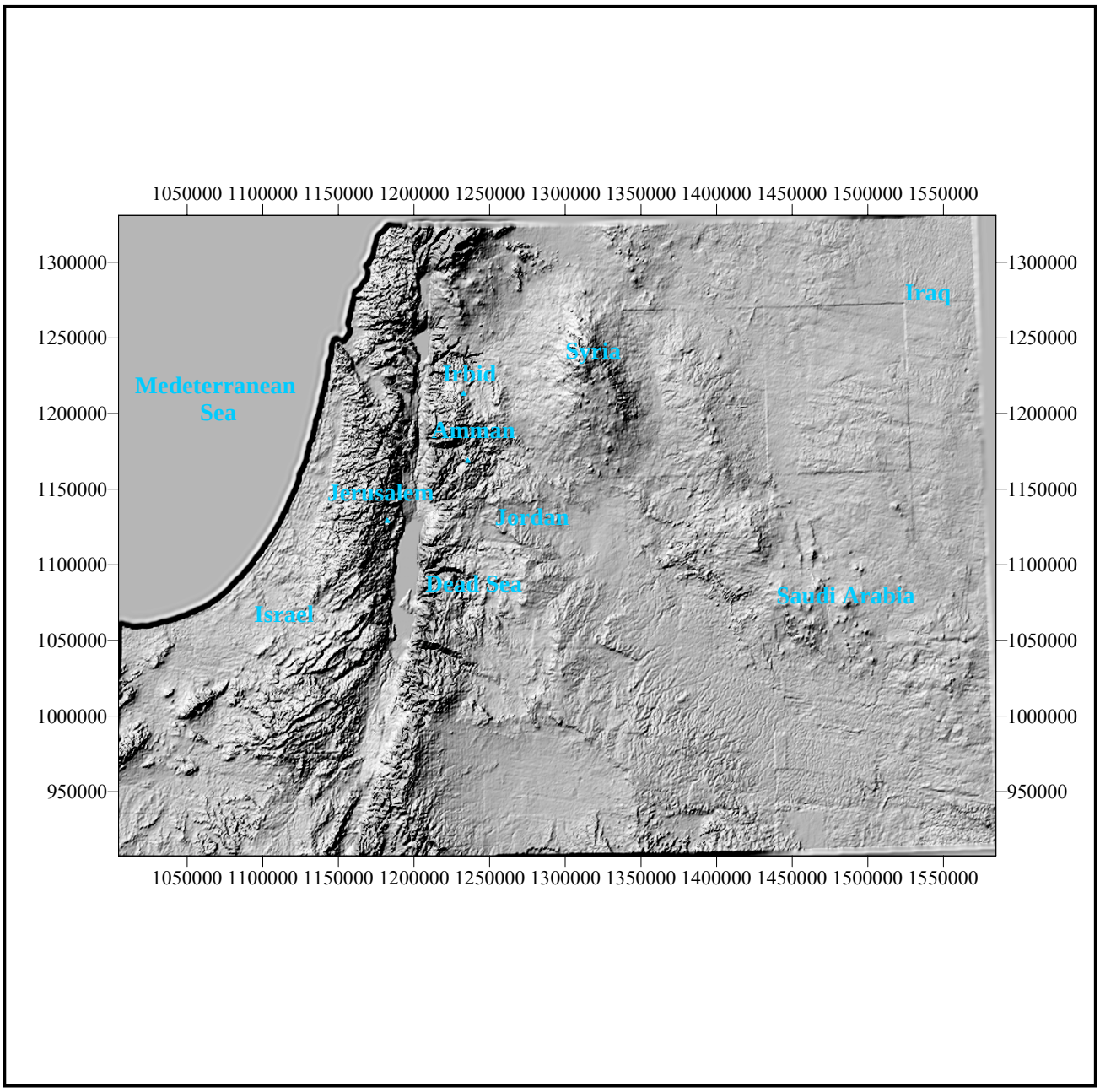

Figure 6: Shaded relief map of Jordan, Palestine, Israel, Syria, Saudi Arabia and west of Iraq. The map is compiled from digitizing 1:50,000 topo maps and from normal surveying during the gravity measurements. (Gettings & Hassouneh 1988; tenBrink 1993).

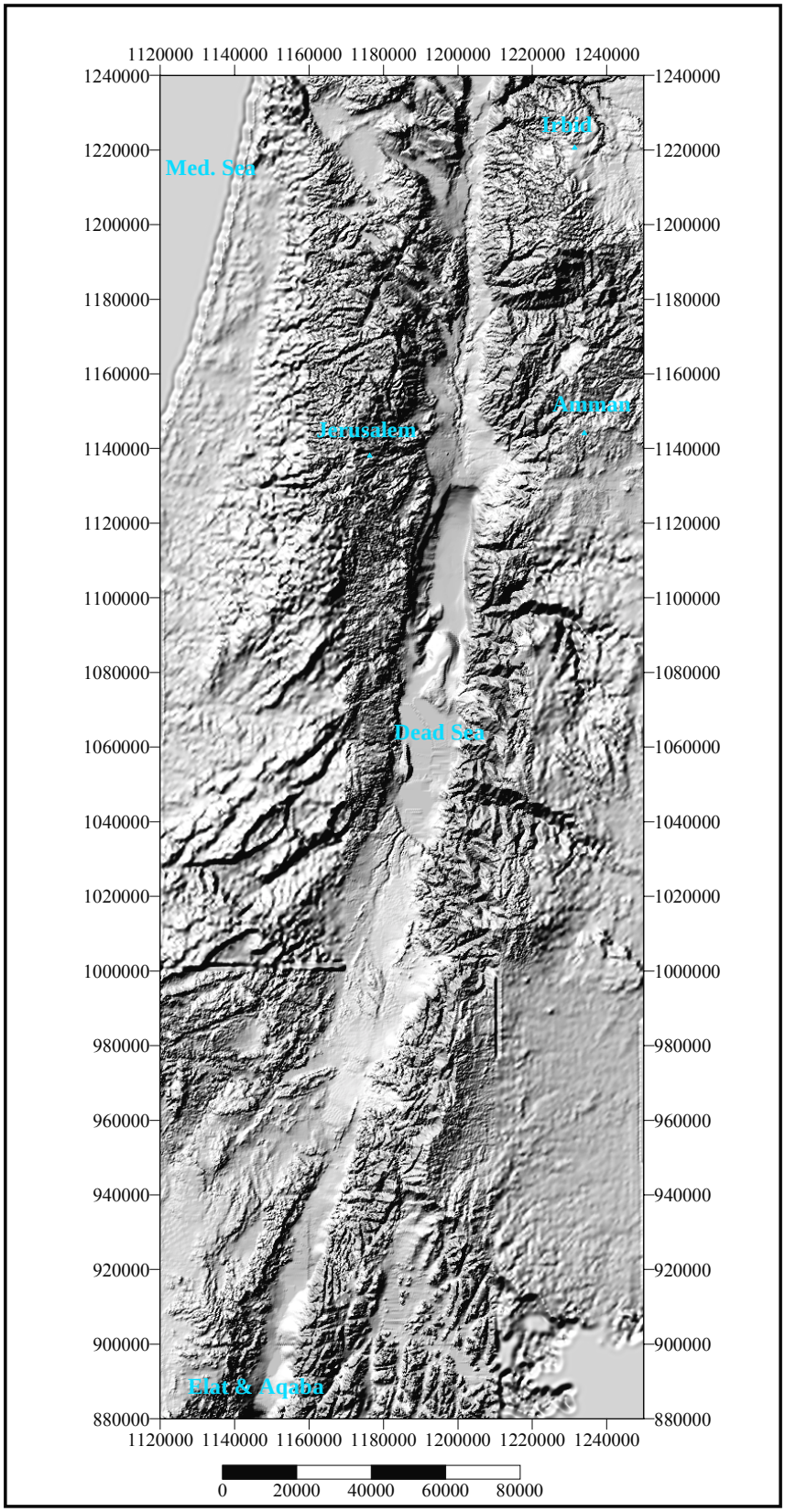

Figure 7: Shaded relief map of the DSR and its surrounding shoulders. This map includes the northernmost tip of the Gulf of Aqaba (Eilat) in the Red Sea, Dead Sea basin, Jordan River, Tiberias Lake, eastern and western shoulders of the rift and Mediterranean Sea. (After Hall 1993, 1994, 1995).

3.3.5 Terrain Correction

The terrain correction Tc corrects for the deviation of the actual terrain from that of an infinite horizontal slab and depends on the average density of the terrain that surrounds the station. The terrain effects were computed here using the DTM described in 3.2.4. The program uses the line-of-mass approximation to estimate the gravity effect of each compartment by replacing the topographic prism with a line of mass along the axis of the prism from sea level to the altitude of the prism. The maximum total terrain correction results in14.16 mGal at station L25 on the east shoulders of the DSR.

3.3.6 Griddling and Contouring

The general approach was to grid the data to produce the final contour maps of the study area. The Kriging method of the SURFER^{R} program was used to interpolate the Arbitrarily distributed gravity data at 1km × 1km grid cells.
A search radius of 6 km was used to determine values at grid positions in areas of sparse data. Through experiment I found that this search radius satisfied the calculation at each grid point within the entire data set. Kriging is very flexible and is geostatistical method that has proven useful and popular in many fields. This method produces visually appealing maps from irregularly spaced data like the data of this study.

3.3.7 Compilation of Jordanian and Israeli gravity data

Jordanian and Israeli gravity data were merged and compiled into one Bouguer anomaly file (Figure 8). The gravity data compilation started in 1998. NRA (Natural Resources Authority) and GII (Geophysical Institute of Israel) have started this joint gravity project by establishing 4 gravity base stations in Jordan and in Israel along their borders in order to build the same gravity datum and control network. The Jordanian network is tied to IGSN 1971, whereas the Israeli network is tied to the Potsdam network. This is why we found a difference of approximately 14×10^{-5} m/s^2 between the two networks. This value was subtracted from the Israeli and marine data before merging the data sets together.

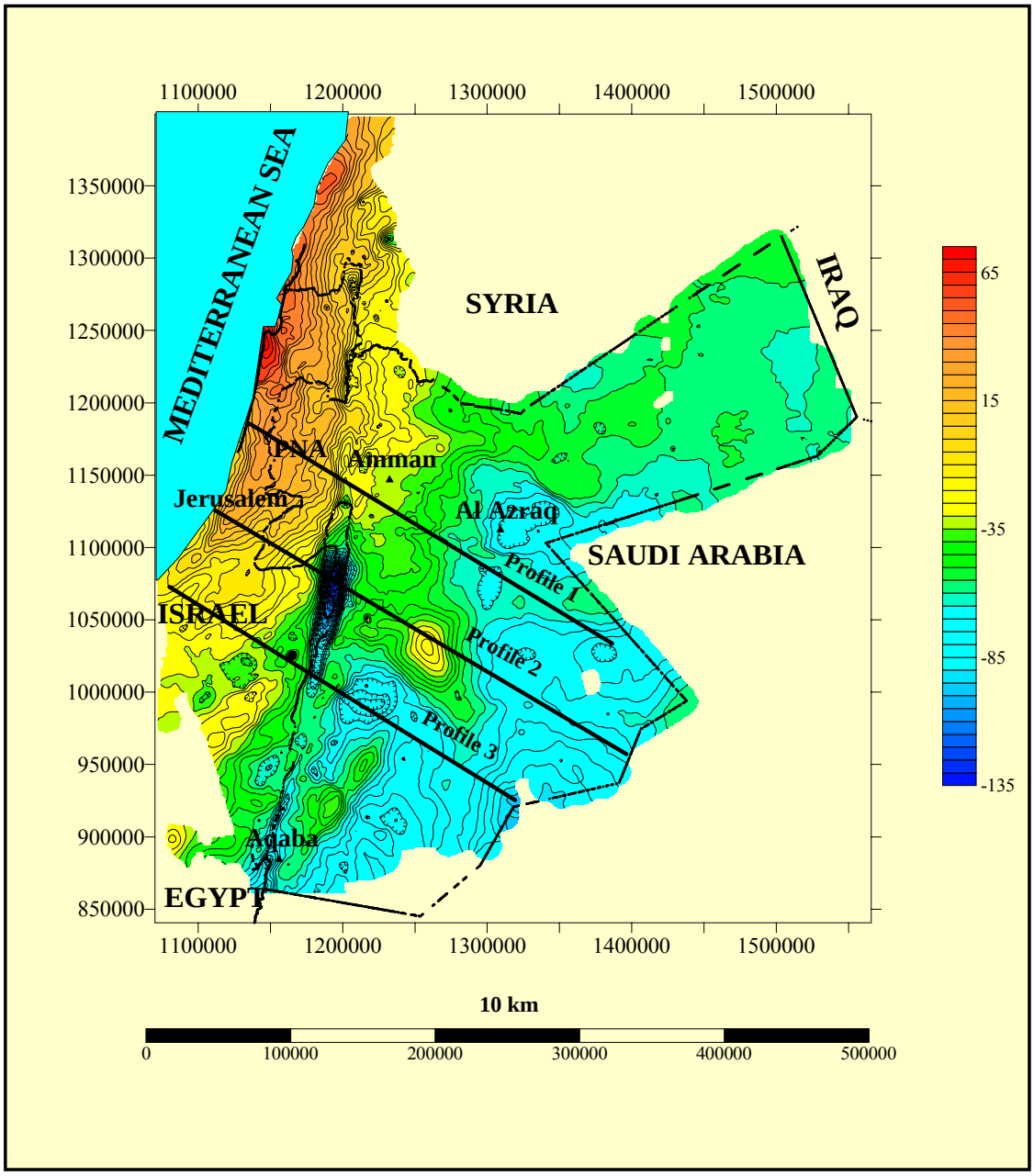

Figure 8: Gravity anomaly map of Jordan, Palestinian National Authority areas, Israel, and the location of the regional 3 NW-SE profiles crossing the Dead Sea rift. Contour Interval = 5 $\times 10^{-5}$ m/s^2.

4 AEROMAGNETIC DATA ACQUISTION, PROCESSING AND COMPILATION

4.1 Introduction

Aeromagnetic anomalies are due to variations in the Earth's magnetic field caused by the uneven distribution of magnetic minerals (primarily magnetite) in the rocks that make up the upper part of the Earth's crust. The features and patterns of the aeromagnetic anomalies can be used to delineate details of subsurface geology including the locations of buried faults, magnetite-bearing rocks, and the thickness of surficial sedimentary rocks (which are generally non-magnetic). This information is valuable for mineral exploration, geologic mapping, and environmental studies.

As part of the Natural Resources Authority (NRA) continuing program to provide basic geological and geophysical data for better understanding of the total geological environment of Jordan and to establish a basic framework for evaluating natural resources potential, the NRA contracted with Phoenix Corporation to provide airborne magnetic survey for the entire area of Jordan.
A total of 378,622 aeromagnetic stations were used (Figure 9), to produce the total field aeromagnetic anomaly map of Jordan (Figure 10).

4.2 Data acquisition

Fall 1979, a total of 54,185 line kilometres of aeromagnetic data were flown by Phoenix Corporation (Figure 9). The survey, which covered the entire Kingdom of Jordan, was divided into three areas:

- Area A, a magnetic survey area, covering Wadi Araba in the rift and the highlands east of the rift, including the outcropping basement rocks of the southern mountains. The flight highs varied between 1500-2000 meters above sea level, depending on the topography beneath the flight line.
- Area B, a survey altitude of 120 meters was maintained except over a small section in the northwest corner where rugged topographic features. Line spacing for area A and B is 1km.
- Area C, a magnetic survey area, covering the largest portion of Jordan (The desert part), survey altitude was 120 meters. Line spacing for this part was 2km.

Doppler navigation was employed in addition to visual navigation through the use of topographic map flight strips, airborne magnetometer (Geometrics Model G803) proton precession magnetometer with sensor mounted in a tail stinger. The magnetometer resolution was 0.5 gammas with a sampling interval of 1.0 second.
In 1996, NRA dumped the data from old large tapes to the recent storage media. The author found that there is an obvious shift of about 50 meters between the location of north-south tie lines and the east west survey lines. The shift caused in some places 30 nT in the total intensity of the magnetic field. It was removed from the data using the SURFER software; as a result a very strong signal of the rift was recorded.

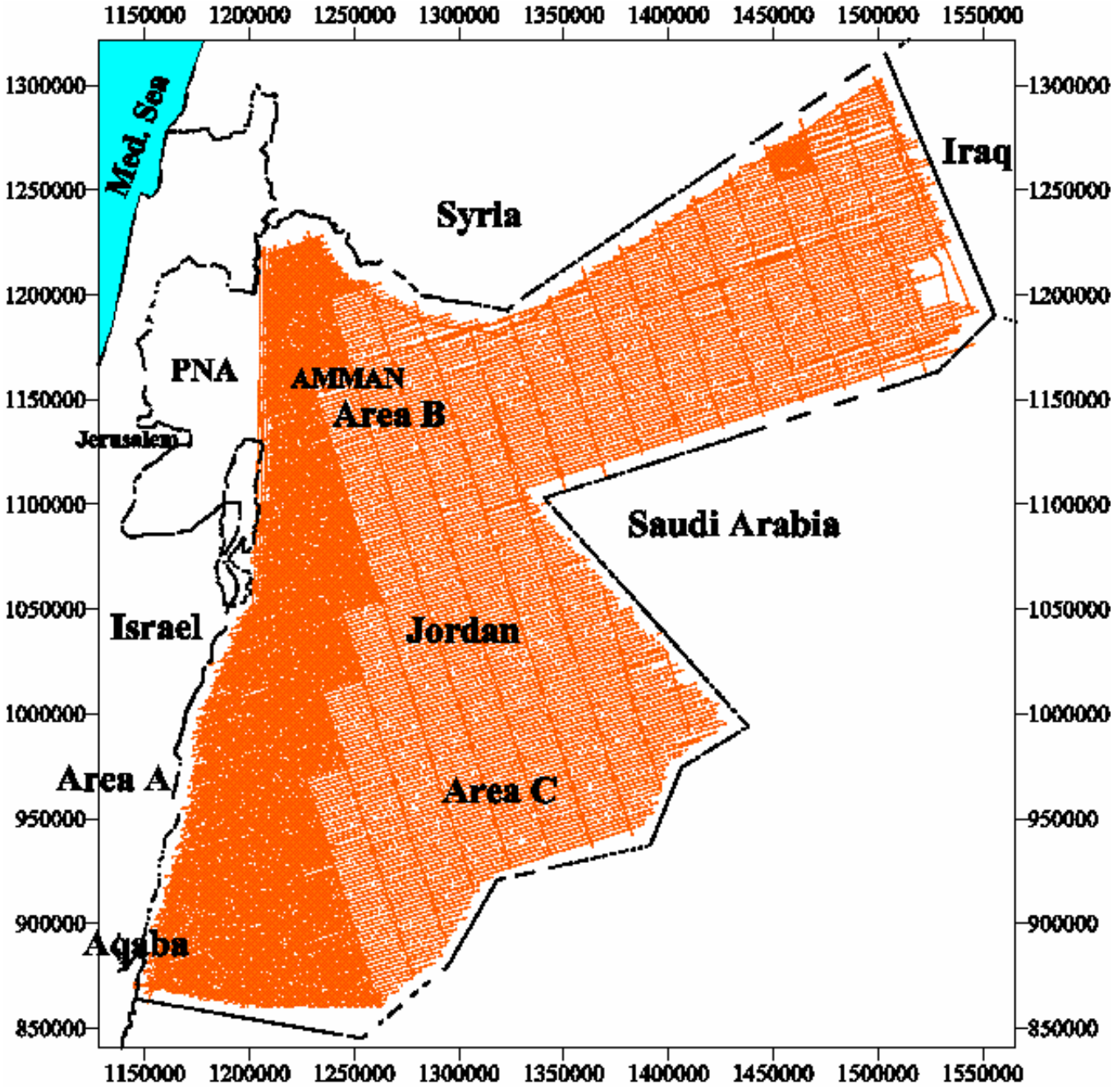

Figure 9: Location of the flight lines of the aeromagnetic surveys in Jordan

4.3 Data processing

The digitally recorded doppler data were processed to produce plots on a scale of 1:50,000 of each line. The processing consisted of simply converting the second by second recordings of track direction and distance into x,y coordinates increments and then producing computer based plots on a line by line basis. All positions were converted to Standard International Universal Transverse Mercator (UTM) coordinates. The author converted the UTM coordinates in geographic coordinates as well as to Israeli, Palestine Cassini-Soldner coordinates, in order to fit in the gravity coordinates.

Shaded relief map of the aeromagnetic anomaly of Jordan

The most remarkable result of the shaded relief magnetic anomaly map of total intensity of the Earth's magnetic field for Jordan (Figure 10) is the view of the magnetic signature of the major tectonic elements in Jordan. Karak-Wadi El-Fayha (KWF) fault system, Disi-Mudawara (DM) fault zone, Quwaira fault (QW), Wadi Araba fault (WA), Fuluq fault (F), Rift valley fault (RV) and other important tectonic features (explained in detail in the following chapters) were shown clearly on this map.

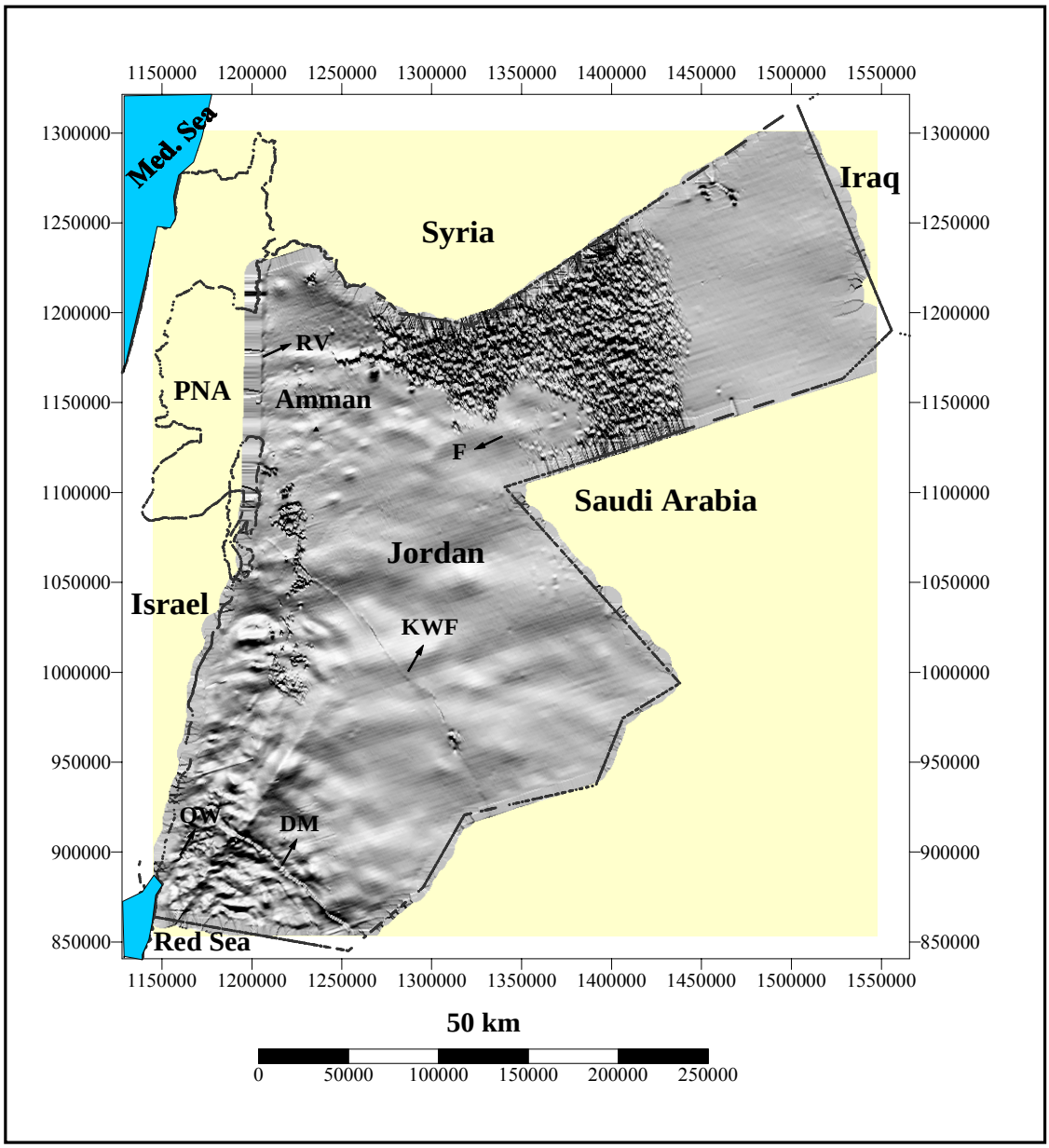

Figure 10: Shaded relief magnetic anomaly map of total intensity of the Earth's magnetic field for Jordan. The light position angles: Horizontal = 90°, vertical = 45°, (illumination from the north). No upward or downward continuation has been used. The abbreviations are: KWF = Karak-Wadi El-Fayha fault system, DM = Disi-Mudawara fault zone, QW = Quwaira fault, F = Fuluq fault, RV = Rift valley fault.

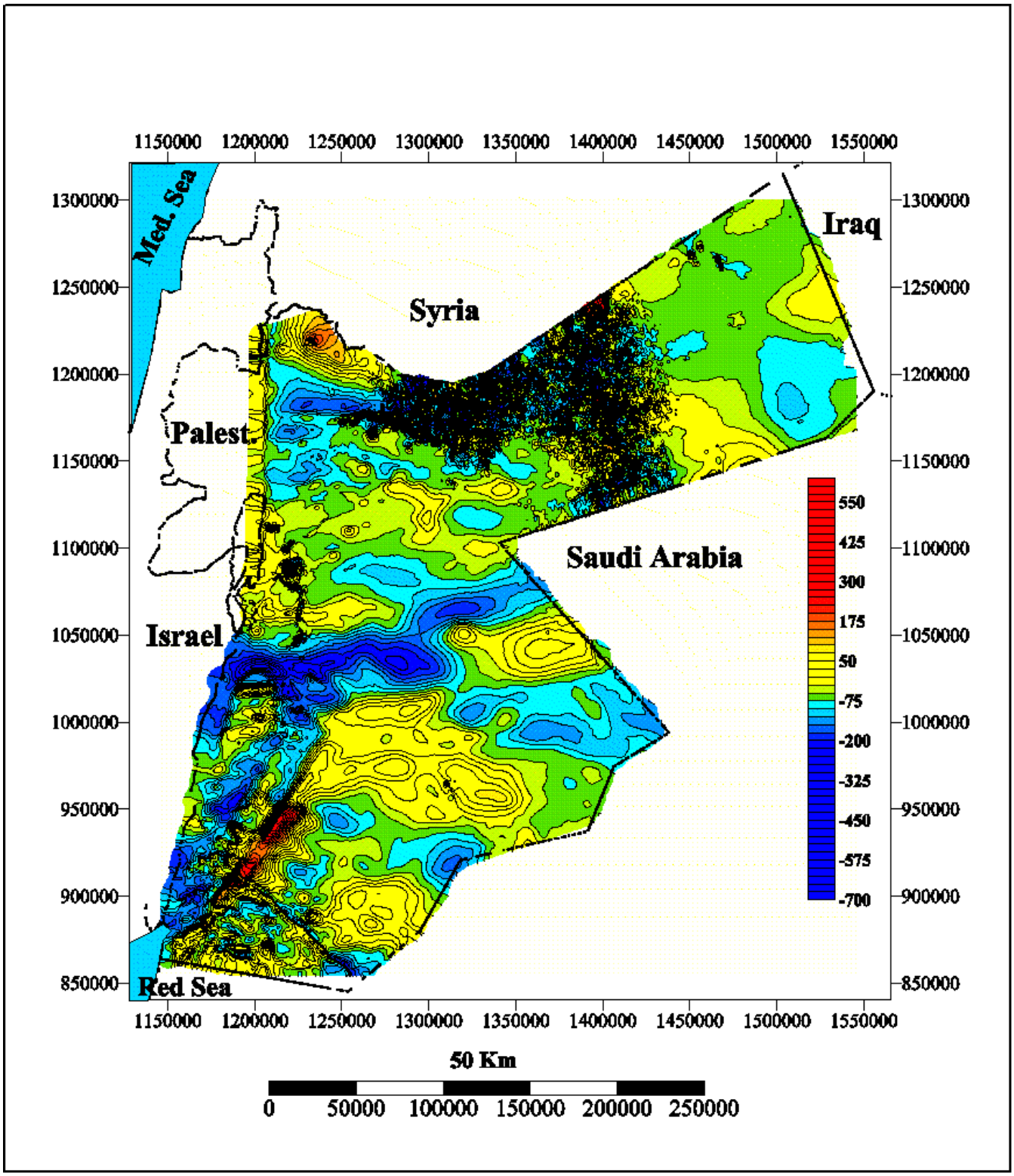

Figure 11: High resolution detailed total field aeromagnetic anomaly map of Jordan, contour interval 25 nT. Coordinates in Cassini - Soldner grid (Palestine + 1000000 m). IGRF was removed.

4.4 Removal of magnetic signal over the basalt flows

The high frequency signal associated with the basalt flows in northern Jordan dominates the magnetic anomaly map (Figures 10, 11) and inhibits qualitative and quantitative interpretation in the region. If we consider the fact that this is a high frequency signal associated with a surficial source then the lower frequency signal associated with basement, and contained in the data but obscure by a higher frequency signal, can be extracted by filtering techniques. High frequency surface signal decays rapidly at higher altitudes.
The data over the volcanic field was filtered by convolution with a set of coefficients derived from an upward continuation operator (utilizing the SURFER software). The convolution operation in the space domain is given by:

$$H(X,Y)=\sum_{\lambda=-x/2}^{x/2}\sum_{\rho=-y/2}^{y/2}\Delta T(x-\lambda,y-P)\ g(\lambda,P)$$

Where $g(\lambda,P)$ is the filter weights. X, Y are the new coordinates after applying the upward continuation operator.

The operator is:

$$O = e-\pi\sqrt{2\mu+2\upsilon}\ h$$

Where μ and υ are the angular frequencies in the x and y directions and h is the level of continuation in data intervals.
For the data over the basalt flow were continued to a height of 4 km. The result map is shown in Figure 12. This map is very useful for constructing the relative flow thickness map because in the upper continuation process, it was noticed that some portions of the volcanic signal disappeared more rapidly than others.

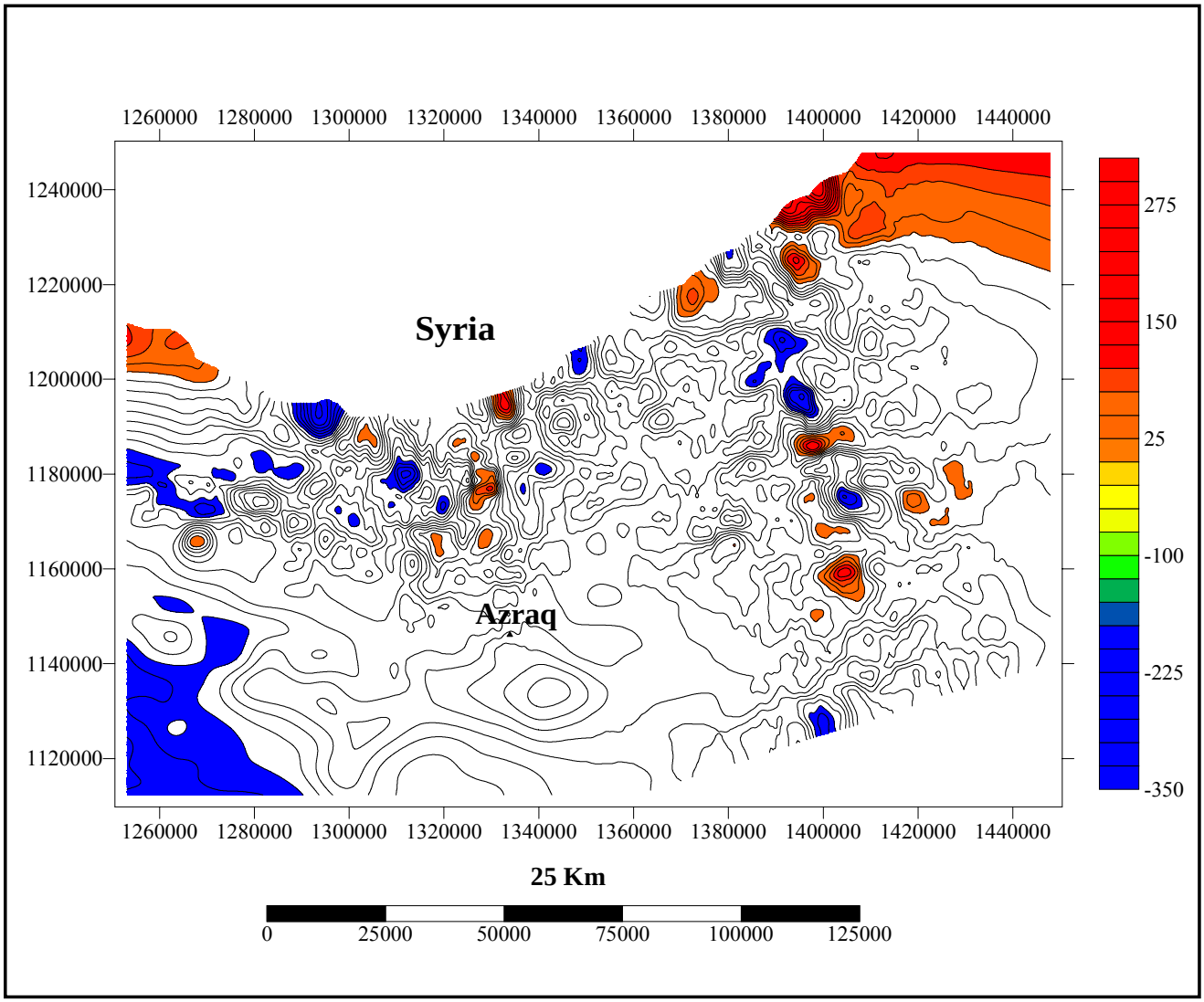

Figure 12: Total field aeromagnetic anomaly map over the Quaternary basalt flow, data upward continued to 4 km. Red areas are the epicentres of the volcanoes.

4.5 Data base compilation

The aeromagnetic survey data over Jordan were collected at different elevations as noted in Figure 10. In order to avoid problems in the interpretation, the data were numerically upwarded to a constant elevation of 2 kilometers. This was accomplished using various spectral techniques (Tsay, 1975, 1976, and Courtillet, et al., 1974) on the individual flight tracks.
In 1998, Jordanian and Israeli aeromagnetic data were merged and unified to one digital data file for the two countries that divide the Dead Sea basin.

4.6 Strike-slip left-lateral motion on the Dead Sea rift

The aeromagnetic anomaly map of Jordan, Israel and Palestine (Rybakov and Hassouneh 1998) (Figure 13) shows obviously the left-lateral movement (LLM) along the Dead Sea rift (DSR). The rate of this movement is 105-107 km, which was calculated according to the same low magnetic value and stratigraphy of the mineral deposits of copper-manganese in Timna (west of the rift, Israel) and in Finan (east of the rift, Jordan). Many authors have described the consequences of this strike-slip motion since 1869. They have suggested that the lateral motion on the DSR occurred during two different episodes. In this scenario there was ~65 km of movement during the Early - Middle Miocene, with the remaining ~42 km in the time period from earliest Pliocene until present.
Lartet (1869) was the first who suggested shift of the Palestine-Sinai sub-plate relative to the Arabian plate of 160 km towards south.
Quennell (1959) suggested 107 km LLM of the plates bordering the DSR. He estimated that the LLM based on the recognition of offset of late Neoproterozoic to Tertiary stratigraphic markers and on similarity of tectonic elements on both sides of the rift.
Freund (1965) assumed 60-80 km sinistral movement along the rift since the late Cretaceous, accompanied by northeast drifting of the Arabian plate.
Freund et al. (1968, 1970) found that all the pre-Tertiary sedimentary and igneous rocks as well as structures and mineral deposits on the eastern side of the DSR are shifted 105 km to the north relative to those on the western side of the rift.
Bender (1970) cites dip-slip motion on hundreds of faults and states that field evidence for strike slip motion is difficult to find, and where observed tends to be very slight compared to dip-slip motion (a few meters for the former compared with up to 1000 m for the latter). He suggests that all strike slip motion is secondary to the major dip-slip motion on the rift.
Zak and Freund (1970) reported actual horizontal displacements of Miocene units.
Ben Menahem et al. (1976) were the first to present geophysical evidence for LLM along the DSR from a study of local and regional earthquakes.
Garfunkel (1989) calculated 105 km of LLM on the DSR according to good matching of the known geologic features across the transform like the lithologic belts in the basement, facies and thickness changes in the Phanerozoic sedimentary cover, lines of erosive truncation, and major structures in the rift.
Barjous and Mikbel (1990) deduced 40 km sinistral offset along the Quweira Fault from the displacement of andesitic rocks.

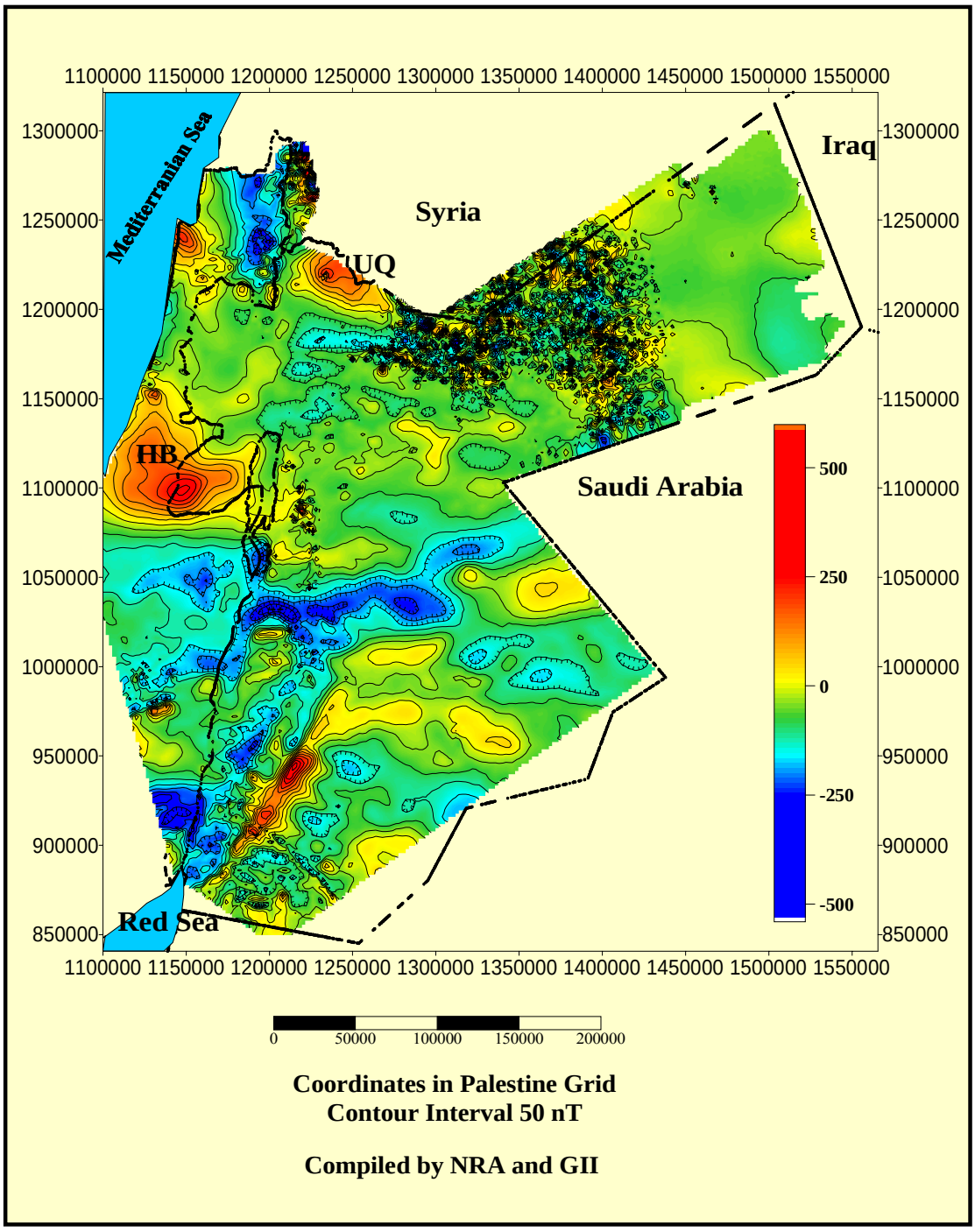

Figure 13: Total-Intensity compiled Aeromagnetic anomaly map of Jordan, Palestine and Israel showing the movement of the Arabian plate (eastern block) northward relative to the African plate (western block) about 107-109 km along the Dead Sea Rift. Note that Um Qeis (UQ) and Hebron (HB) used to be one structure.

5 INTERPRETATION OF THE GRAVITY AND AEROMAGNETIC DATA OF JORDAN

5.1 Introduction

The goal of the present gravity and magnetic data interpretation is to provide a new picture of the subsurface geology that will contribute to the analysis of exploration for hydrocarbons, minerals and water resources. Qualitative interpretation of gravity anomalies describes and explains the location, shape and magnitude of these anomalies. A reduction of gravity data using accurate rock densities is required for this purpose. The term anomaly is used to refer to a particular gravity feature that occurs on a map or profile which differs from the surrounding gravity or magnetic values.

5.2 Qualitative Interpretation and general discussion of the gravity anomaly map of Jordan

Bouguer anomaly map of Jordan Figure 5 shows that the main dominant tectonic feature in the region is the Dead Sea Rift (DSR). The Bouguer values range from +2 $.10^{-5}$ m/s^2 over A'jlun area to less than – 132 $.10^{-5}$ m/s^2 in the central part of the DSR. The gravity gradient from A'jloun (northern highlands) to the Jordan River in the rift valley is 4.10^{-5} m/s^2 /km, but this gradient is 8.10^{-5} m/s^2 /km between Karak Castle and the Lisan Penunsuila of the central part of the DSR. In this region, the contours of the gravity anomaly are trending north-south.
Along the DSR itself the Bouguer anomaly field is characterized by a serious of negative gravity closures (could be basins) with different size, shape and depth. The basins, generated as a result of the relative plate motion and fault geometry, are detected in the gravity field because of the low density of their fill (2000-2200 kg/m^3 relative to the surrounding rocks (2500-2670 kg/m^3) (tenBrink, et al., 1993; tenBrink, et al. 1999). The amplitude of Bouguer anomaly decreases from Lake Tiberias to the central part of the Dead Sea Basin (DSB). The amplitude at Lake Tiberias is $–15.10^{-5}$ m/s^2, at Bet She'an basin (30 km south of Tiberias) is $–24.10^{-5}$ m/s^2 , at Damia basin (50 km south of Bet Shea'an basin) is $–30.10^{-5}$ m/s^2, at Jericho basin (20 km south of Damia basin) is $–35.10^{-5}$ m/s^2 and at the central part of the DSB the amplitude of Bouguer anomaly is $–132.10^{-5}$ m/s^2. The decreasing amplitude of Bouguer anomaly from north to the central part of the DSB indicates a considerable increase of crustal and/or sedimentary thicknesses in this direction (more detail in the 3D modelling, chapter 9).

The high structure on the central part of the gravity map indicates a shallow high density limestone or dolomite. This structure was surveyed by Fina Oil Company in 1989. The seismic shows no anticline exist below this structure (Figure 14).

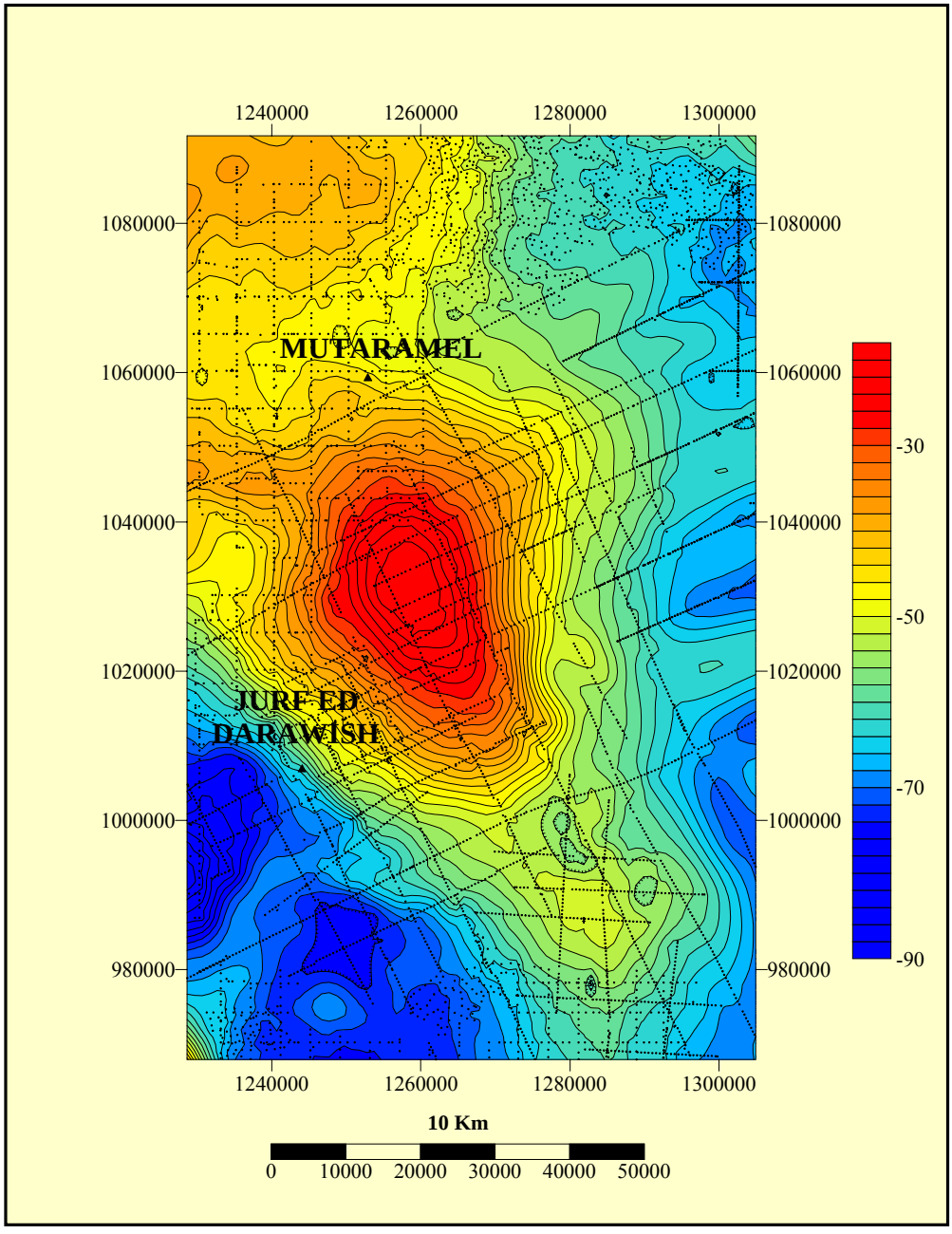

Figure 14: Gravity map of the central part of Jordan shows the high gravity structure at the central part of the gravity anomaly map of Jordan. Contour intervals 2×10^{-5} m/s^2.

In southern Jordan, where Precambrian rocks crop out and are intruded by dykes, the gravitational field correlates with the magnetic anomaly and both delineate 4 major fault zones: Disi-Mudawara (DM) fault zone striking SE-NW, Quwaira (QW) fault zone striking north, Ma'an (MA) fault striking NE-SW and Wadi Araba (WA) fault striking SSW-NNE (Figure 15). These fault zones are called Aqaba - Araba complex.

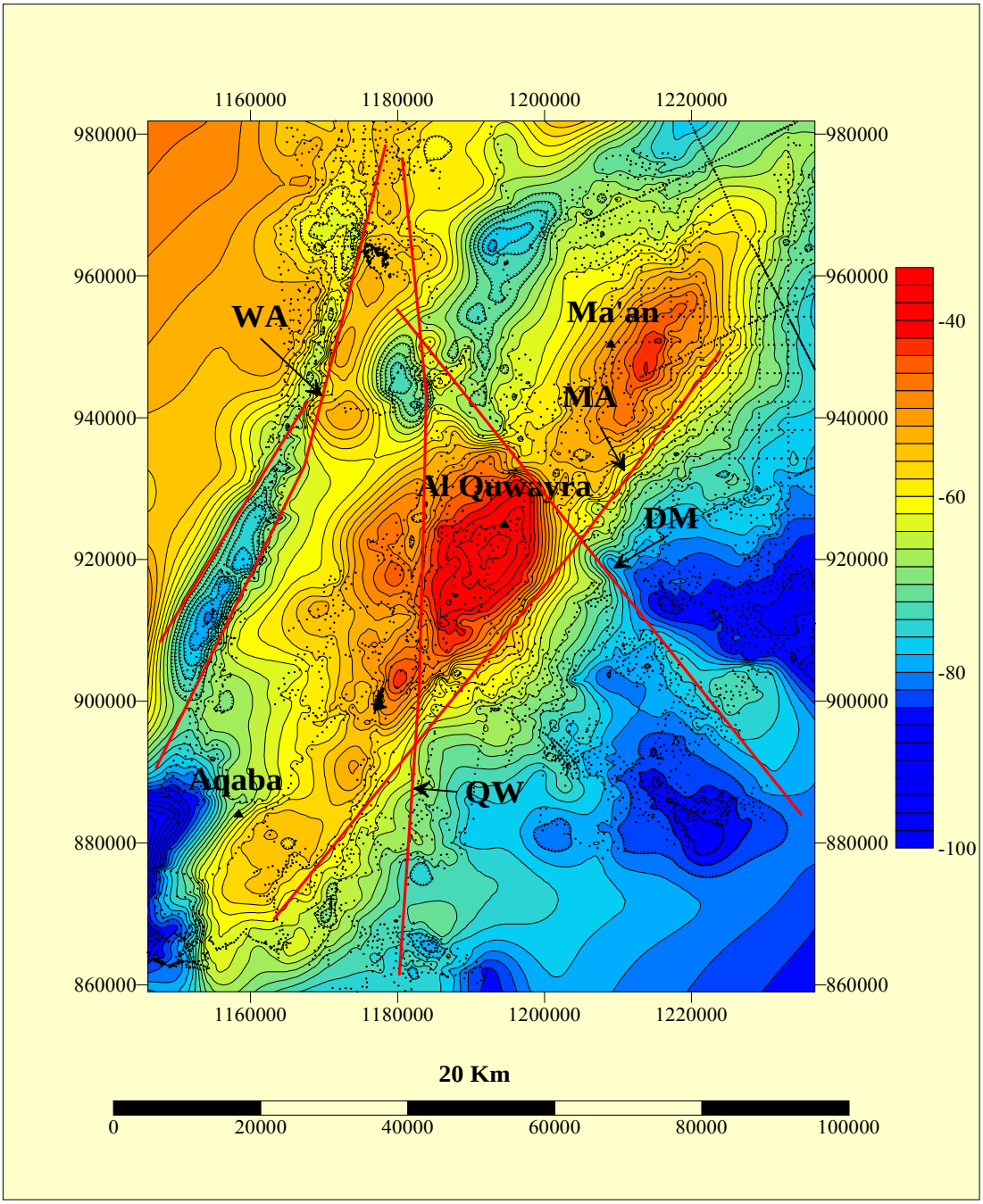

Figure 15: Gravity map of the southern part of Jordan shows 4 major fault zones in the area. Disi-Mudawara (DM), Quwaira (QW), Ma'an (MA) and Wadi Araba (WA) fault zones. Contour intervals 2×10^{-5} m/s^2.

Further northeast of this anomaly at El i'nab (Wisad) area, a very low gravity structure -96.10^{-5} m/s^2 exists. This low structure could be attributed to basement depression (resulting from a major subsidence of the basement). It is very important for oil exploration in future because of its great thickening of sediments.

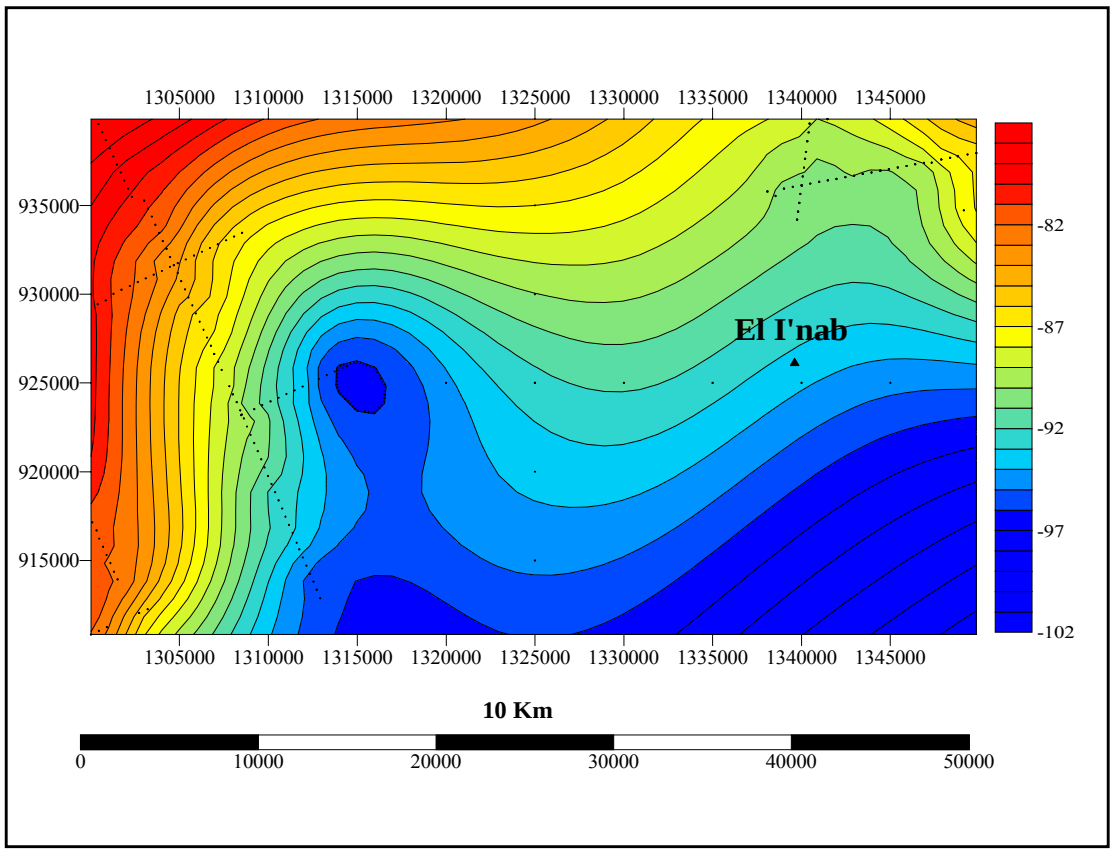

Figure 16: Bouguer anomaly map of Al I'nab area in the southern part of Jordan shows the low structure (could be attributed to basement depression) in the area. Contour interval 1.10^{-5} m/s^2.

Further north east of Al I'nab anomaly in al Sirhan area, Figure 17 shows the east portion of Swaqa fault zone. This fault formed two high structures which could form be an anticline structures in Wadi Huseidat Um Ghudran and Qasr Tuba and formed two low structures could be basement depressions in Wadi El Ghamr and Bayir.
The large high and low structures in this area are very important for oil exploration in Jordan in future.

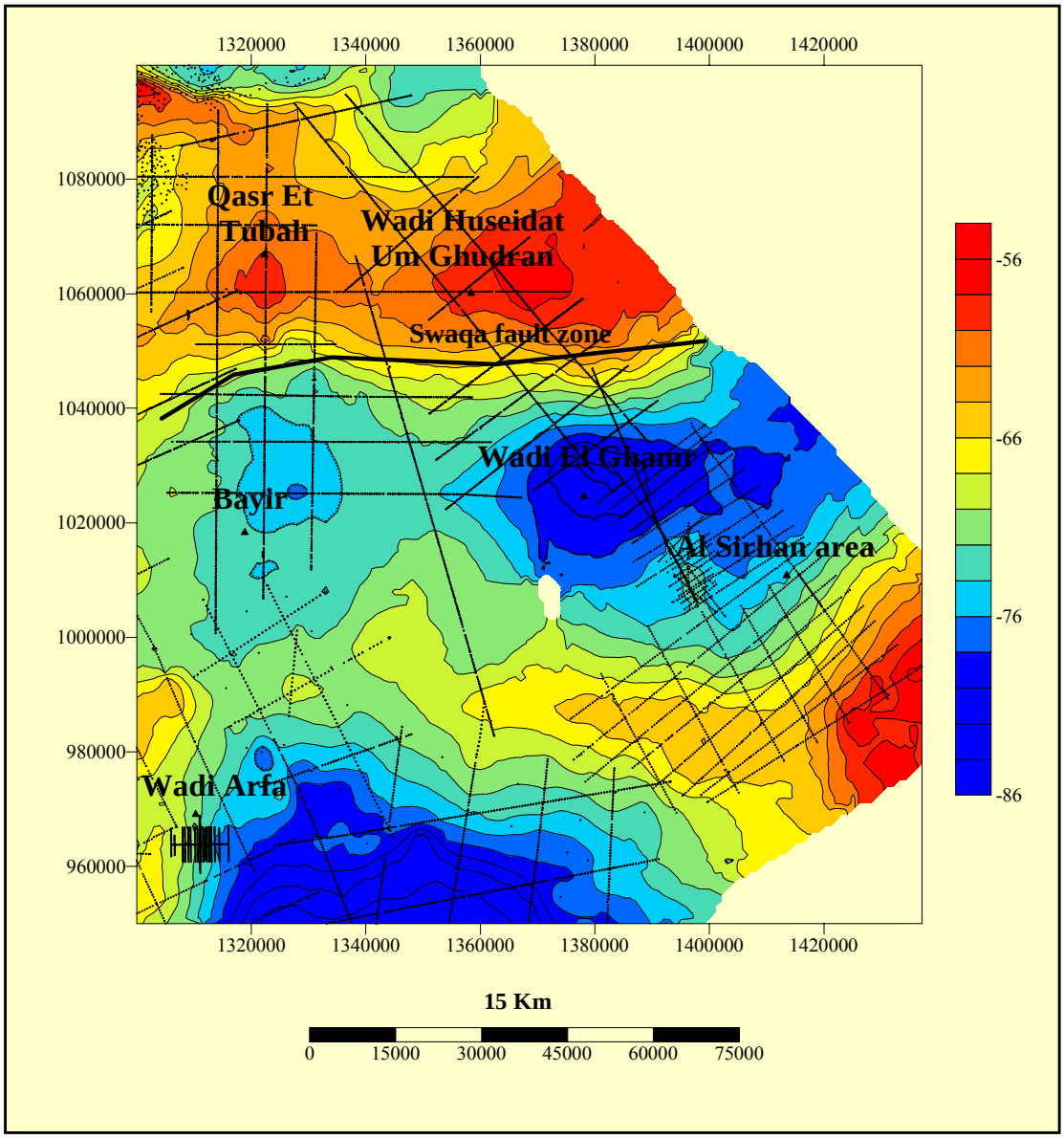

Figure 17: Bouguer anomaly map of Al Sirhan area in the southern east part of Jordan showing two high structures could be anticlines in Wadi Huseidat um Ghudran and Qasr Et Tuba, and two low structures which could be basement depressions in Wadi el Ghamr area and Bayir. Contour interval 2.10^{-5} m/s^2.

In the neighbourhood of El Risha gas field (Figure 18) the large low structure could be attributed to basement depression in Wadi El Athna at the Iraqi border and the two high structures, in Wadi Mudeisis and in Wadi Judhei', could be interpreted as anticlines or major relief on the magnetic basement. The low structure has been tested by several drill holes, a gas field was found in that area.

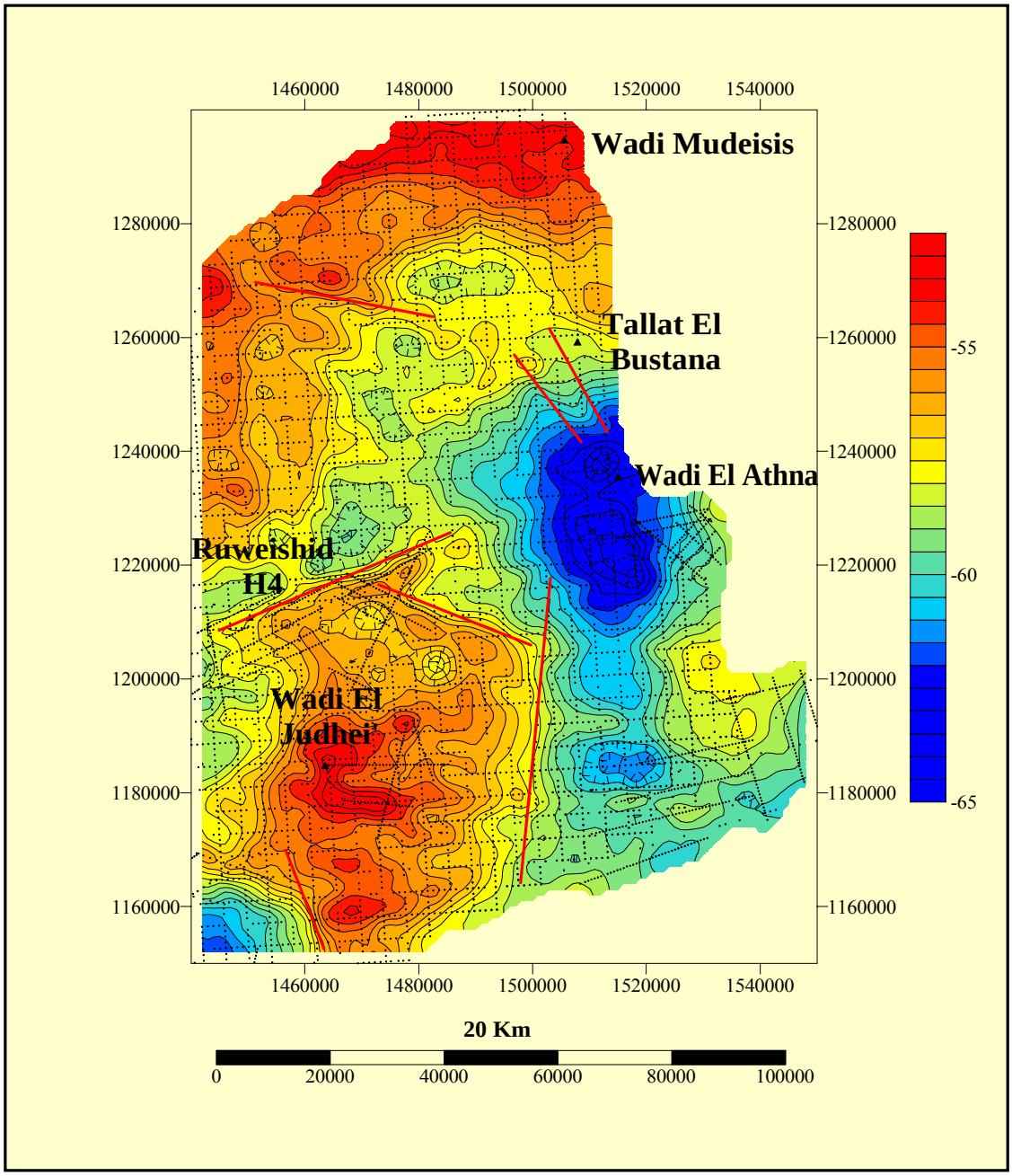

Figure 18: Bouguer gravity anomaly map of the Risha gas field area showing large low structure at Wadi el Athna which could be as a basement depression. Contour intervals 0.5×10^{-5} m/s^2.

In the middle of Harat Al Sham basaltic plateau, at Wadi El Abd area, the gravity map (Figure 19) shows a high structure (H1) which can be interpreted as a horst structure and as two low structures L1 and L2; one to the north of the horst structure along the Syrian borders and the second to the south of the horst structure along the Saudi Arabian borders. This suggests that considerable thickness of sediments exist under the basaltic plateau along the Syrian and Saudi borders. According to this, it is assured that this area is very important for future oil exploration in Jordan. To the west of the previous structures, the Fuluq fault zone, a major NW-SE fault stretching from the basalt plateau along Jabal Qirma and continuing into Saudi Arabia, as obviously shown on the gravity map. This fault has a downthrown of 3-4 km to the southwest with a high gravity gradient. This fault could have formed the Al Azraq basin.
To the southwest of the Al Fuluq fault zone, a large low gravity structure exists (L3). This structure is Al Azraq depression. To the northwest of this fault, a large high gravity structure (H3) exists to the west of the Safawi and extends until Qasr El Hallabat. This structure could be interpreted as an anticline or as a horst structure.

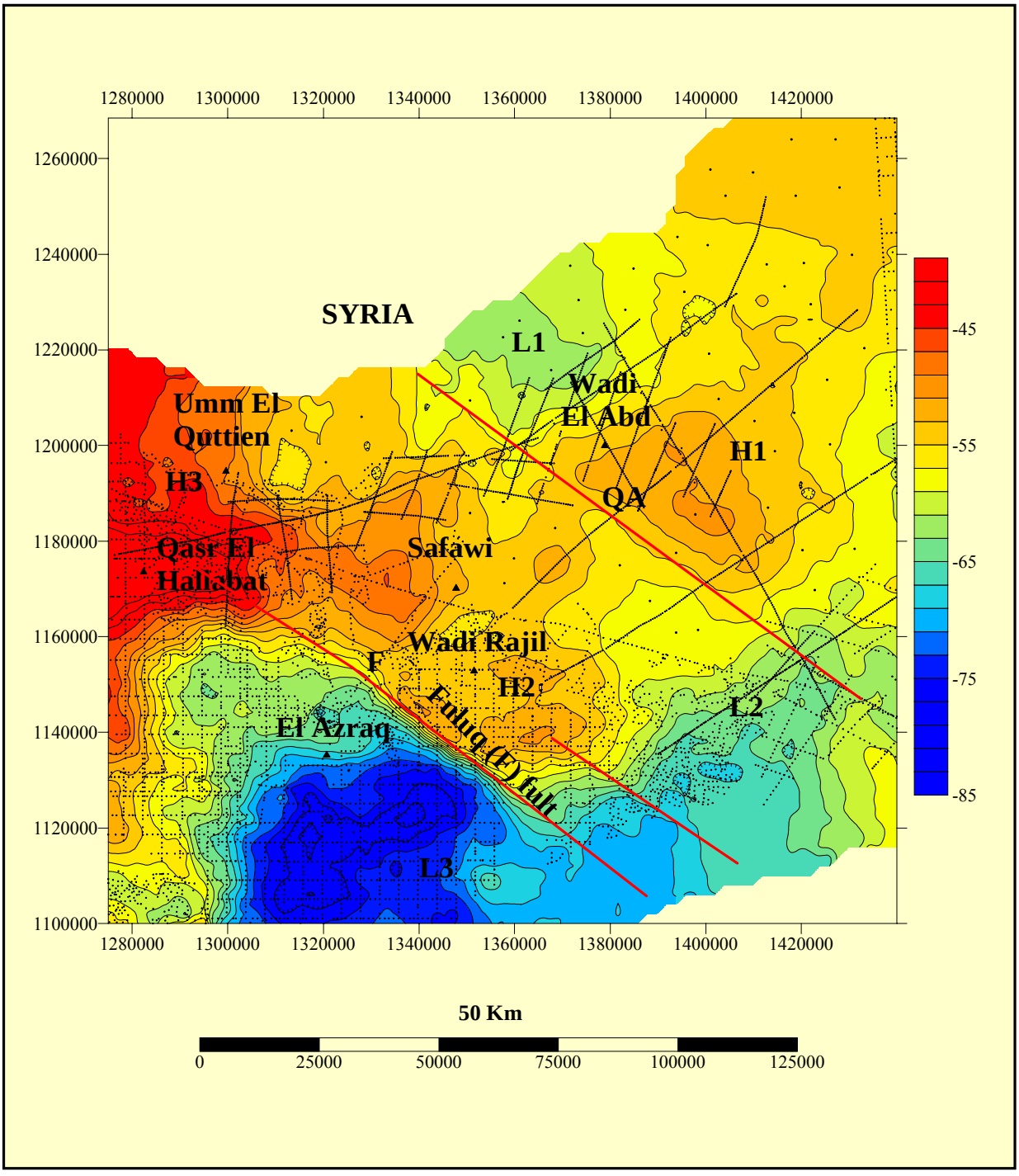

Figure 19: Bouguer gravity anomaly map of the basaltic plateau (Harrat El Sham). The abbreviations are: L1, L2, L3 = low gravity structures, interpreted as basement depression and H1, H2, H3 = high gravity structures which could be interpreted as anticlines or horst structures. QA = Qitar Al A'bed fault zone, F = Fuluq fault zone. Contour intervals 2×10^{-5} m/s^2.

In northern Jordan, an anticlinal structure called A'jlun dome is shown in Figure 20. This structure has the highest gravity value observed on the gravity anomaly map of Jordan (+ 2.10^{-5} m/s^2**)**. This high gravity could result from the high density Permian carbonates. Several lineaments interpreted as faults trending N-S (Rift faults), NW-SE and NE-SW are clearly seen on the map (Figure 20). Other small closures with

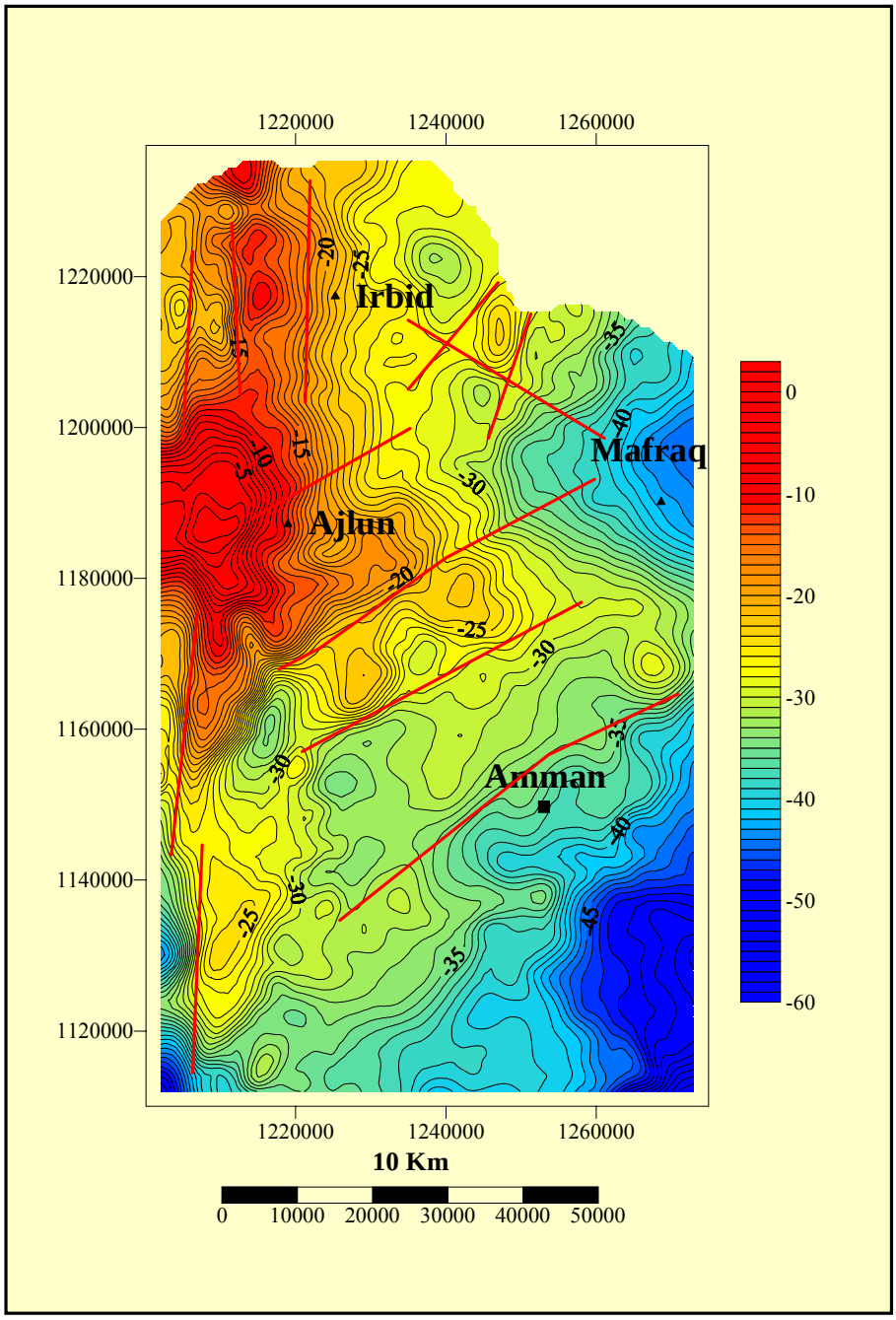

Figure 20: Bouguer gravity anomaly map of northern Jordan showing A'jlun Dome structure and several lineaments interpreted as faults striking N-S, NE-SW and NW-SE. Contour intervals 1×10^{-5} m/s^2**.**

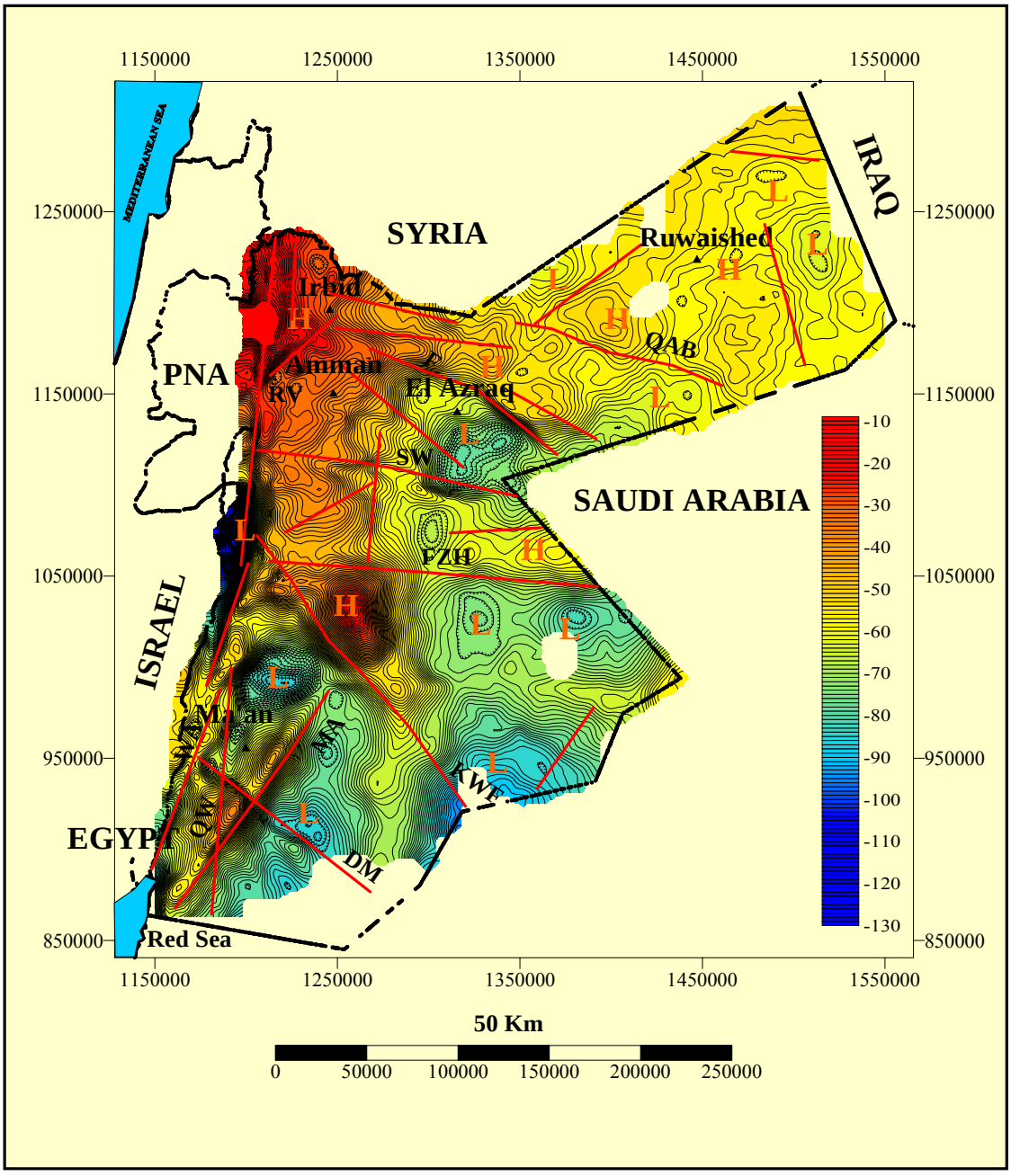

Figure 21: Generalized interpretation of the complete gravity anomaly map of Jordan showing major tectonic features in Jordan. The abbreviations are: DM = Disi-Mudawwara fault zone (FZ), QW = Quwaira FZ, WA = Wadi Araba fault, MA = Ma'an fault, KWF = Karak Wadi El Fayha FZ, FZH = Finan Zukimat Al Hasa FZ, SW = Swaqa FZ, QAB = Qitar El A'bed FZ, RV = Rift Valley strike-slip fault. Contour intervals 2×10^{-5} m/s^2.

5.3 Qualitative interpretation and general discussion of the aeromagnetic anomaly map of Jordan

The magnetic map Figure 7 reflects the basic structures of the geology of Jordan.
The total field aeromagnetic anomaly map is dominated by high frequency signals associated with the basalt flows in northeast of Jordan. The large area of Quaternary basalt and several areas of Quaternary mafic rocks in central western and southern Jordan east of the Dead Sea rift produce a strongly contrasting pattern of short wavelengths, high frequency anomalies of low amplitude. This is related to surface highly magnetic mafic rocks.
The high frequency signals are associated with surficial sources and the lower frequency signals are associated with basement. Gridded data in the area of the volcanic field was filtered by a convolution using Surfer upward continuation operator (Figure 12). The high frequency surface signal decays quite rapidly and thus is reduced at higher altitude. The aeromagnetic data continued upwards to a height of 3-4 km by Matrix Smoothing which is most effective for removing noise or small-scale variability in the grid (for more details see chapter 4.4).

In southwestern corner of the magnetic map, the basement rocks cropping out are responsible for most of the magnetic anomalies in addition and 2 major fault systems seem to correlate nicely with the magnetic pattern in this region Figure 13:

- Disi-Mudawara(DM) fault zone striking NW-SE. It associated with Quaternary basalt flows.
- Quwaira (QW) fault zone, striking N-S, where the Paleozoic sandstones are brought in contact with the crystalline basement rocks along this fault.

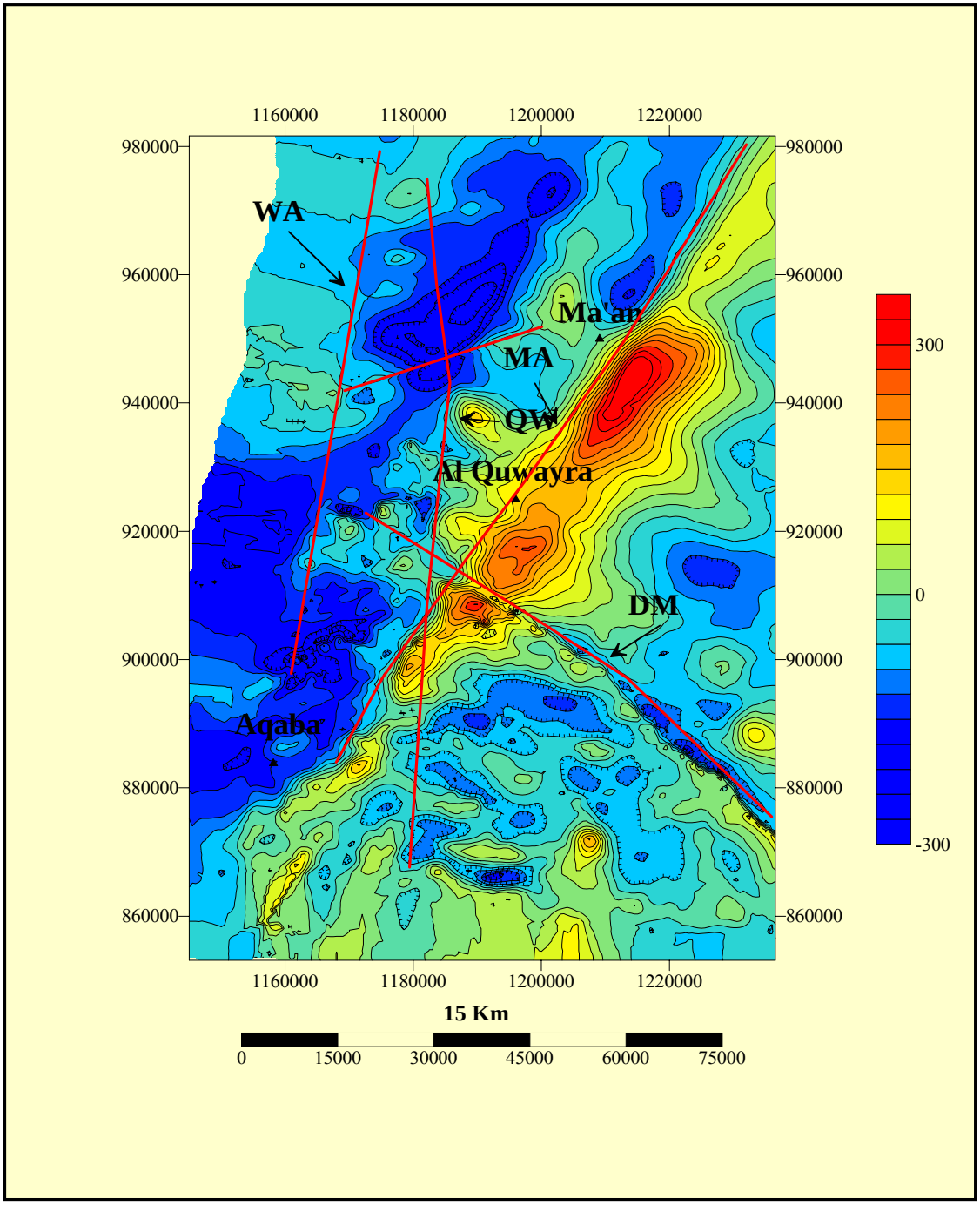

Figure 22: The total field aeromagnetic anomaly map of the southern part of Jordan shows 4 major fault zones: Disi-Mudawara (DM), Quwaira (QW), Ma'an (MA) and Wadi Araba (WA); Contour Interval = 30 nT.

Other major tectonic features clearly shown on the magnetic map (Figure 24):

- Karak-Wadi El-Fayha (KWF) fault system. This fault system consists of a serious of faults striking NW-SE forming horst and graben structures and crossing the country from the Dead Sea to several hundred kilometers in Saudi Arabia. The length of this fault zone in Jordan is about 200 km. Portions of this major fault zone correlate very strongly with a set of very small NW-oriented interruptions in the large EW-dominant anomalies in south-central Jordan Figure 13.
- The Swaqa (SW) fault striking E-W and crossing the country from the Dead Sea to Saudi Arabia borders.
- Finan-Zukimat al Hasa (FZH) fault zone striking E-W.
- Fuluq (F) fault striking NW-SE, on the west side of the basaltic plateau.

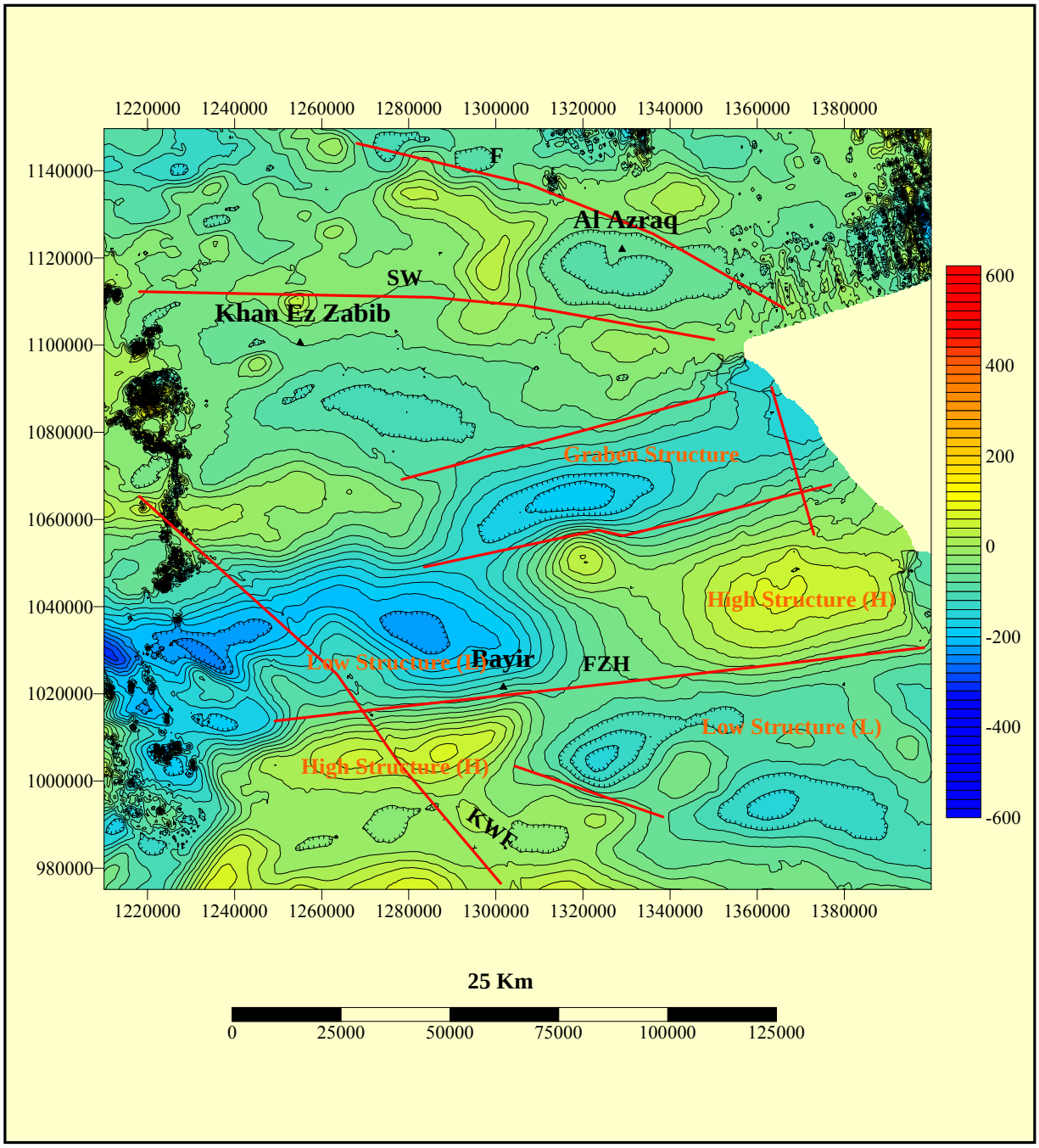

Figure 23: Total field aeromagnetic anomaly map of the central part of Jordan showing 4 major fault zones in the area: Karak-Wadi Al Fayha FZ (KWF), Finan-Zukimat Al Hasa FZ (FZH), Swaqa FZ (SW), and Fuluq fault (F); contour Interval = 20 nT.

Small size local anomalies (Figure 10, 11, 12 and Figure 22) are very common on the magnetic map. Some of these seem to be in positive and negative pairs such as in southwestern Jordan where Precambrian rocks crop out in Wadi Araba, along the north part of the DSR, along the Al Karak-Wadi Al Fayha fault zone, along Swaqa fault zone, along al Fuluq fault, in Amman, in Zarqa and many in the basaltic Plateau over the volcanoes centres. These anomalies could be caused by intrusives and shallow magnetic bodies.

Large size closures could be caused by large intrusions above the basement as shown on the magnetic map such as the two closures on the central part of the magnetic map, along Quwaira fault zone, in Wadi El Ghamr at Saudi Arabia borders and at the far south-eastern corner of the map.

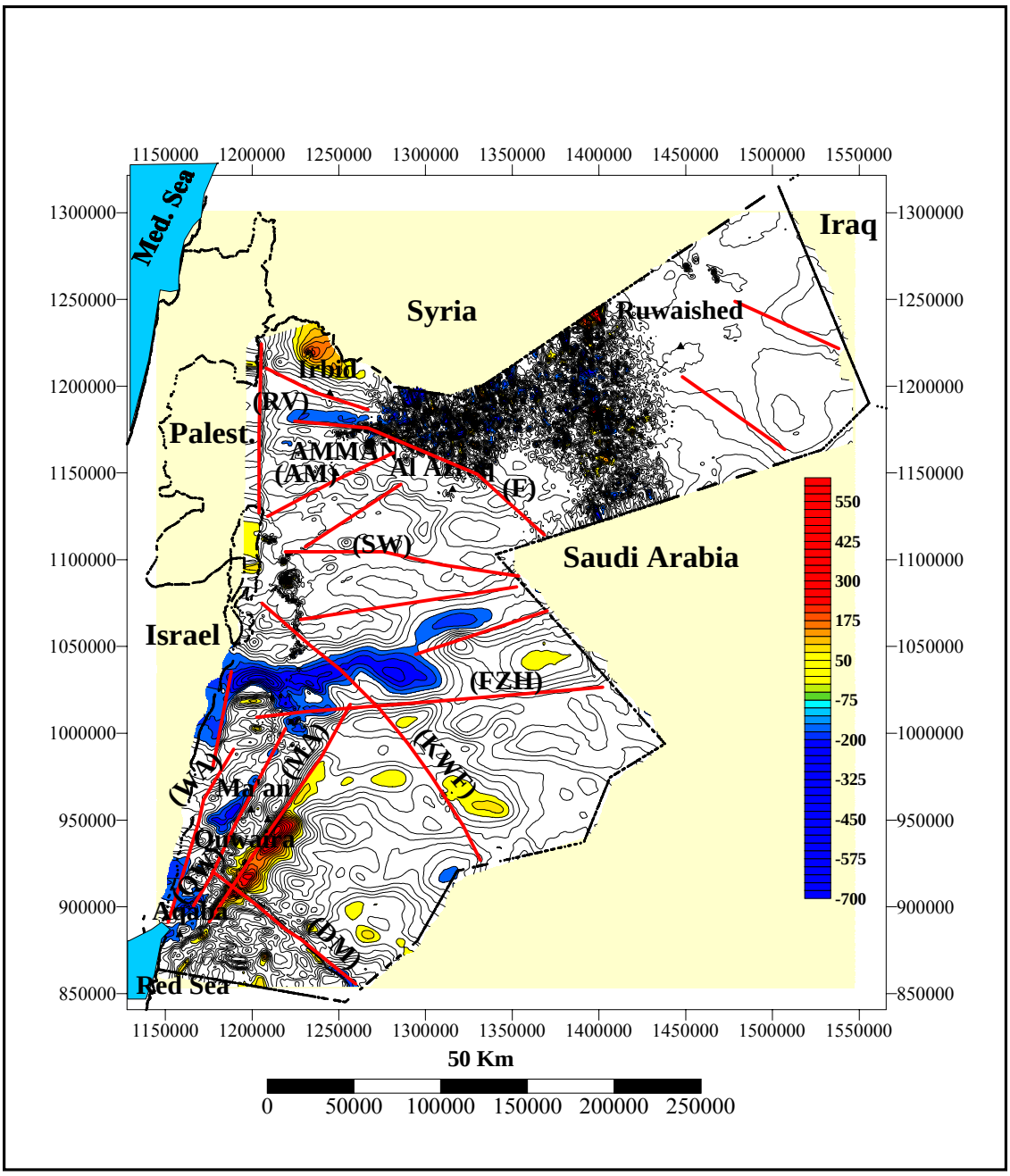

Figure 24: Generalized interpretation of the total field aeromagnetic anomaly map of Jordan. The abbreviations are: DM = Disi-Mudawwara fault zone (FZ), QW = Quwaira FZ, WA = Wadi Araba fault, MA = Ma'an fault, KWF = Karak Wadi El Fayha FZ, FZH = Finan Zukimat Al Hasa FZ, SW = Swaqa FZ, RV = Rift Valley strike-slip fault; contour interval 25 nT.

5.4 Comparison of gravity anomaly, aeromagnetic anomaly and structural geology map of Jordan

Many major fracture systems on the gravity and magnetic maps are correlating strongly with the structural geology map of Jordan published by Bender (1974) Figure 25. Tectonic features traced from the gravity and aeromagnetic anomaly maps are shown on Figures 21, 22, 23, and Figure 24.
In southwestern Jordan, the Disi-Mudawara (DM) and Quwaira (QW) fault zones in the crystalline basement rocks are correlating nicely with the structural map of Jordan.
The intrusive and extrusive units; gneisses, schists gabbros, diorites, granites, etc., along these faults are strongly magnetized and are characterized by high density contrast with the surrounding rocks. The intrusion of the dykes in the Neoproterozoic crystalline basement rocks reflect the tectonic activity at the end of the Neoproterozoic. Planes of structural contacts between dykes and basement are reactivated during the Cenozoic tectonic activity (Bender, 1968). This can be inferred from the linear contacts with the Neoproterozoic crystalline basement rocks and the development of veins along these dykes. The dyke intrusions have been dated between 560 Ma and 570 Ma (Ibrahim and Mc Court, 1995). The thickness of these dykes reaches up to 25 m; they were observed in two locations, north of Quwaira village and north of Ad Disi village.

In southwestern Jordan, Wadi Araba fault can be seen in the gravity map and correlates with Bender's structural map. This fault is the southern segment of the Dead Sea rift. It extends from the Gulf of Aqaba in the south up to the Dead Sea basin in the north trending NNE. It is responsible for the existence of the Wadi Araba depression and the topographic differences to the east and west shoulders in the rift Figure 6 and 7.

The Karak Wadi al Fayha (KWF) fault zone on the magnetic map corresponds strongly with Bender's structural map. This fault zone trend NW-SE is believed to be of Pre-Cretaceous age (Bender, 1968). The strong magnetic anomalies along this fault could be caused by the basaltic flows associated with it. To the northeast of this fault, in Wadi Al Ghamr area, there is a high gravity and magnetic structure. This structure could be an intrusion or a substantially elevated basement (basement highs).This structure is not seen in Bender's structural map. To the south of this structure and close to the oil exploration well (WS-3) in the Sirhan area, there is a major fault called Finan Zukimat Al Hasa (FZH) fault zone, this fault is very obvious on the magnetic and gravity maps (Figures 21, 23, 24) and correlate nicely with Bender's map. Because of the notable vertical displacement, this fault creates at Bayir and Al Sirhan areas four important structures (Figure 23); two high structures could be interpreted as anticlines or horsts and two low structures which could be interpreted as basement depressions. The downthrown (inclination) of this fault is to the north and has a large horizontal extent reaching around 250 km.
The Al Fuluq (F) fault (Figures 19, 23, 24), with 3-4 km vertical throw, associated with a very prominent gravity gradient due to the very substantial vertical throw across this fault zone, it correlates strongly with a magnetic anomaly and Bender's maps.

The Swaqa (SW) fault striking E -W, is shown obviously on the magnetic maps (Figure 23 and 24), it correlates well with the gravity anomaly. Bender's map shows the western part of this fault correlates strongly with gravity and magnetic maps, but the central and eastern parts of this fault are not seen on Bender's map. This means that

the newly compiled magnetic and gravity data will perfectly coincide with the structural map of Bender.
In the Risha area where the NRA discovered the gas field, the aeromagnetic map Figure 24, shows two very interesting structures separated by a fault striking NW-SE. The low magnetic structure could be interpreted as basement depression and the area of the high magnetic structure (where the NRA discovered the gas), could be interpreted as an anticline. These structures on the magnetic map correlate poorly with the gravity and Bender's structural map.

On the basaltic plateau, the most distinctive structural feature is Qitar El Abid (QA) fault zone (NW-SE) (Figure 19). This fault is associated with basalt intrusions and correlate strongly with the filtered aeromagnetic map (Figure 12) and with Bender's map. According to Bender (1974) the fissure effusions of many kilometres in length are considered to belong to the youngest eruptions and are present as a row of volcanoes (90 km in length). The magnetic map is proving what Bender concluded about this fault zone.
In A'jlun area in the northern part of Jordan, the high anticline structure (Figure 20), correlates very well with gravity, magnetic and structural map of Bender. Finally, gravity, magnetic and Bender's structural map show very strong correlation in the northern segment of the Dead Sea rift (see chapter 6 for more details).

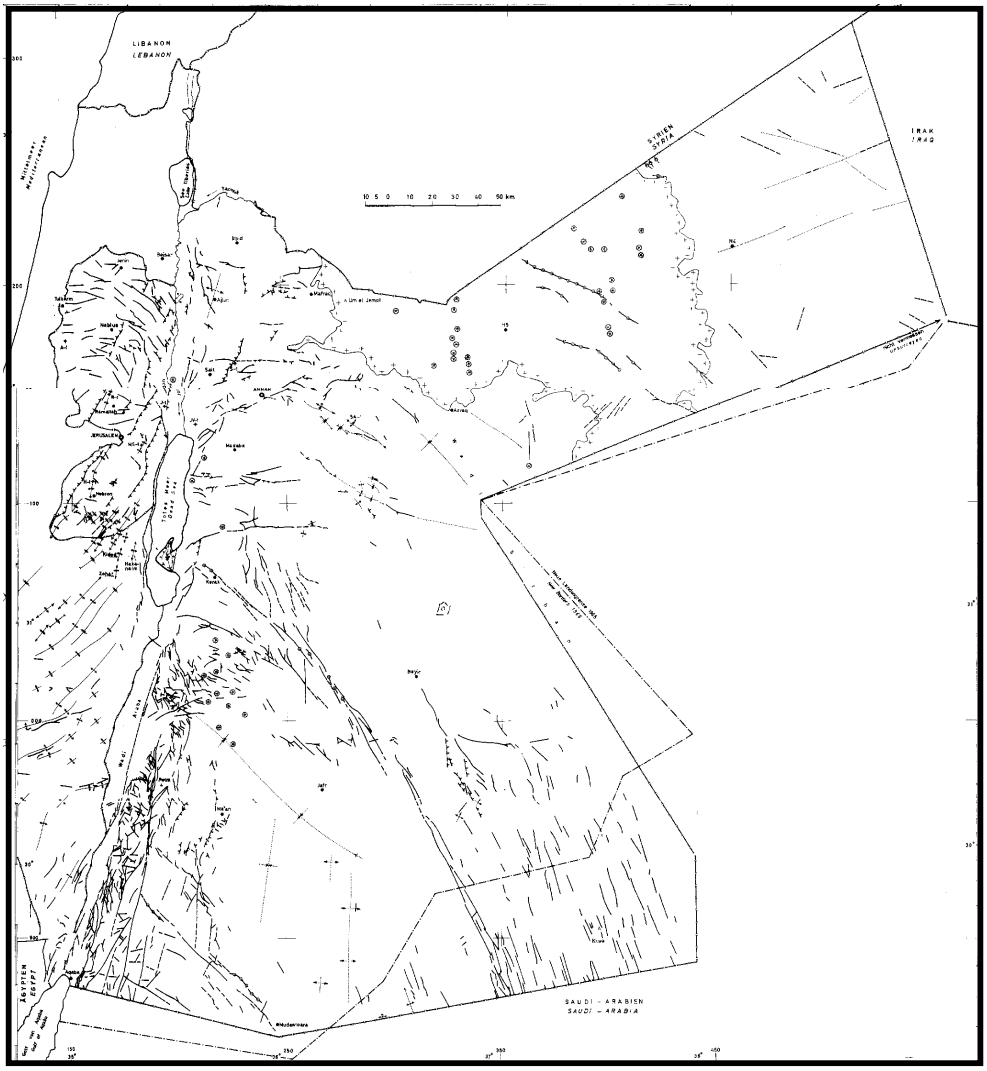

Figure 25: Structural geology map of Jordan. (After Prof. F. Bender, German Geol. Mission in Jordan 1961-1966)

6 INTERPRETATION OF THE GRAVITY ANOMALY DATA IN THE NORTH AND IN THE SOUTH SEGMENTS OF THE DEAD SEA RIFT

6.1 Introduction

The Jordan Rift Valley extends 370 km from the Gulf of Aqaba (Elat) to Lake Tiberias and consists of 3 major segments. The northern segment, called Jordan valley segment, extends from the Dead Sea shore to Lake Tiberias and trends N-S. The southern segment called Araba segment, extends along Wadi Araba and the southernmost part of the Dead Sea and trends SSW-NNE. The last segment is the central Dead Sea basin. The gravity anomaly map of the northern segment of the Dead Sea rift Figure 26 shows the prominent left-slip fault, in addition to some marginal normal faulting (Garfunkel et al., 1981). North of Bet Shean the rift is flanked by volcanic fields of Middle Miocene-Quaternary age. There are several basins with low gravity values which built the northern segment of the Dead Sea: Lake Tiberias, Al Bakura, Bet Shean, Damia and Jericho (tenBrink et al., 1999). The Jericho basin is shallow (800 m deep) asymmetric basin, plunging westward and terminating against a west-dipping strike-slip fault (Rotstein et al., 1991). A buried monocline parallels this segment of the fault on the west and is indicative of local transpressive motion (Rotstein et al., 1991). The Damia basin is a shallow (~ 250 m deep) basin and occupies the central Jordan River Valley. The Bet Shean basin to the north plunges asymmetrically toward the east (Shaliv et al., 1991; M. Gardosh, 1998). The Bakura basin occupies the upper Jordan River valley and extends into the southern Lake Tiberias (Ben-Avraham et al., 1996; Y. Ben-Gai and M. Rezhnikov, 1997). It is narrow (~6 km) and long symmetric basin (Rotstein et al., 1992). The presence of many gabbros and basalt layers explains the small gravity high over this basin.

The Bouguer gravity anomaly map of the southern segment of the DSR (Figure 27) defined very well the major Wadi Araba fault and shows the other structural elements (dykes, joints, anticlines, synclines, major and minor faults) in the area. Aqaba-Gharandal, Wadi Rahma, Gharandal-Abu Burqa, Ras-Al Naqab and many other faults are shown clearly on the gravity map and they are related to the major Wadi Araba fault. The faults are vertical to sub-vertical and show horizontal and vertical movements on their surfaces. From the Gulf of Aqaba (Elat) to about 90 km northward along Wadi Araba fault, there are three basins that become successively narrower and shallower to the north (tenBrink et al., 1999). They include the Aqaba (Elat) basin, which extends from the offshore, the newly discovered Timna (Qa-Taba) basin, which is offset in an en echelon from the Aqaba basin, and a string of basins, which called the Gharandal basin. The basins are oriented diagonally to the axis of the Rift Valley.

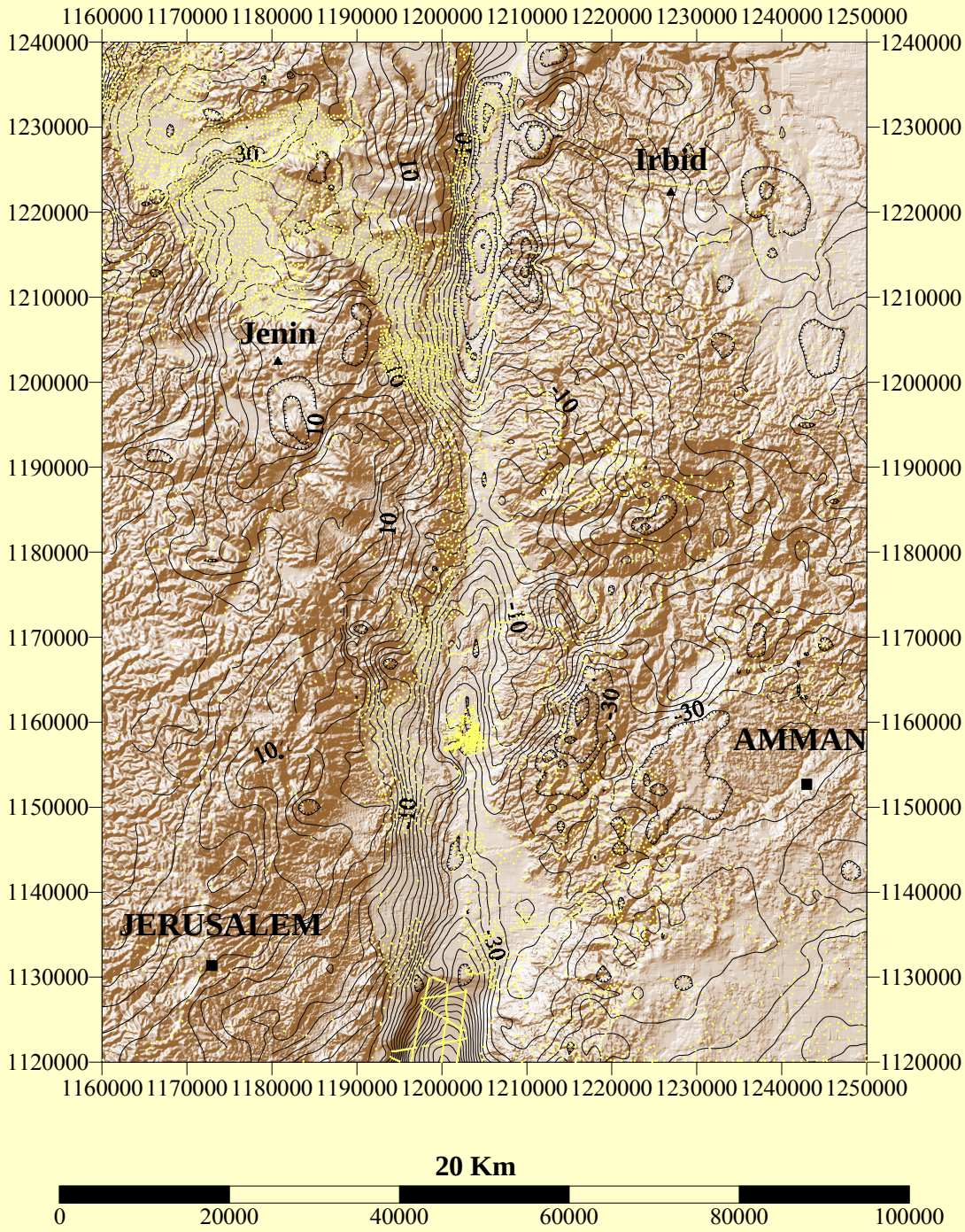

Figure 26: Gravity anomaly map of the northern segment of the Dead Sea rift superimposed on the shaded relief map of the area. Contour Interval $2.5.10^{-5}$ m/s^2. Yellow dots are the location of the gravity measurements in the area.

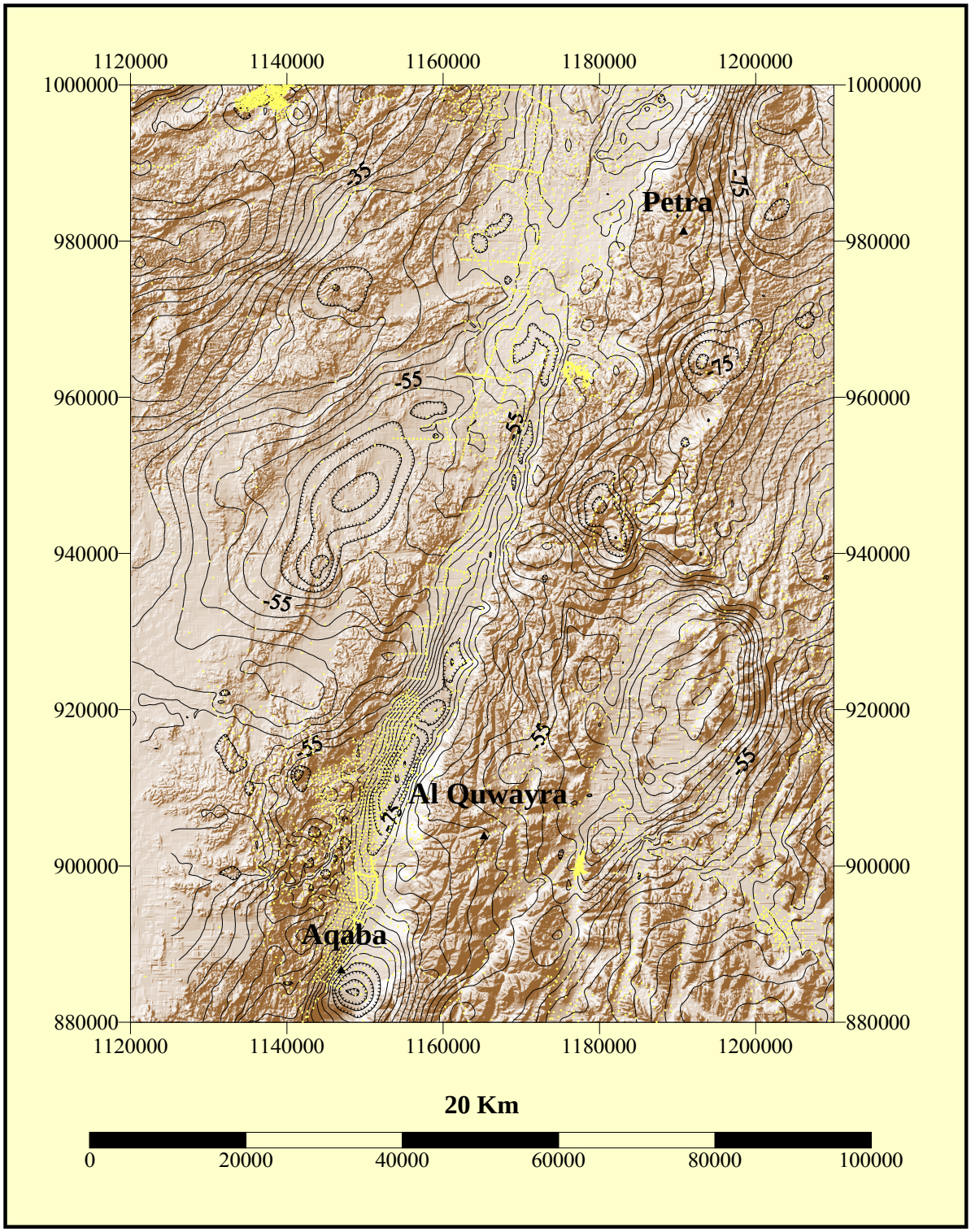

Figure 27: Bouguer gravity anomaly map superimposed on the shaded relief map of the southern segment of the DSR. (Contour Interval $2.5.10^{-5}$ m/s^2). Yellow dots are the location of the gravity measurements in the area.

6.2 The residual Bouguer gravity anomaly and the first horizontal derivative of the northern segment of the DSR

The residual gravity anomalies and the first derivative of the northern segment of the DSR, Figure 28 and Figure 29, have delineated very well the major tectonic features in the area and emphasizing the gradients of a Bouguer anomaly

The residual gravity field can be separated from the gravity anomalies by wavelength filtering. It is numerically assured that short wavelengths are caused by superficial structures while long wavelength will be caused by deep seated bodies. Digital filtering was used to remove either the short or long wavelength anomalies. For oil and water exploration, we are interested in short wavelength anomalies caused by shallow sources. In the area that influenced by the Jordan valley transform fault, we may expect anomalies on a regional scale, from infra-basement lithological variations as well as from structure at even greater depth, and we may expect anomalies on a residual scale, from the density variations within the Phanerozoic overlying the crystalline Precambrian basement.

The residual map shows, as expected the negative values in the rift valley and positive values on the shoulder of the DSR. The major rift faults and the shallow basins in the rift can be traced very precisely from the residual map. The anticline structures in A'jlun and near Amman (Suweileh) have been seen obviously on the residual map. The gravity gradient on the Jordanian side is higher than in the west side of the rift. The residual anomaly and first derivative maps outline horizontal extension and the location of the faults bounding the basins along the east and west sides of the rift.

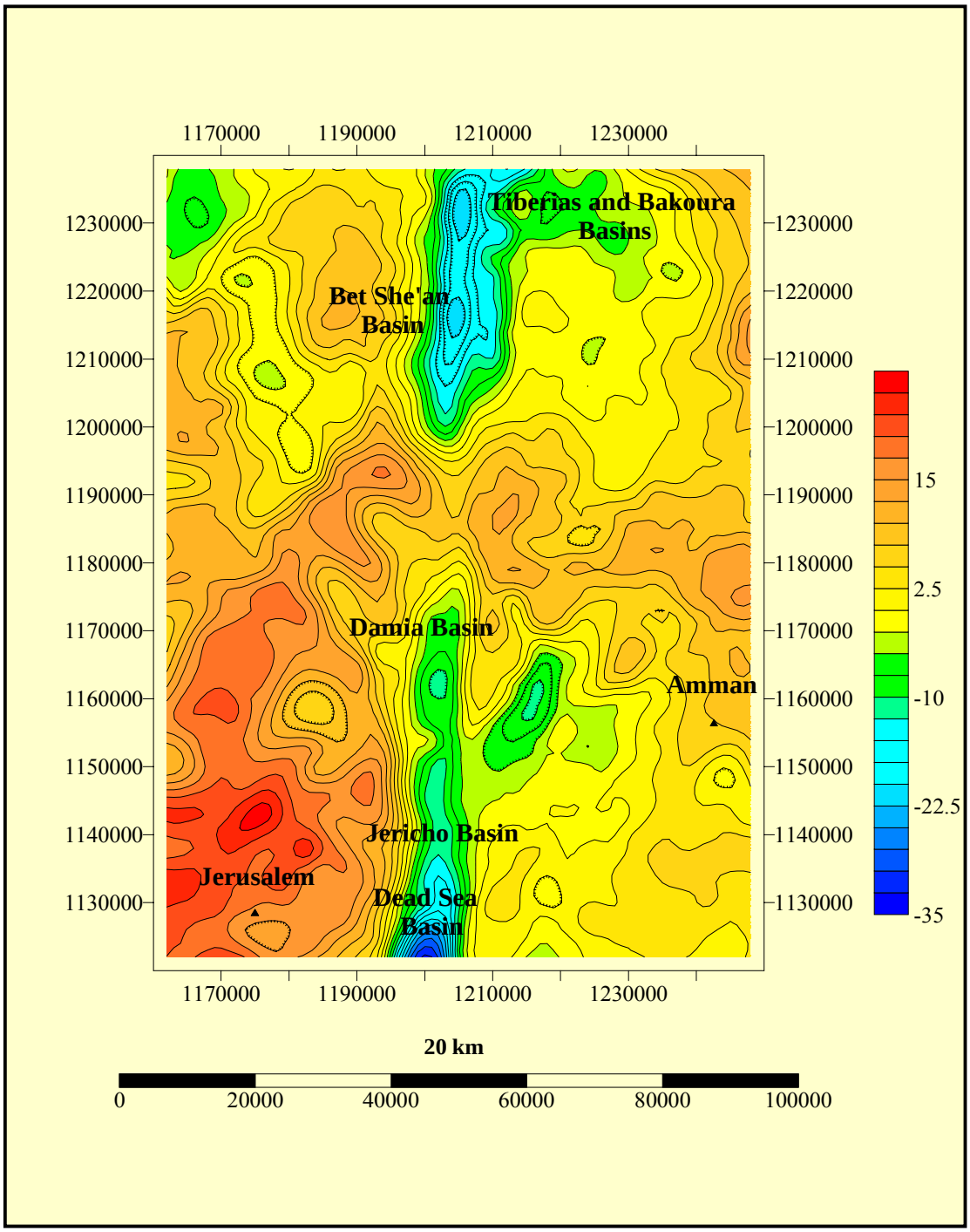

Figure 28: Residual gravity anomaly map of the northern segment of the DSR shows the major tectonic basins in the north part of the rift (contour interval $2.5.10^{-5}$ m/s^2).

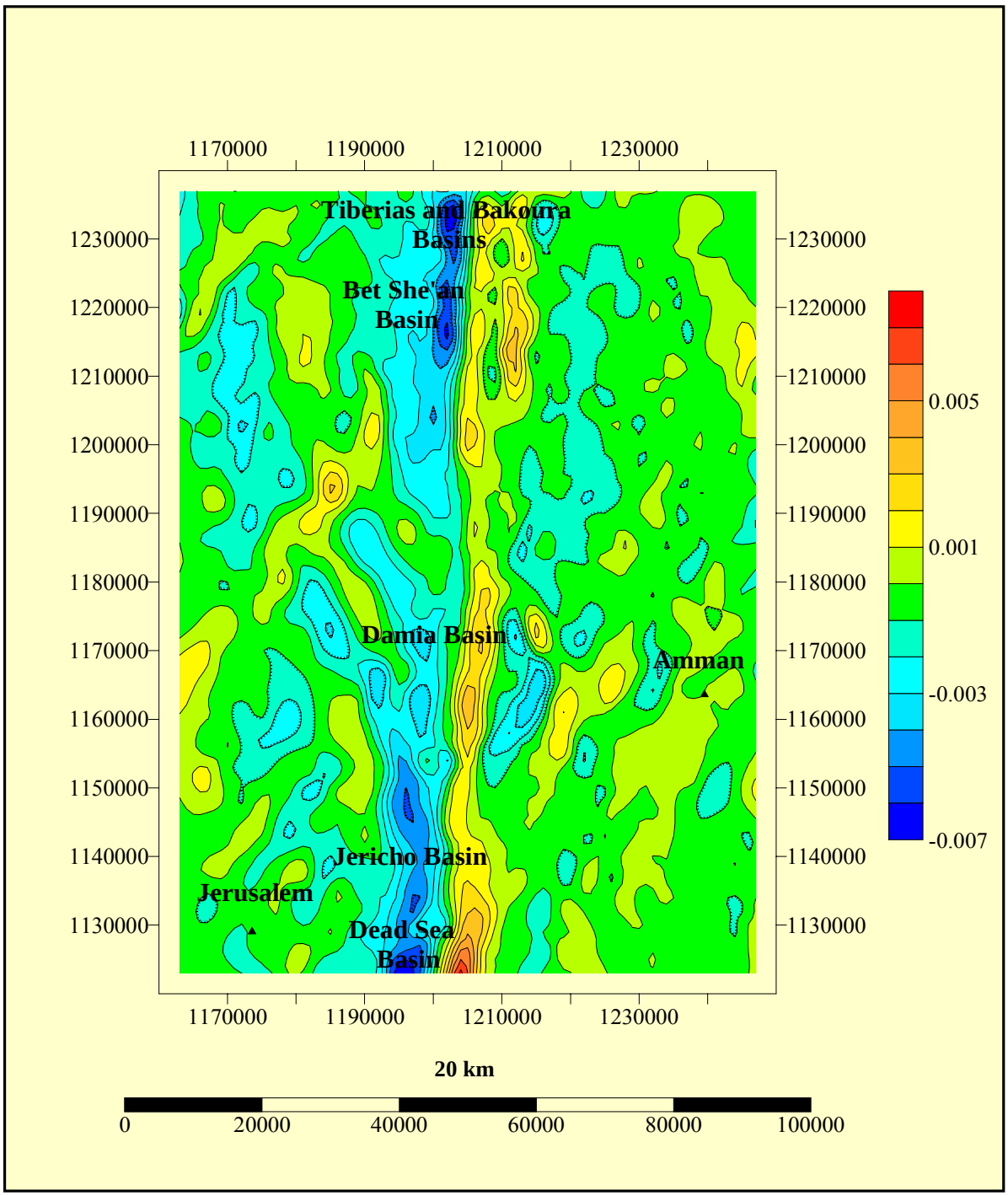

Figure 29: The first horizontal derivative of the Bouguer gravity anomaly of the northern segment of the DSR shows the major tectonic basins in the rift.

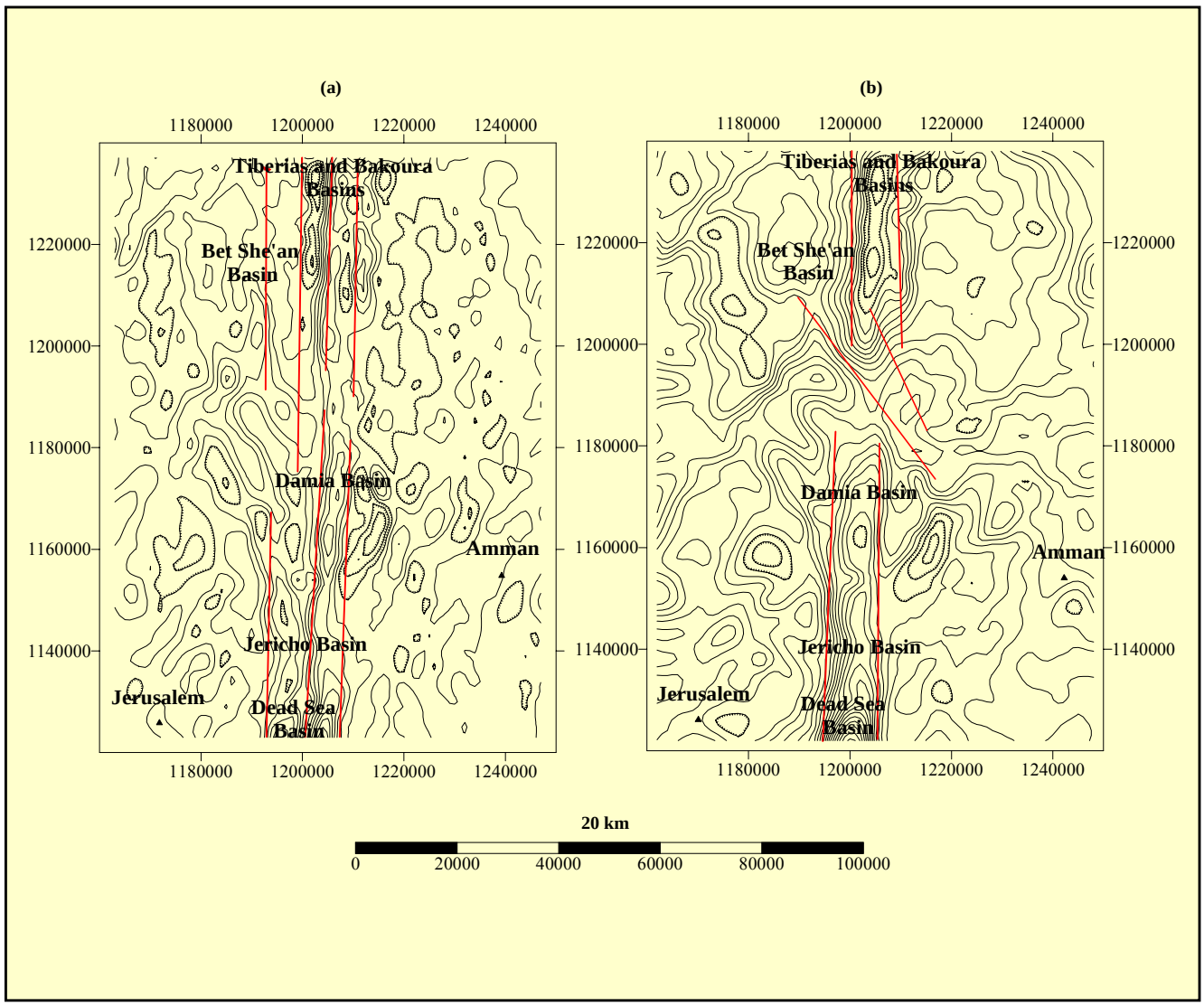

Figure 30: Interpretation map of the structural elements on the first derivative (a) and the residual (b) anomaly maps of the northern segment of the DSR. The major strike slip faults and the shallow basins are clearly shown on the maps.

6.3 The residual Bouguer gravity anomaly and the first horizontal derivative of the southern segment of the DSR

The residual gravity anomalies and the first derivative of the southern segment of the DSR, (Figs 31, 32, 33) delineate very well the major tectonic features in the area. The major Wadi Araba fault trending NNE-SSW extends from the Gulf of Aqaba in the south to the Dead Sea basin in the north, about 120 km long. It is responsible for the existence of the Wadi Araba depression and the topographic differences to the east and west in the region. The Aqaba-Gharandal fault can also be traced very well on the maps. The movement on this fault has both horizontal and vertical components (ZainAldeen, 2000). About 30 km to the north of Aqaba where Cretaceous and younger rocks are exposed in a down-faulted block, the downthrown on the fault is about 1200 m (Ibrahim, 1991). The Wadi Rahma fault striking N-S is slightly oblique to the Wadi Araba fault and has 3.3 km sinistral offset (Ibrahim., 1991). The Gharandal–Abu Burqa fault strikes NW-SE to NNW–SSE and changes to the north to N-S and NNE-SSW. Sinistral movement of 3 km is indicated along it (Abu Taimeh, 1988). The Ras Al Naqab escarpment can be traced along a fault system trending NW-SE. Most of the NW-SE trending faults are truncated by NNE-SSW to N-S trending faults indicating that the formers systems are older than the latter (ZainAldeen, 2000). The residual anomaly map shows clearly the Timna (Qa' Taba) basin. The dimensions of this basin are about 18 km long, 8 km wide and 1.3 km deep. The depth of this basin was calculating from 2-dimensional model (tenBrink, et., al 1999).

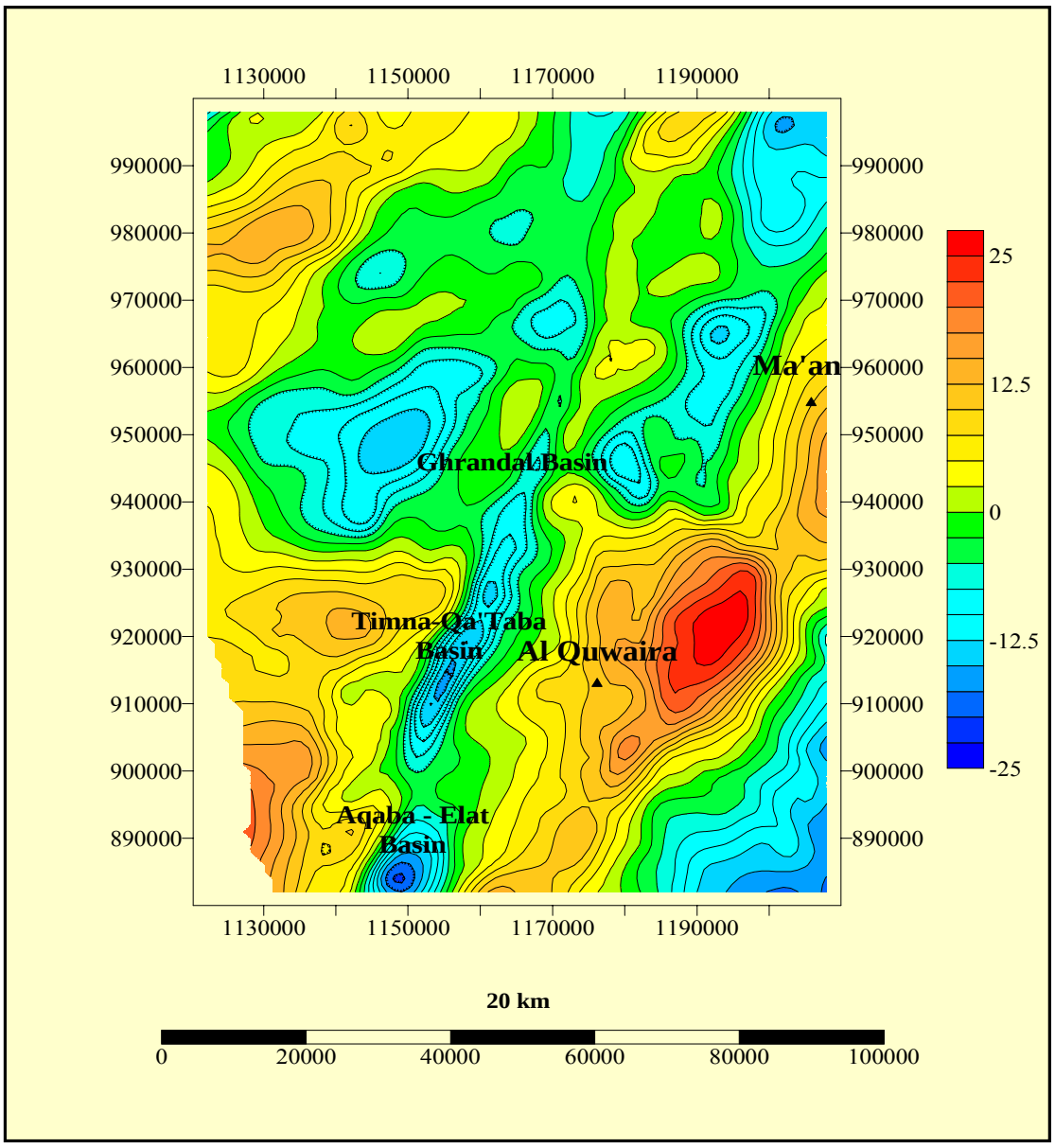

Figure 31: Residual gravity anomaly map of the southern segment of the DSR shows the major tectonic basins in the rift. (contour interval $2.5.10^{-5}$ m/s^2).

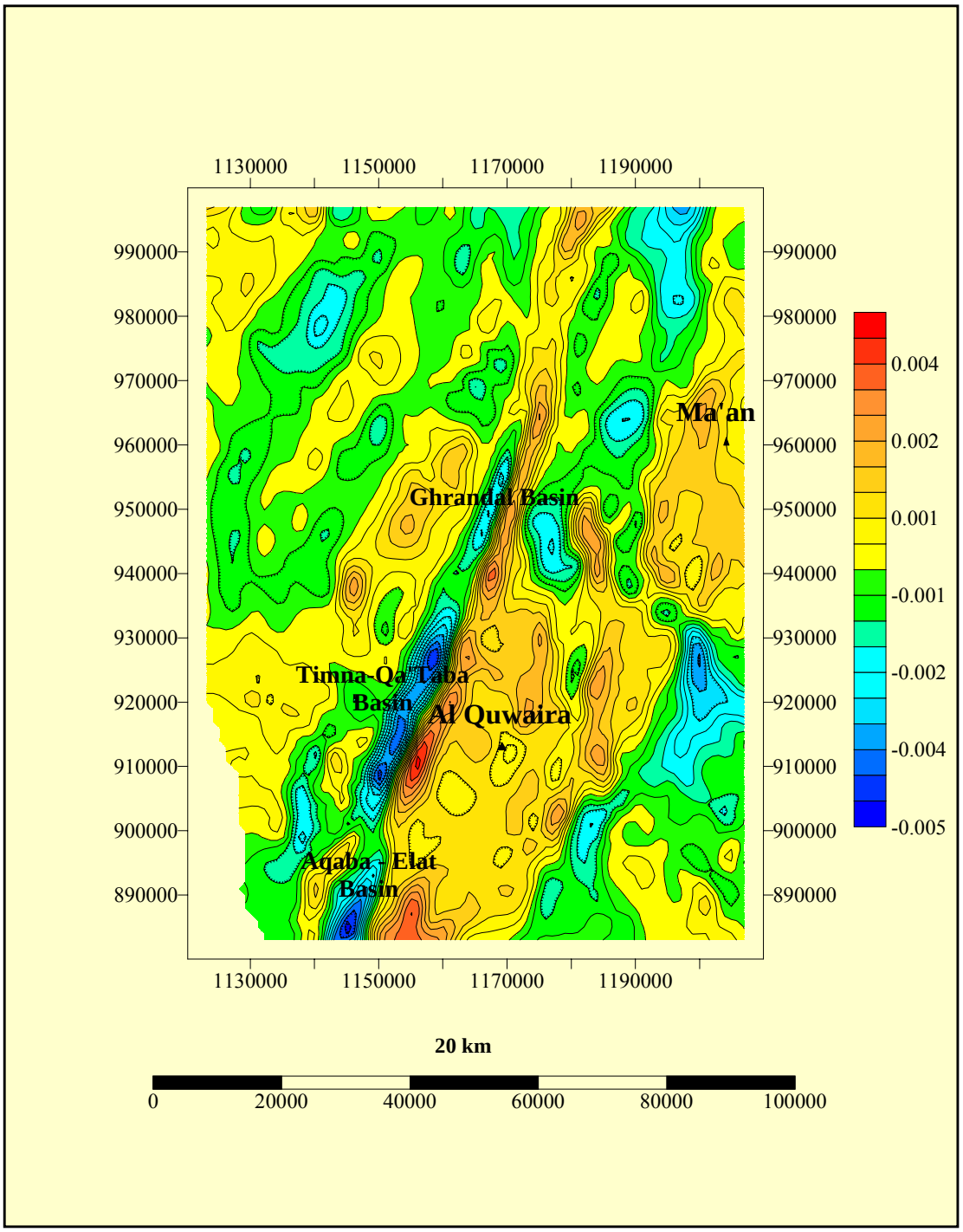

Figure 32: First derivative map of the southern segment of the DSR shows the major tectonic basins in the rift.

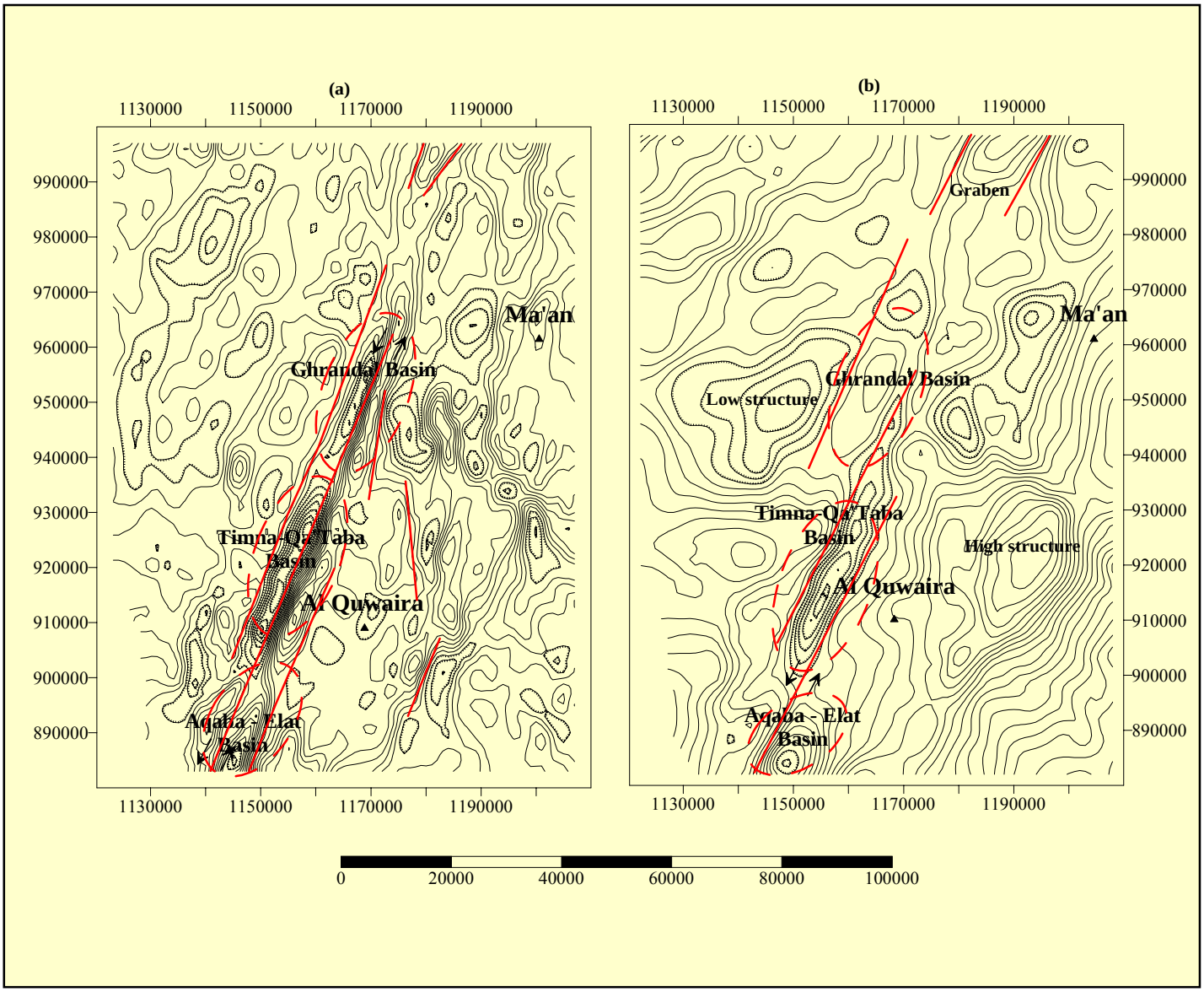

Figure 33: Interpretation map of the structural elements on the first derivative (a) and the residual (b) anomaly maps of the southern segment of the DSR. The major strike slip faults (solid red lines) and the shallow basins (dashed red lines) are clearly shown on the maps.

7 DETAILED QUANTITATIVE INTERPRETATION OF THE COMPLETE BOUGUER AND FREE-AIR GRAVITY ANOMALY MAPS OF THE DEAD SEA BASIN

7.1 Introduction

The purpose of quantitative gravity interpretation is to find physical models of anomalous bodies which are able to explain the observed gravity anomalies in full. The calculation of the first and higher derivatives of the gravity potential of a model of an anomalous body of known dimensions, shape, density and depth (position) are the basic factors of quantitative interpretation.

A Bouguer anomaly gravity map of the Dead Sea basin, Figure 34, delineates the shape and dimensions of the basin. The length of the basin is about 130 km and its width varies from 15 km in the center to 7 km in the northern and the southern ends. The Bouguer anomaly along the axis of the basin deepens gradually from both the northern and southern ends to a 30 km long central region where the anomaly is essentially flat and is about 100×10^{-5} m/s^2 more negative than the surrounding shoulders. (tenBrink, et., al., 1993). The shape of the Bouguer anomaly minimum within the basin suggests that the Dead Sea basin is a full-graben. The map shows that the central part of the basin, the Lisan Peninsula, is bounded on the eastern and western sides by two lineaments striking N-S of high or very steep gravity gradient which are interpreted as the boundary major rift faults. The two longitudinal faults are approximately vertical. The gravity gradient is approximately 8×10^{-5} m/s^2 /km on the eastern side and 6×10^{-5} m/s^2 /km on the western side of the basin. The high gravity gradients are explained by the changes in thickness of the crust and the compensating effects of the changes in thickness of the low density sedimentary toward the central part of the DSB. The very low gravity value of -130×10^{-5} m/s^2 in the central part of the study area is fairly flat and marks the deepest part of the basin. The deepest part of the basin is a salt diaper originating from layers which were deposited in this area during the Plio-Pleistocene (Ben-Avraham, et al. 1990). The Bouguer map shows high positive gravity at the north-west corner of the map towards the Mediterranean could be due to the thickness of the Crust increasing in this direction. The Bouguer map shows low negative anomaly could be attributed to a syncline structure at the south east corner of the map.
The Free-air gravity anomaly map (Figure 35) shows that the large positive free-air gravity anomalies are found over the highlands and the large negative anomaly is over the basin. This suggest that the topography is not isostatically compensated at these wavelengths (< 60 km); hence the free air gravity anomaly map primarily reflects the topography; the axis of the Judea Mountains shows as high as $<100\times10^{-5}$ m/s^2 gravity anomaly in the NW corner of the map, the NE-SW monoclines are identifiable farther south as NE trending steps in the gravity field, and the free-air gravity anomalies over the eastern highlands are fairly flat (tenBrink, et., al., 1993). The long-wavelength component of the gravity field consists of a regional trend decreasing to the east and presented by the Bouguer anomaly Figure 34. It was modeled by ten Brink et al. (1990) to result from crustal thickening from ≤ 12 km in the Mediterranean Sea to 35 km in the Arabian Desert, the majority of which probably occurs west of the basin. The regional trend is apparent in the free-air map only when peak-to-trough differences are compared. The maximum peak-to-trough differences between the Judea Mountains in Israel and the Dead Sea $<335\times10^{-5}$ m/s^2 is 100×10^{-5} m/s^2, larger than that between the

Moab Plateau in Jordan and the Dead Sea (Figure 34), although both flanks are at similar elevations (Figure 7).

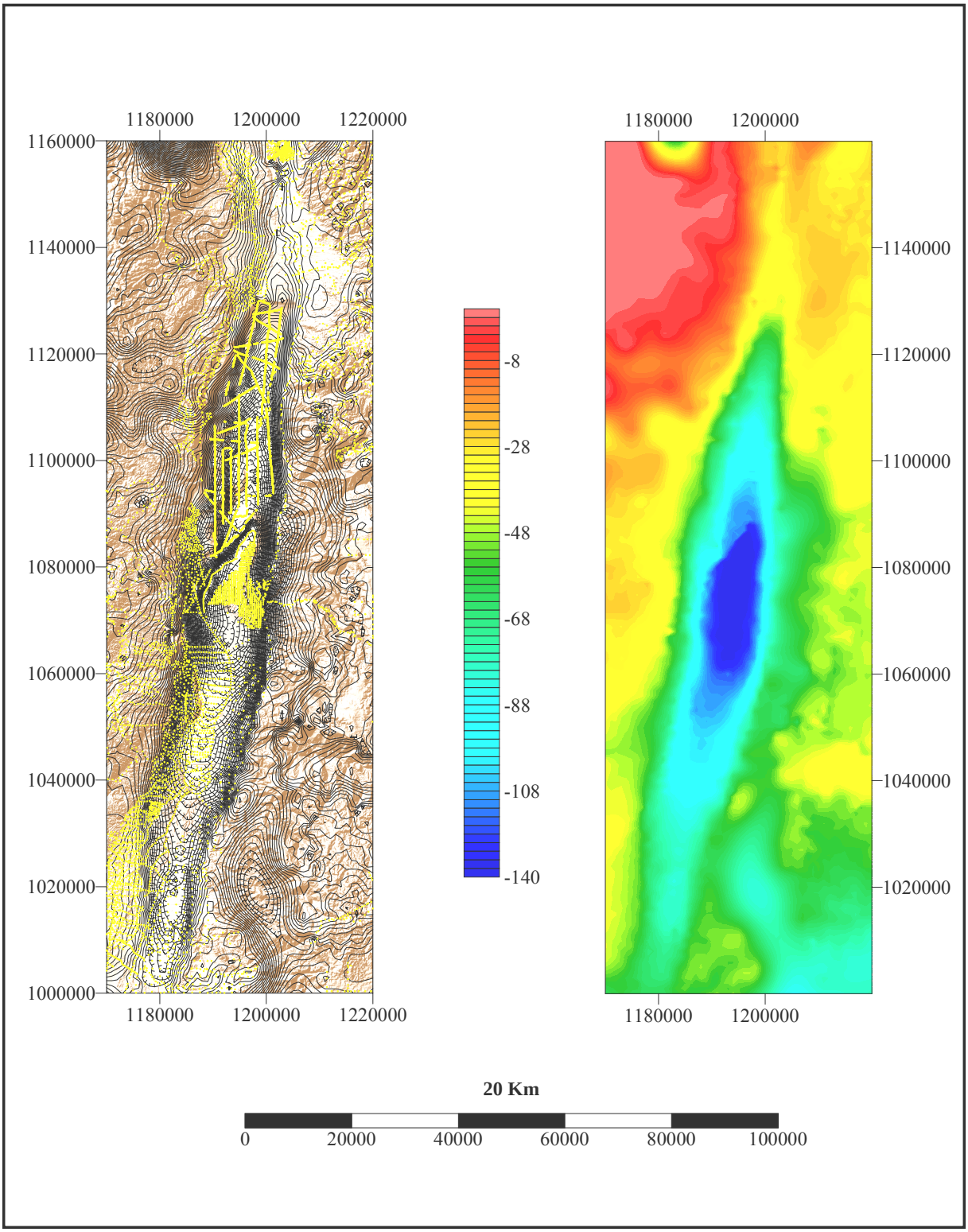

Figure 34: Bouguer gravity anomaly map of the Dead Sea basin and the shaded relief map of the basin. Contour intervals 2×10^{-5} m/s^2.

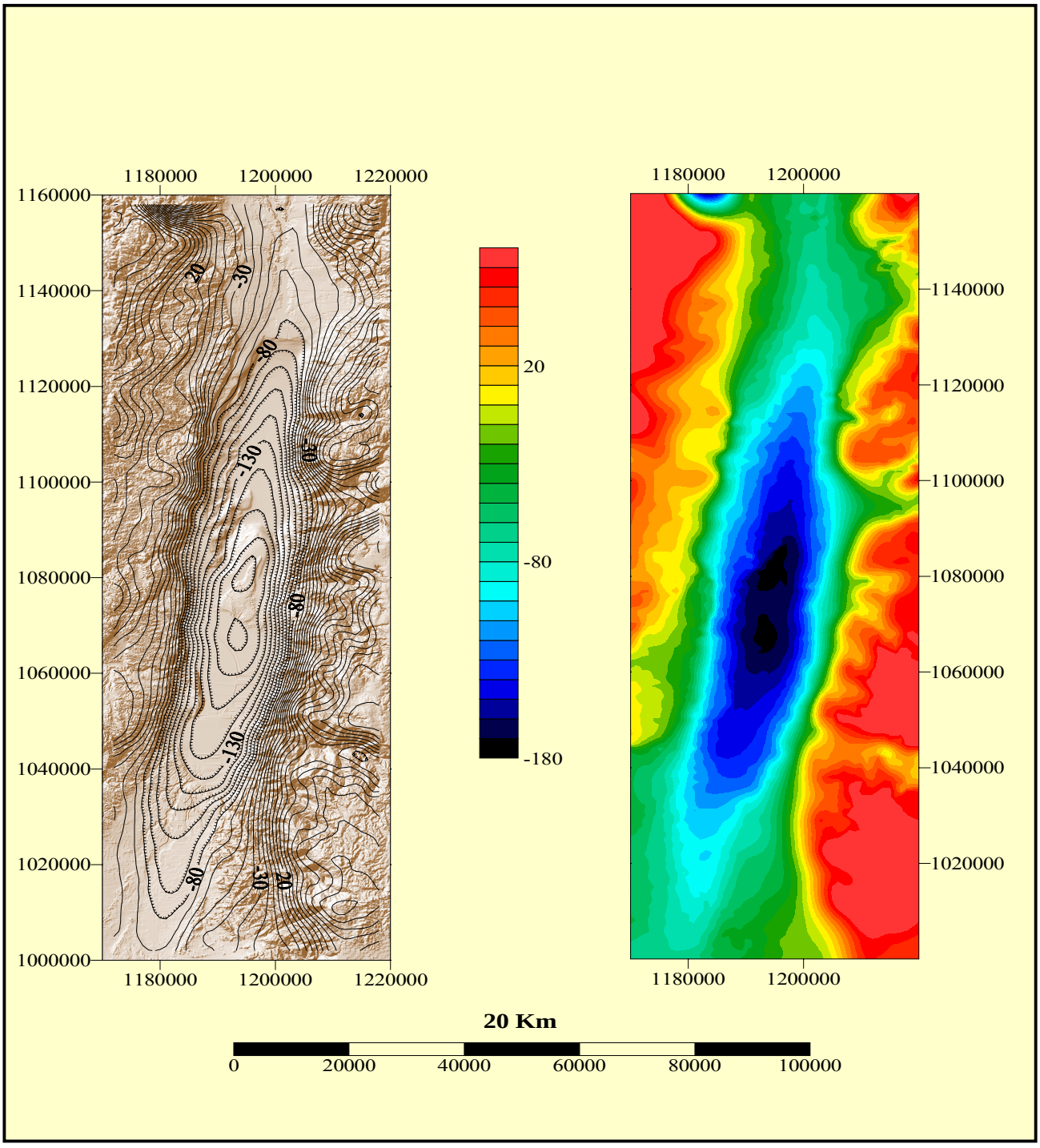

Figure 35: Free-Air gravity anomaly map on the shaded relief map of the DSB.

7.2 Comparison of topography, measured gravity (OG), Free-Air, Simple Bouguer gravity anomalies along 3 E-W profiles crossing the Dead Sea transform

Figure 36, Figure 37 and Figure 38 show plots of surface elevation (red line, surveyed to the nearest 10-15 cm), observed gravity (OG), (dark blue line), free air anomaly (brown line) and simple Bouguer anomaly (green line) for three E-W profiles extending from the Mediterranean Sea crossing the rift valley to the east until the Saudi Arabia borders with about 225 km length (Figure 8).
Profile 1 and Profile 3 are located outside the Dead Sea basin and profile 2 is crossing the central part of the Dead Sea basin. The three profiles show the positive correlation between topography and free air anomaly. The observed gravity correlate inversely with topography. There is weak correlation of the Bouguer anomaly with topography in the profiles 1 and 3 and strong correlation between them in profile 2 which is crossing the DSB. When the Bouguer anomaly correlates positively with topography as in profile 2, it means that the anomalies are caused by the high density contrasts beneath the central part of the DSB. The simple Bouguer gravity anomaly decrease to the east in profile 1 and 3 is caused by a decrease in the density of the rocks in this direction. Part of this decrease is probably caused by an increase in the thickness of the crust in this direction. Note that the Bouguer anomaly equals the free-air anomaly at sea level.

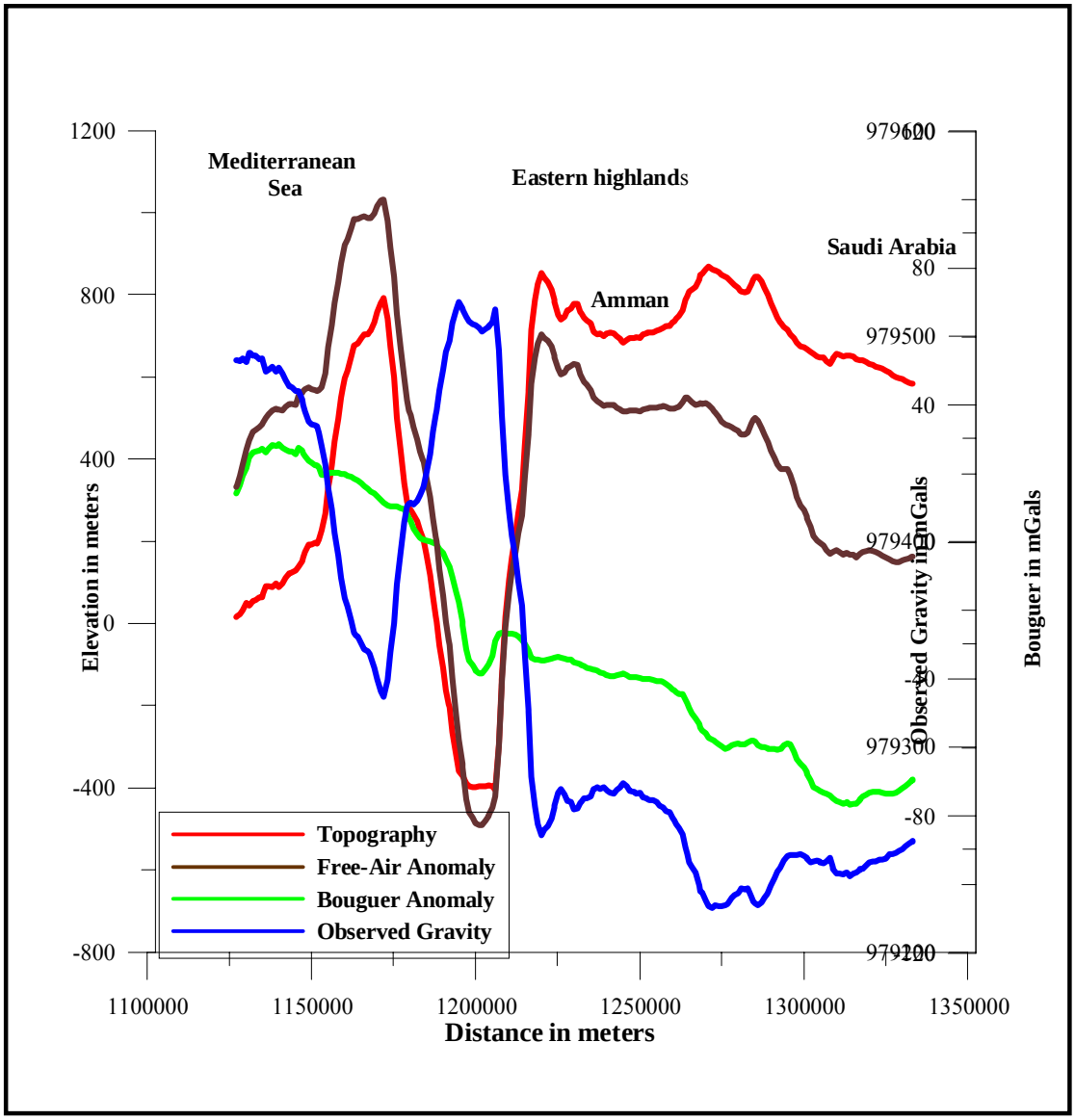

Figure 36: Regional profile Nr.1 of topography (red line), free-air gravity (brown), simple Bouguer gravity (green line), and observed gravity (Dark blue line) crossing the southern part of the Jordan rift valley (to the north of Jericho city) outside the DSB.

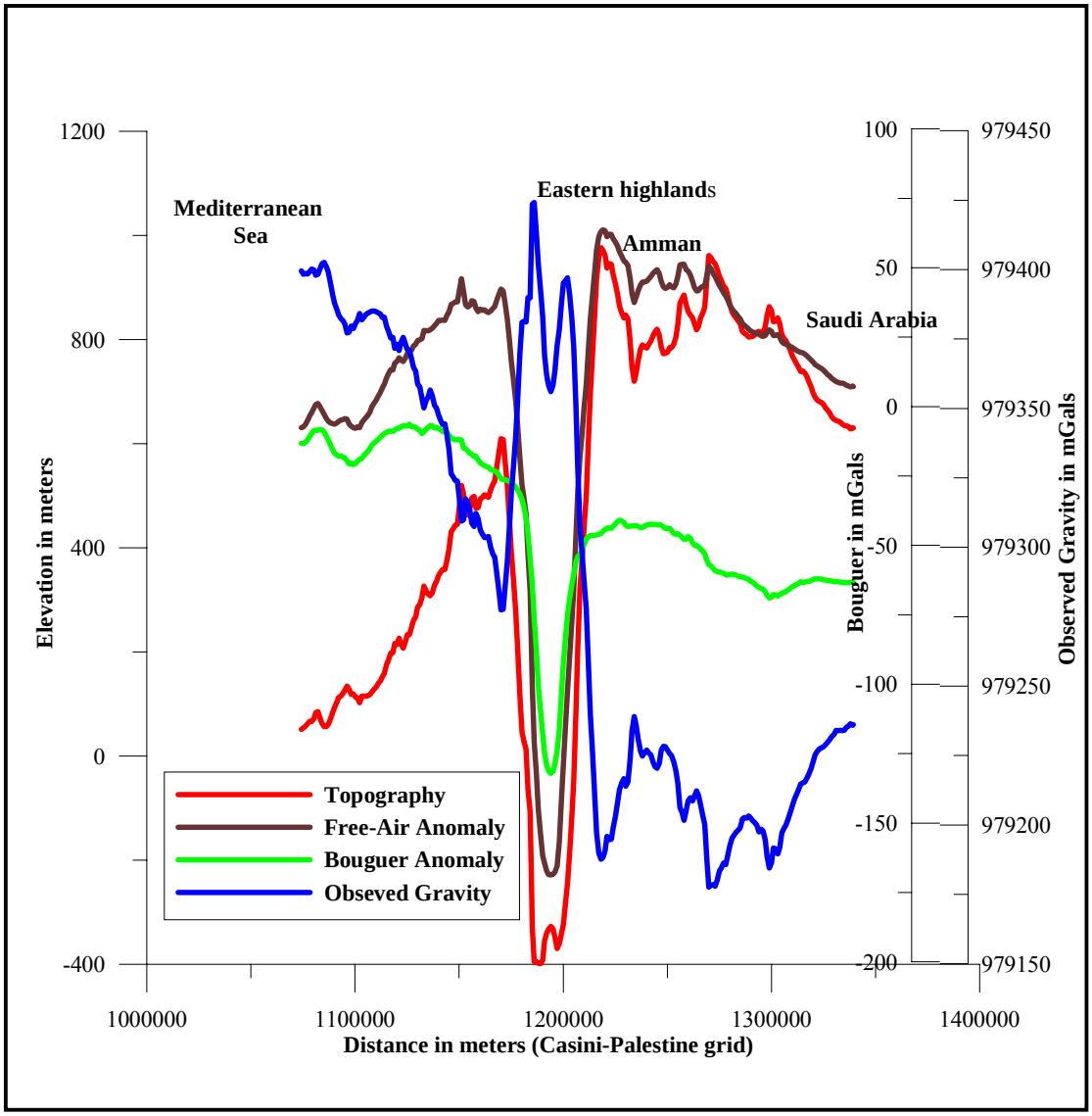

Figure 37: Regional profile Nr.2 of topography (red line), free-air gravity (brown), and simple Bouguer gravity (green line), and observed gravity (Dark blue line) crossing the central part of the Lisan Peninsula of the DSB.

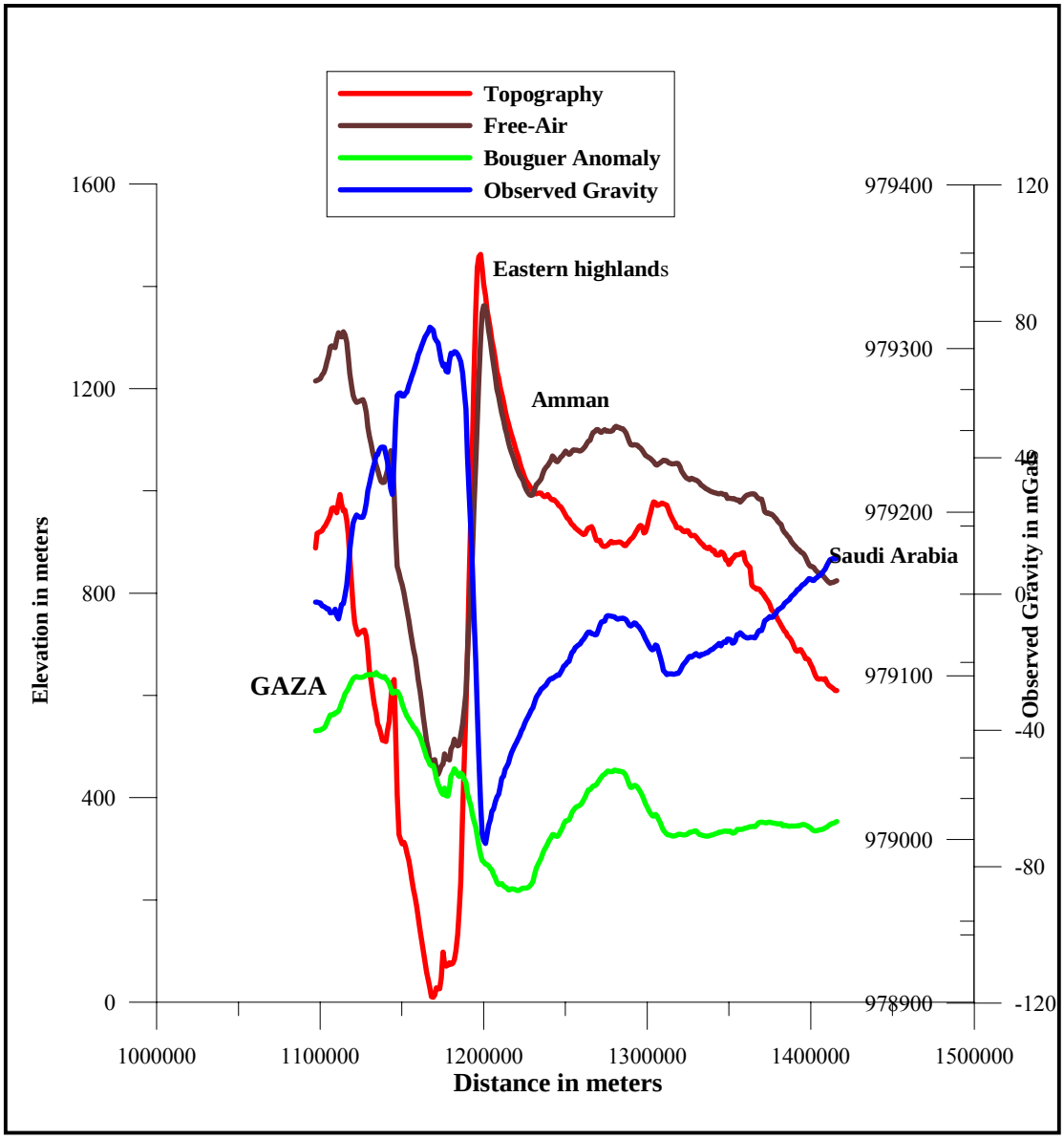

Figure 38: Regional profile Nr.3 of topography (red line), free-air gravity (brown line), and simple Bouguer gravity (green line), and observed gravity (Dark blue line) crossing the northern part of the Wadi Araba segment outside the DSB.

7.3 Interpretation of the Residual and First horizontal derivative of the Bouguer gravity anomaly of the Dead Sea basin

Interpretation of the residual and first derivative maps of the DSB, Figure 39 and Figure 40, emphasizes the short wavelength features of the Bouguer anomaly. The basin is bounded on the eastern and western sides by two "crests" connecting zones of maximum gravity gradient. The crests become closer to each other, but do not meet at the southern and northern ends. A linear "valley" connecting zones of minima is enclosed between the high-gradient crests (except in ~20 km long area north of the Lisan peninsula) and probably marks the axis of the deepest part of the basin. There are a few minor offsets along the valley of low gradient, which may be attributed to subsurface diagonal faults (tenBrink, et., al., 1993). Provided the crests of maximum gradient represent faults, the skew ness of the horizontal gravity gradient around the peak gradient can be used to deduce the dip of the fault (Bott, 1962). A vertical fault will produce a symmetric peak, a reverse fault will produce a steeper slope toward the basin, and a normal fault will produce a steeper slope toward the flank (tenBrink, 1990). The eastern crest appears to represent a generally vertical or slightly reversed fault, whereas the western crest represents a generally normal fault, except at the northernmost end (at 1110000 Northing, Casini-PAL. Grid) where it is a vertical to reverse fault. The northernmost end of the western crest follows the trace of the Dead Sea strike-slip fault which is indeed slightly reversed (Rotstein et al., 1991).

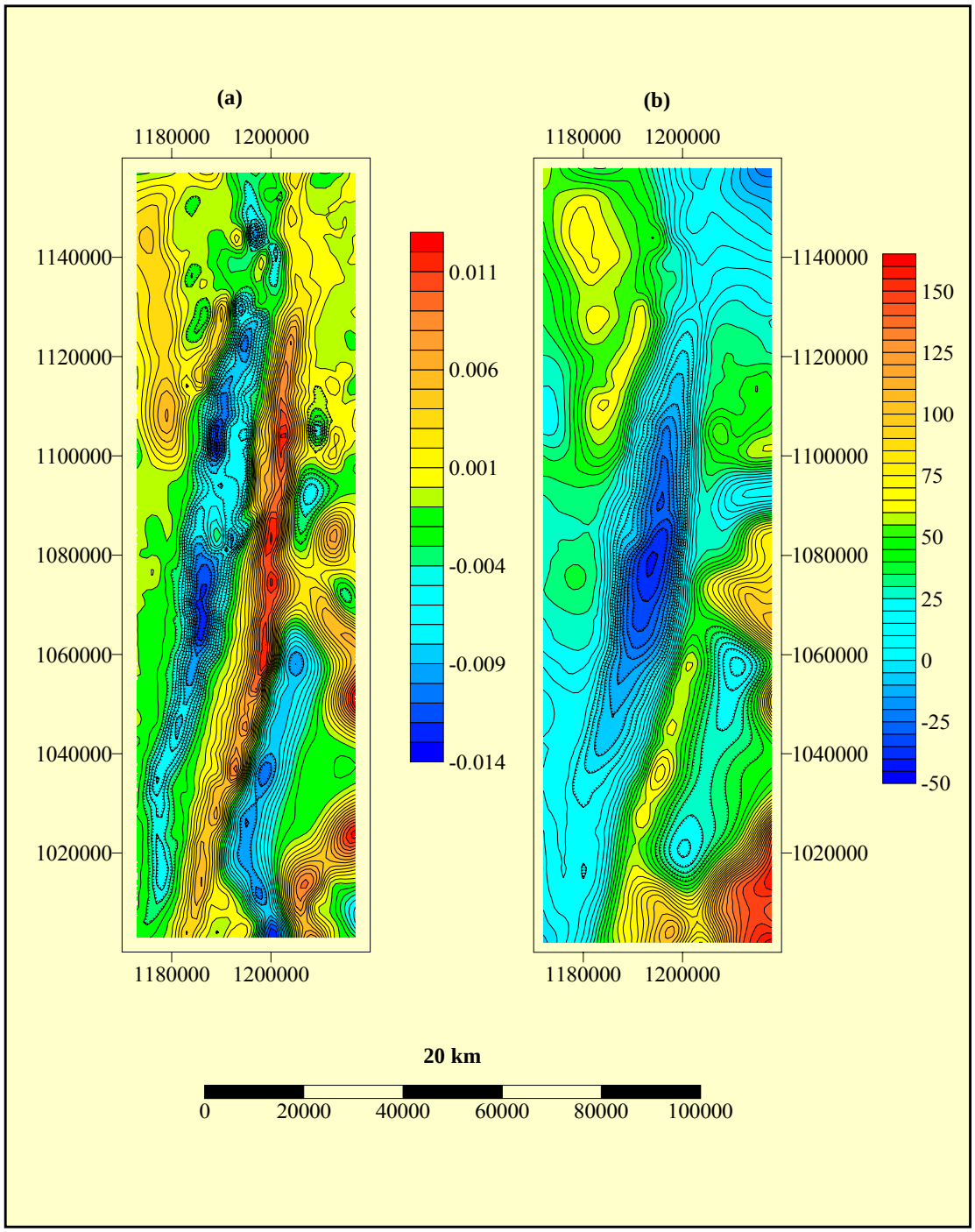

Figure 39: First horizontal derivative (a) and Residual (b) Bouguer gravity anomaly maps of the Dead Sea basin.

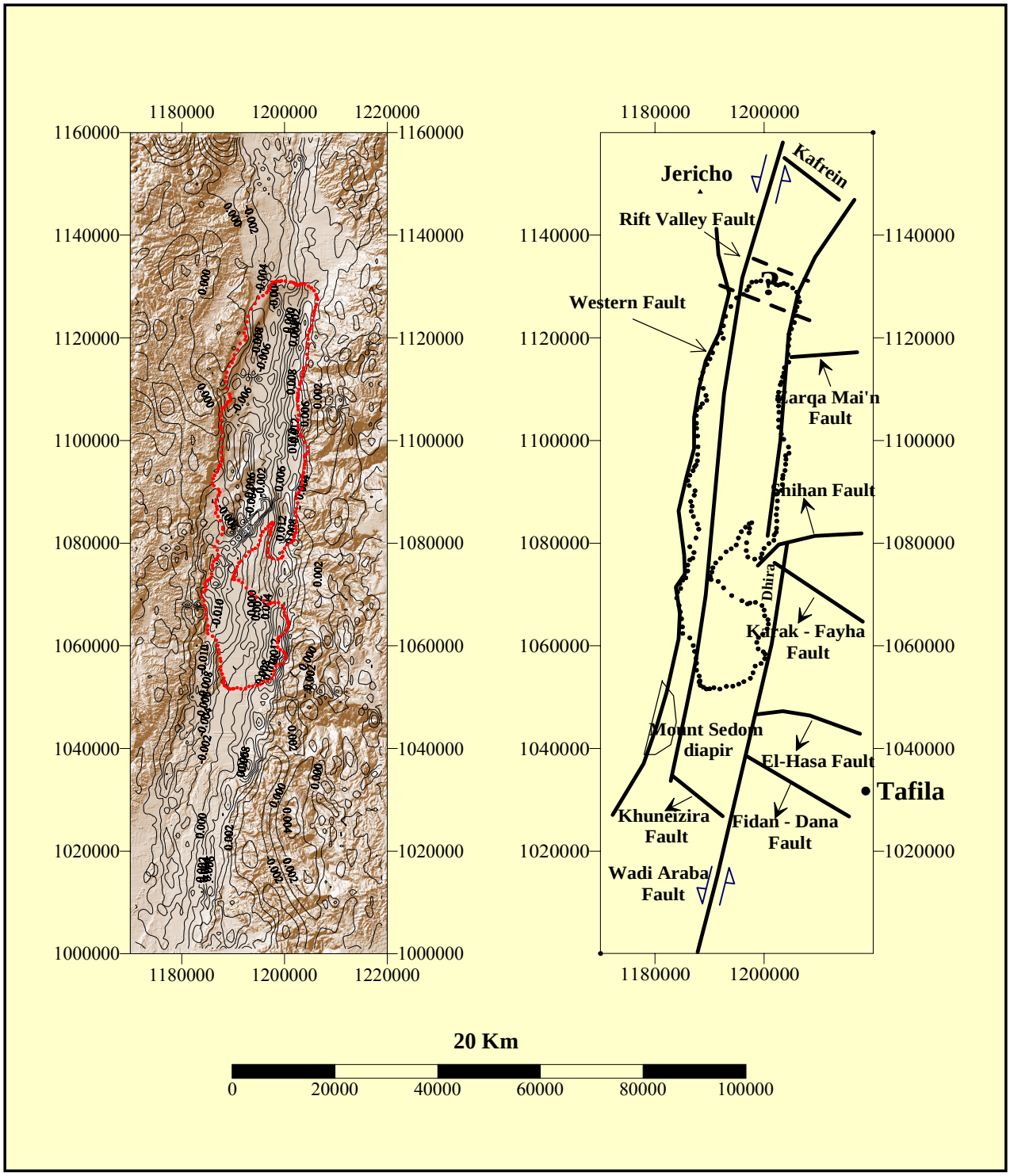

Figure 40: The interpretation of the first horizontal derivative of the Bouguer gravity anomaly map of the Dead Sea basin (DSB).

8 3-DIMENTIONAL GRAVITY MODELING OF THE CENTRAL AND SOUTHERN PARTS OF THE DEAD SEA BASIN

8.1 Introduction

Analysis and modeling of gravity data were used to investigate the structure of the Dead Sea Basin, and discuss the processes involved in its formation. In this research a 3-dimensional interactive modeling was done using the interactive gravimetry and magnetic analysis System (IGMAS) program package (Schmidt and Götze, 1995). IGMAS is an extended new version of the interactive gravimetry and magnetic application system (IGAS) developed by Götze and Lahmeyer (1988). IGMAS is modified to be installed at workstations and has many extra functions. Both programs (IGAS and IGMAS) are based on algorithms developed by Götze (1976, 1978).

IGMAS is an interactive, graphical computer system for 3D interpretation of potential fields (gravity and magnetics) by means of numerical simulation (*Götze, 1978*; *Götze, 1984*; *Götze and Lahmeyer, 1988*). The modeling procedure is based on 'trial and error' methods. The algorithm used for potential field calculation bases on triangulated polyhedron (*Götze, 1978*), and has been revised and extended in 1995 (Götze, pers. comm.). At the moment a simultaneous modeling of the following field elements is possible:

- Gravity field (x, y and z components),
- Gravity gradients (x, y and z components),
- Mass attraction potential,
- Geoidal undulations,
- Magnetic field (x, y and z components) and
- Total magnetic field (induced field and remanent magnetization).

The data structure, required for the description of three dimensional model geometry has to be simple and flexible enough to cover the wide field of gravity or magnetics modeling: It should facilitate representations of geological information, such as vertical or horizontal cross sections, surface and depth contour maps, 3D visualization, as well as volume and mass calculations.

These requirements lead to the following basic elements of the input data: The structures (geological bodies) to be modeled are bounded by triangulated surfaces (layer boundaries), which limit domains with constant density and/or susceptibility.

The definition of these triangulated surfaces may be given in two different ways:

1. By defining polygons (lines) along vertical, parallel cross sections. The triangulation between the vertical planes is always done automatically. The data input is two-dimensional, whereas the construction of the final 3D model structures is performed by IGMAS and does not require detailed knowledge about topology, data structures or triangulation techniques.

2. Importing externally triangulated surfaces (*gocad* triangulation format).

3. A combined import of both formats is possible.

Interactive modification of model parameters, e.g. geometry, density and susceptibility, access to the numerical modeling process and direct visualization of both, calculated

and measured fields of gravity and magnetics. This enables the interpreter to design the model as realistic as possible. In this context, a 'realistic' model means, that inconsistencies of existing information should be restricted to a minimum. A basic requirement for modeling is the existence of ideas and hypothesis on the investigated area, i.e. the availability of quantitative or qualitative constraints. Towards this end, geophysical modeling aims in the combination and compilation of (all) existing information. The lack of information, which always exist, has to be filled by inter-or extrapolation, and contradictions of different data sources have to be clearly identified, e.g. by means of statistical methods.

The outlined procedure applied to complex interpretation tools requires a synoptically visualization of the necessary constraining data, which have to be selected and activated by the user. Modern Geo-Information Systems (GIS) handle this task. Today these systems are based frequently on relational data banks, and will be replaced by object orientated systems (OOS) in the near future. The advantage of OOS is an increasing affectivity, because of direct access to data and information by the definition of 'geo-objects' (*Breunig et al., 1999*; *Breunig et al., 2000*; *Schmidt & Götze, 1998*; *Schmidt & Götze, 1999*).

The 3D model of the DSB covers an area of 2475 km^2, and consists of 30 E-W planes crossing the DSB (Figure 41). Two of them are considered as margin planes which are situated about 500 km away from the first and the last planes (P2 and P29) at both sides of the modeling area, as the distance must be large enough (Schmidt and Götze, 1995) in order to reduce edge effects as much as possible.
The 3D model consists of six densities: the Dead Sea water (1280 kg/m^3), the sediment fill (2150 kg/m^3), the Mesozoic carbonate platform (2550 kg/m^3), Cretaceous, (Amman, Wadi Essir, Shueib, Hummar, Fuheis, Na'ur and Kurnub Sandstone), (2400-2500 kg/m^3), Upper Cambrian, Lower Ordovician (Disi Sandstone), (2700 kg/m^3) and the crystalline basement (2670 kg/m^3). The 3D model used all available geological and geophysical information including bathymetry, location of faults in surface geology (Picard and Golani, 1965; Bentor et al., 1965), the first derivative gravity map of the DSB, Figure 39, and the depth to crystalline basement map Figure 47. Sample of model parameters and configuration file of the 3D model of the DSB are listed in Appendix 3.

8.2 Previous geological and geophysical models of the DSB

Models interpreted the evolution of the DSB have been developed since 30 years. The simplest model for the evolution of the DSB envisioned an extension across a jog between two strike-slip faults strands, which created a rhomboid hole bounded by diagonal normal faults (Freund and Garfunkel, 1976). More recent models suggested asymmetric extension over a mid-crustal detachment fault. In this model the southern end of the basin is bounded by a series of large diagonal listric faults, whereas the northern end warps down (Arbenz, 1984; Reches, 1987). Models of fracture propagation, dislocation, and displacement discontinuity predict asymmetric subsidence near the tips of the en-echelon strands which coalesce to produce a larger strike–slip basin (Segall and Pollard, 1980; Rodgers, 1980; Bilham and King, 1989). These models have been successfully applied to shallow pull-apart basins.
Kovach (1986) from Stanford University has developed a 2D gravity model for a profile crossing the eastern Mediterranean and the Dead Sea rift. His model illustrated

that the gravity anomaly is produced by 8-9 km of low density (2000 kg/m^3) material so that the bordering faults must extend to at least that depth.
Recent hypothesis interpreted the evolution of the DSB given by tenBrink et al., 1993. They show from 2D and 2 1/2D gravity models that the north-south extension of the upper crust is concentrated in the deepest part of the basin (Lisan Peninsula) where the two strands of the strike-slip possibly overlap. Extension and subsidence continued thus, the upper crust sank and became partially ductile. Outside the area of concentrated extension the basin simply sagged toward the hole. The sagging indicates that the upper crust lost its foundation over a wider area than just the deepest part pf the basin. Thus, the crust within the pull-apart basin appears to be stretching only from above by subsidence and ductile flow.
In May, 2001 Al-Zoubi and Uri ten Brink presented a modern example of a large salt diapir in the Dead Sea pull-apart basin; the Lisan diaper, which was formed during the Quaternary due to basin subsidence. They used seismic and gravity data and they determined the size of the diaper to be 13 × 10 km. From 2D gravity model, they found that the maximum depth of the Lisan diaper is 7.2 km (Al-Zoubi, 2001).

8.3 Discussion of the 3-dimension model of the DSB

The interpretation of this model assumes that the Bouguer anomalies are entirely due to high density contrast between the salt body (2150 kg/m^3), the Mesozoic sediments (2550 kg/m^3) and the crystalline basement (2670 kg/m^3), (Figs 42, 43, 44).
Several features are consistent in all the models for the 28 east west planes: A full graben or close to a full graben occupies the central part of the Dead Sea basin. The faults bounding the full graben have close to vertical (> 80°) dips. Tilted fault blocks, several kilometers wide, are located along the western side of the basin and smaller tilted bocks may be located on the eastern side. (tenBrink, 1993). The total width of the basin is 17-19 km. The gradual decrease in the gravity from the northern and the southern ends of the basin indicates that the basin sags from the two ends toward the center. The basin is slightly asymmetric along its axis with the deepest part of the basin located in the Lisan Peninsula of the DSB. The basin has three depth levels, the deepest level, 10-12 km, is located under the Lisan Peninsula, an intermediate level (4-6) km extends ~ 20 km to the north and to the south of the deep level, and a sallow level (2 km) occupies the southernmost 3 km. The three depth levels are probably separated by fault zones Figure 45.
The crests of maximum gravity gradient delineate the eastern and western boundary faults of the basin whereas the valley of the minimum gravity gradient delineates the axis of the full graben. The crests of maximum gravity gradients do not close on the southern and northern ends of the basin. The crests do not meet, they become closer to each other at the northern and southern ends, indicating that the basin narrows at its ends where it is also the shallowest (<3000 m). This suggests that widening by the collapse of blocks accompanied the deepening of the basin. The western high gradient crest between latitude 50N and 110 N runs parallel at about 1 km eastward of the escarpment that marks the western boundary of the basin, supporting the interpretation that the escarpment is the surface expression of a normal fault (Picard ad Golani, 1965; Bentor et al., 165).
High gravity gradients within the basin immediately north of the Lisan peninsula may indicate that active subsidence is also taking place here (tenBrink, et al., 1993). Appendix 2 shows a sample of the input data of one of the 30 planes calculated to

produce the 3D image of the DSB. Appendix 3 shows the results of the computed crustal model along southern, central and northern parts of the DSB.

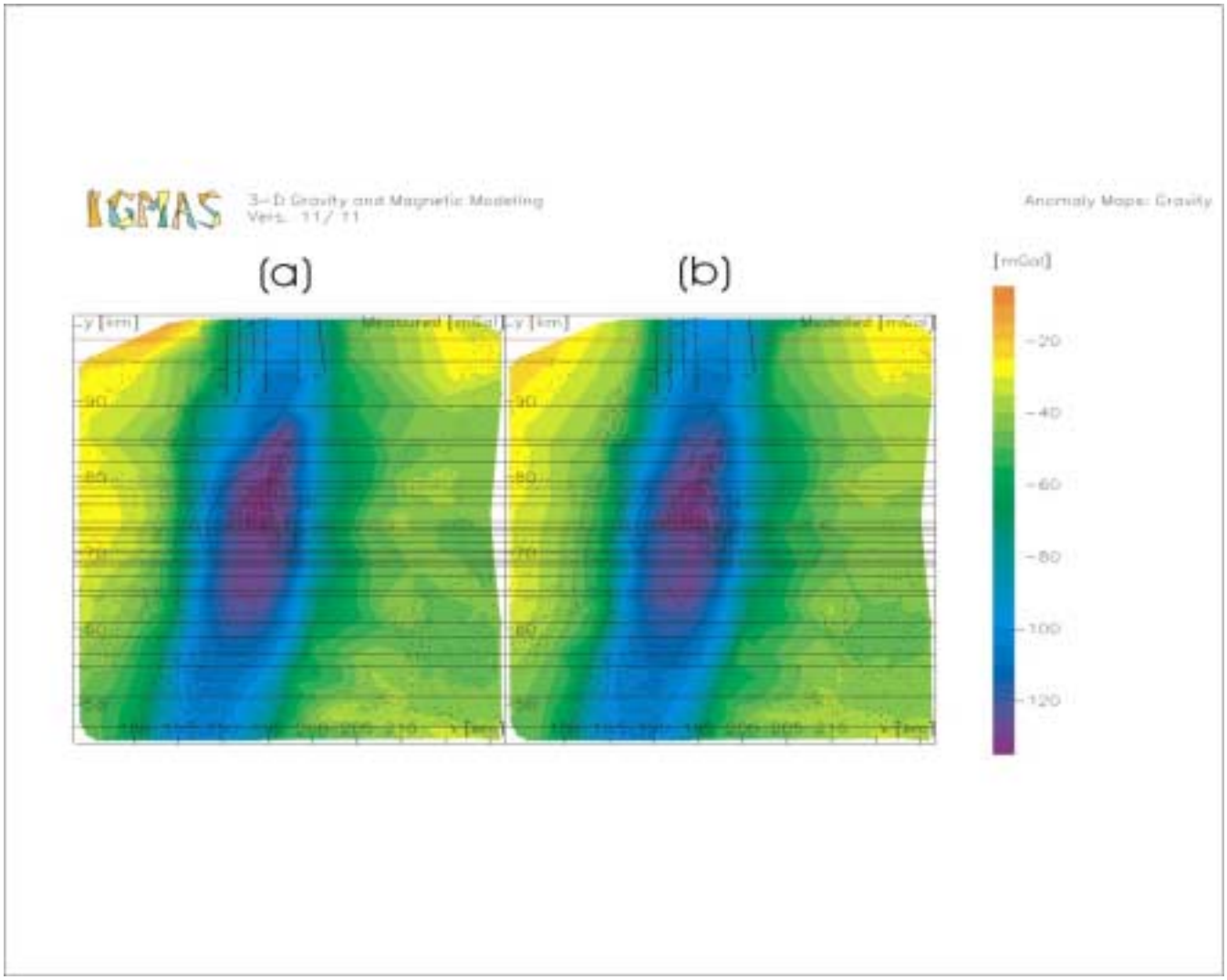

Figure 41: Comparison between measured (a) and modeled (b) Bouguer anomaly maps of the DSB. 30 E-W planes are shown on the map.

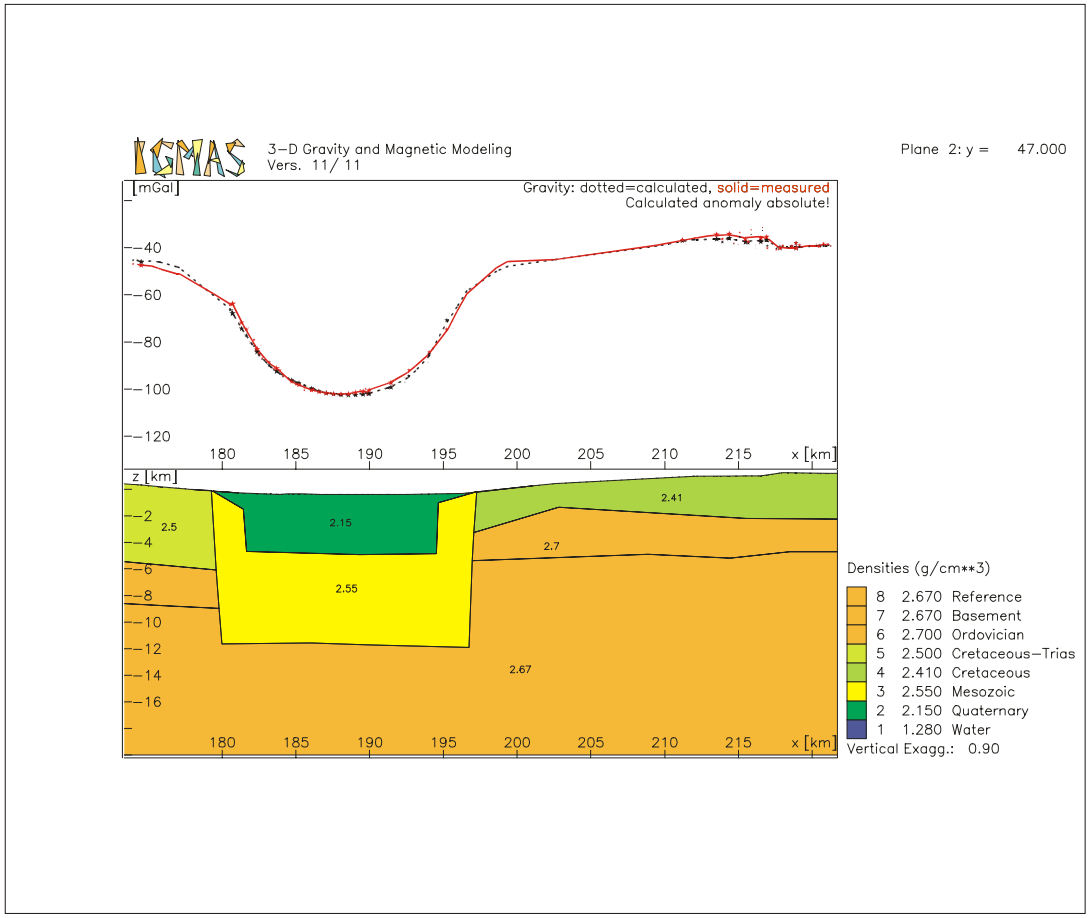

Figure 42: Computed crustal model for the DSR along the southern planes Nr. 2. Northing = 1,047,000 m in Palestine grid.

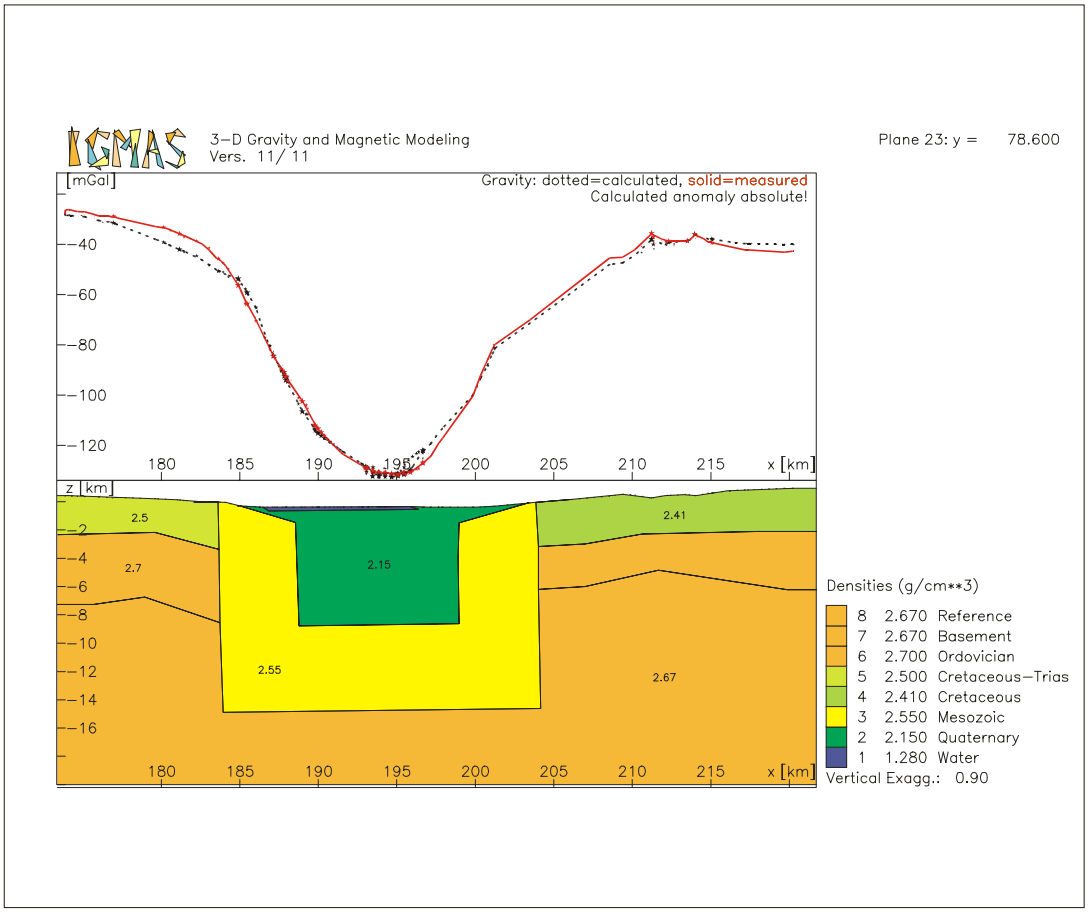

Figure 43: Computed crustal model for the DSR along the central part of the DSB in the Lisan Peninsula. Northing = 1,078,600 m in Palestine grid.

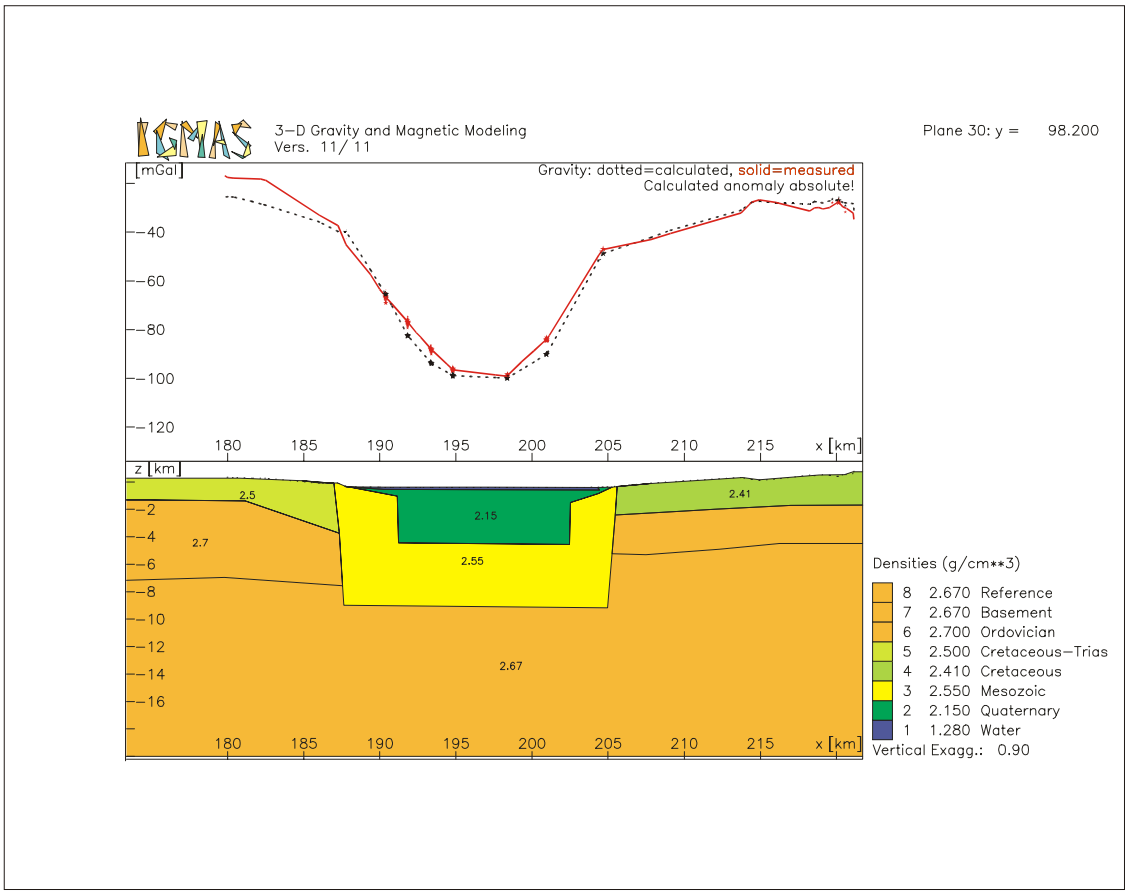

Figure 44: Computed crustal model for the DSR along the north plane Nr. 30. Northing = 1,098,200 m in Palestine grid

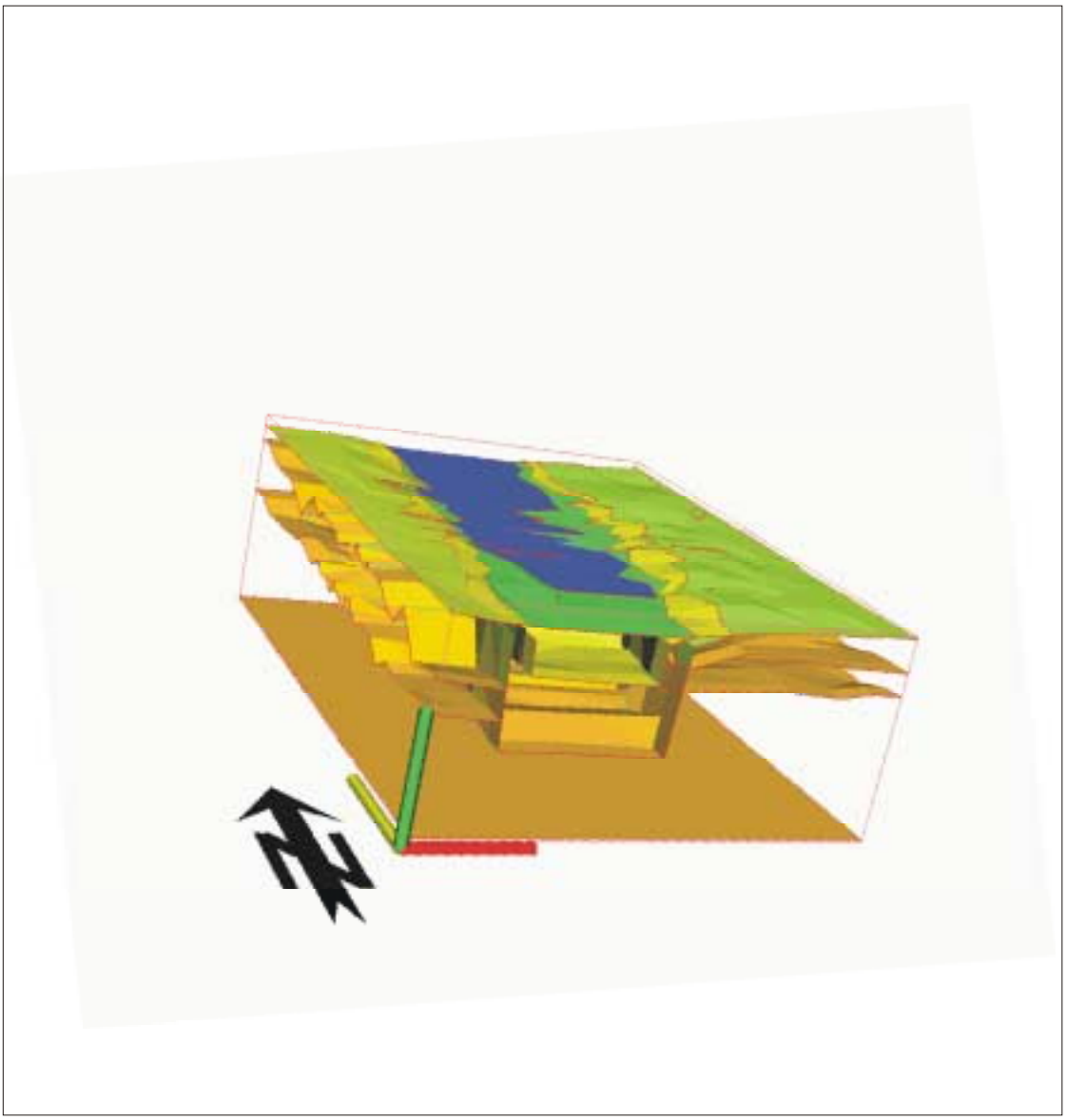

Figure 45: 3D image of the subsurface structure of the DSB.

9 RELATIVE DEPTH TO CRYSTALLINE BASEMENT ESTIMATION BENEATH JORDAN AND BENEATH (IN) THE JORDAN RIFT VALLEY AS INTERPRETED FROM GRAVITY AND AEROMAGNETIC DATA ANALYSIS

9.1 Introduction

Accurate quantitative estimates of the depth to the top of the bedrock can be calculated from the gravity models and aeromagnetic map of Jordan which reflects the magnetic basement, because bedrock usually has a high susceptibility value than the overlying cover. The estimation of the depth to the bedrock requires an accurate regional-residual separation, knowledge of the density contrast between the basin fill deposits and bedrock, gravity models that reasonably represent the geologic situation in the area of interest and well logs from deep boreholes. The previous requirements are available for this research. More than 60 deep boreholes for oil exploration were drilled by NRA in different areas in Jordan. Samples of the well logs were shown in Appendix 2.

Several profiles for depth determination have been chosen on the selected closures (sphere shape) of magnetic anomalies, Figure 46. The profiles provide a basis for determining the depth to the top of the source body (e.g. depth to crystalline basement). Significant characteristic of a magnetic anomaly is its variation with the depth between the magnetometer and source; the deeper the source, the broader the anomaly.
There are several different methods for estimating the depth to the top of the source body from potential field data, the simplest one is the half-width method: the depth to body is half the width of an anomaly at half its maximum amplitude. It is the horizontal distance between the principal maximum (or minimum) of the anomaly (assumed to be over the center of the source) and the point where the value is exactly one-half the maximum value. This rule is valid only for simple shaped forms such as a sphere (dipole).

The results of the magnetic depth determinations have an uncertainty of about ± 15%.

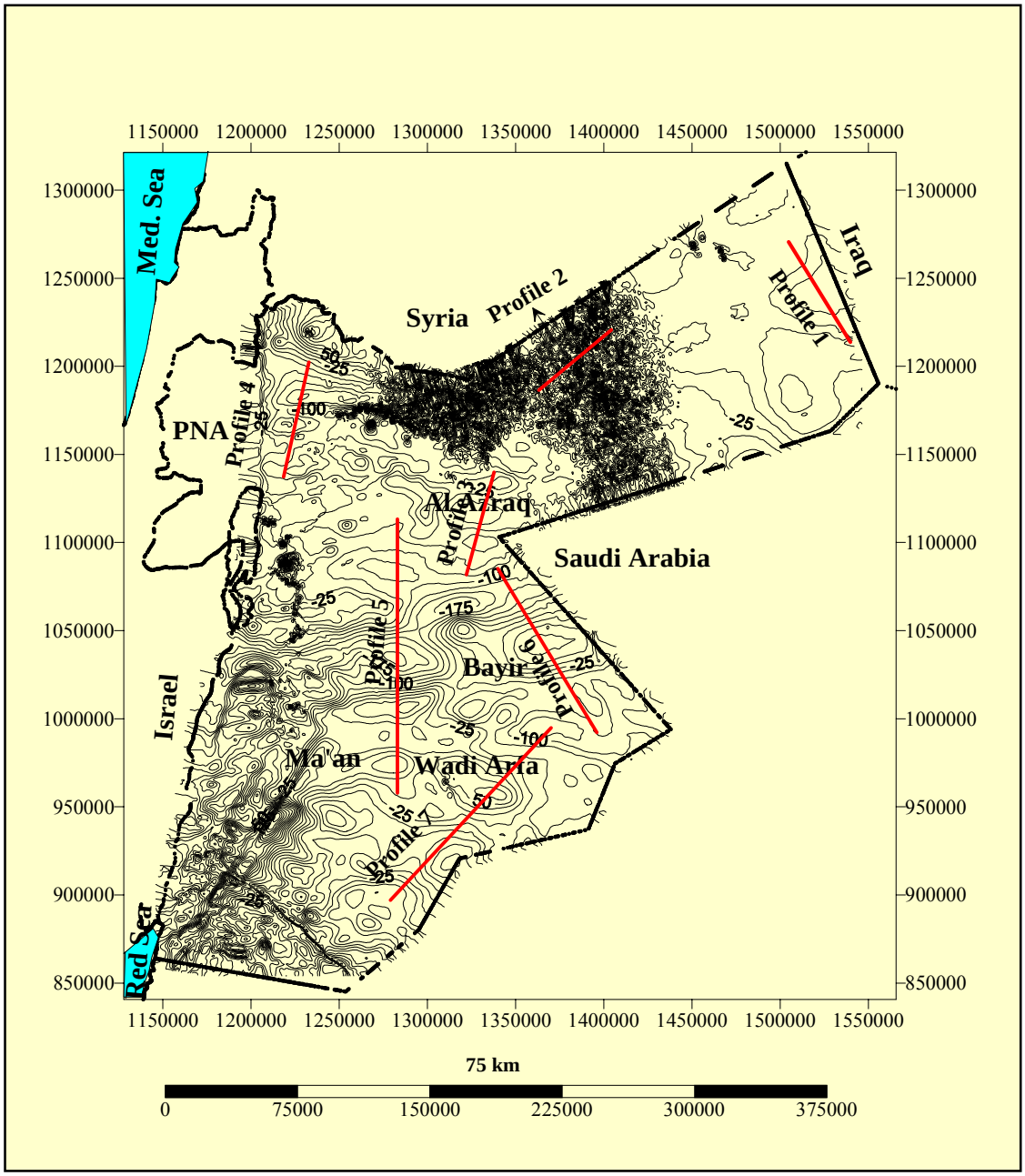

Figure 46: Aeromagnetic anomaly map shows several profiles along the selected closures of the magnetic anomaly map of Jordan.

9.2 Depth to the bedrocks estimations utilizing half-width method

Half-width method for depth to bedrocks estimating was used in the present research a long several selected profiles.
Profile 1 (Figure 47), 60 km long, is located in the Risha area, starting about 8-10 km south of Wadi el Mirba at the Iraqi borders, crossing Tallat el Bustana and ended up about 5-6 km north of Wadi Mudeisis. The following investigation oil boreholes are drilled along this profile: RH-15, RH-32, RH-09, RH-20, RH-06, RH-03, and RH-05. The depth of the previous exploration oil wells is between 3200-5000 m and reached to the Ordovician Dubaydib formation where the deposits of gas where found. It is apparent in the Risha area that the magnetic structures have a relationship with the location of the gas field.

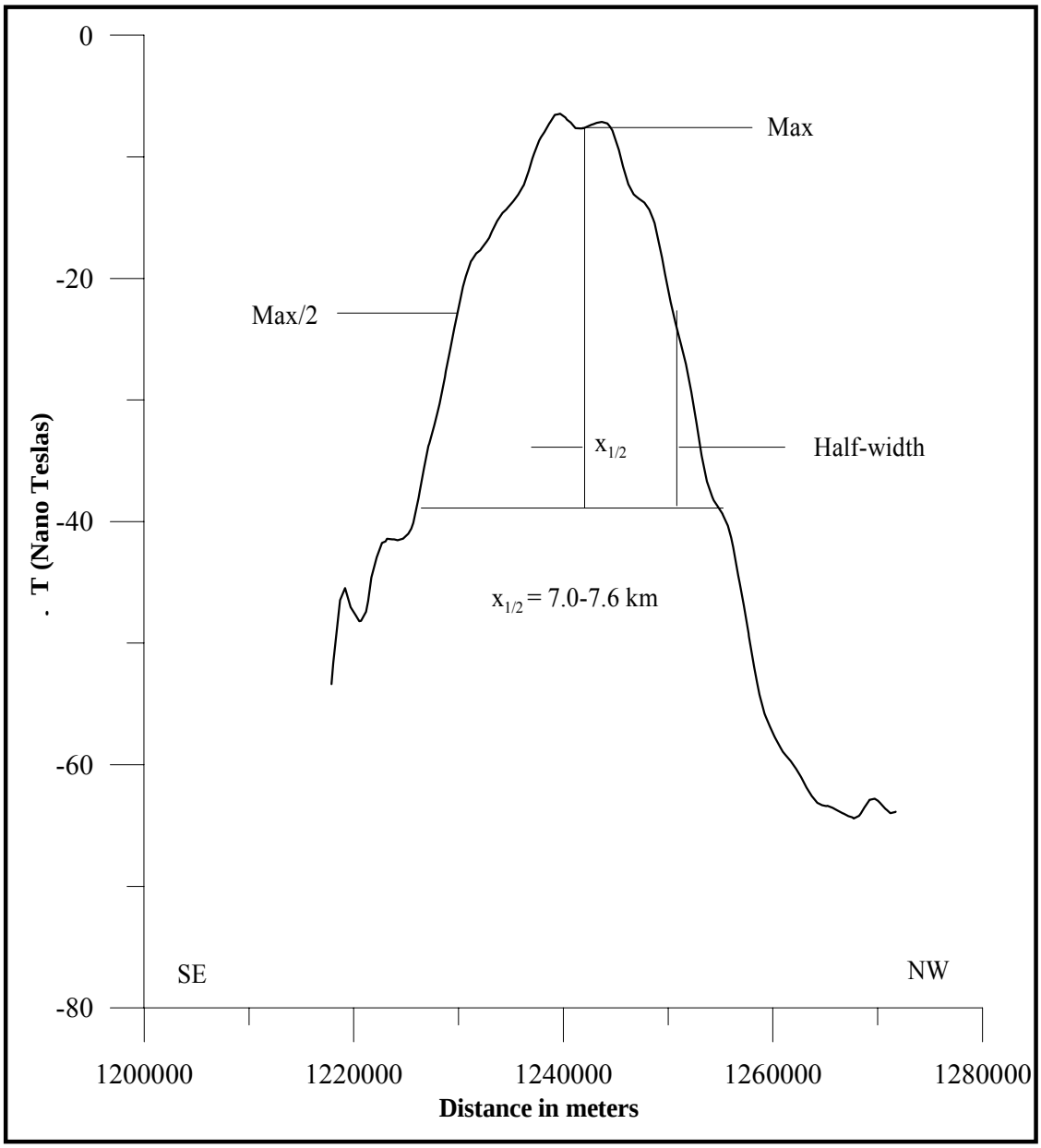

Figure 47: Total field magnetic anomaly along profile 1 in the Risha area. The depth to the bedrocks beneath this profile is approximately 7.0-7.6 km.

Profile 2, Figure 48, 40 km long, is located in the north east of the basaltic plateau starting about 7 km to the north of Wadi Al A'bd and ended up about 5-6 km south of Tulul esh Shahba area. One investigation oil well called Al A'bd-1 was drilled in Wadi Al A'bd area. The depth of this borehole is 4700 m reached to the Ordovician formation. The depth to the basement beneath this profile is approximately 5.6-6.2 km.

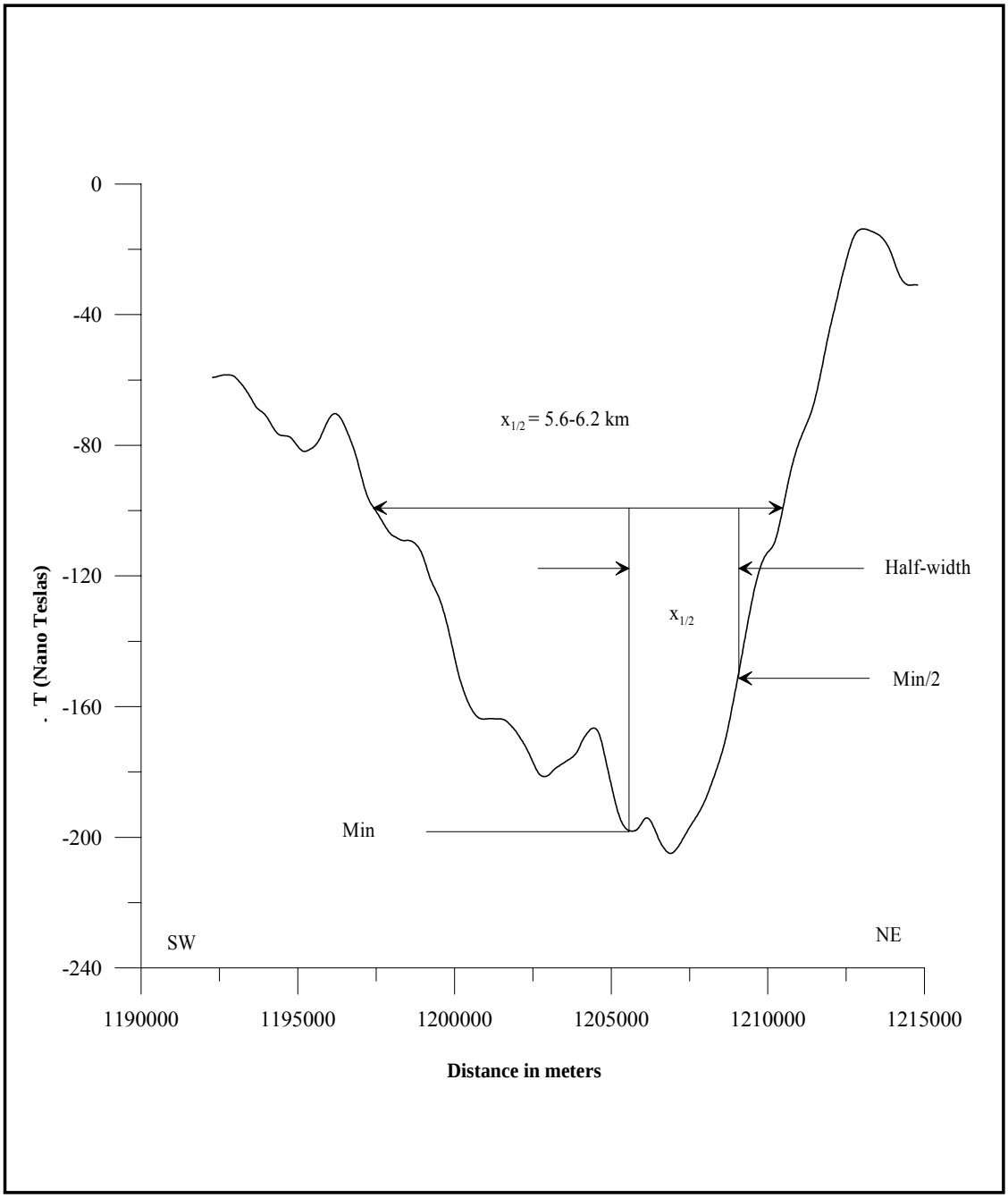

Figure 48: Total field magnetic anomaly along profile 2 in the north east of the basaltic plateau. The depth to the bedrocks beneath this profile is approximately 5.6-6.2 km.

Profile 3, Figure 49, 50 km long, is located in Al Azraq area, starting about 2 km of Qasr Et Tuba, crossing Wadi el Ghadaf and ended up about 3 km south of Al Azraq city. Several investigation oil wells were drilled along the area of this profile such as HZ1, HZ2, and HZ14. Oil shows found in Al Kurnub sandstone. NRA still producing oil from this area. The depth of these boreholes is 3700-5200 m reached to the Ordovician formation According to half-width method, the depth to the bedrock beneath this profile is approximately 5.5-6.0 km.

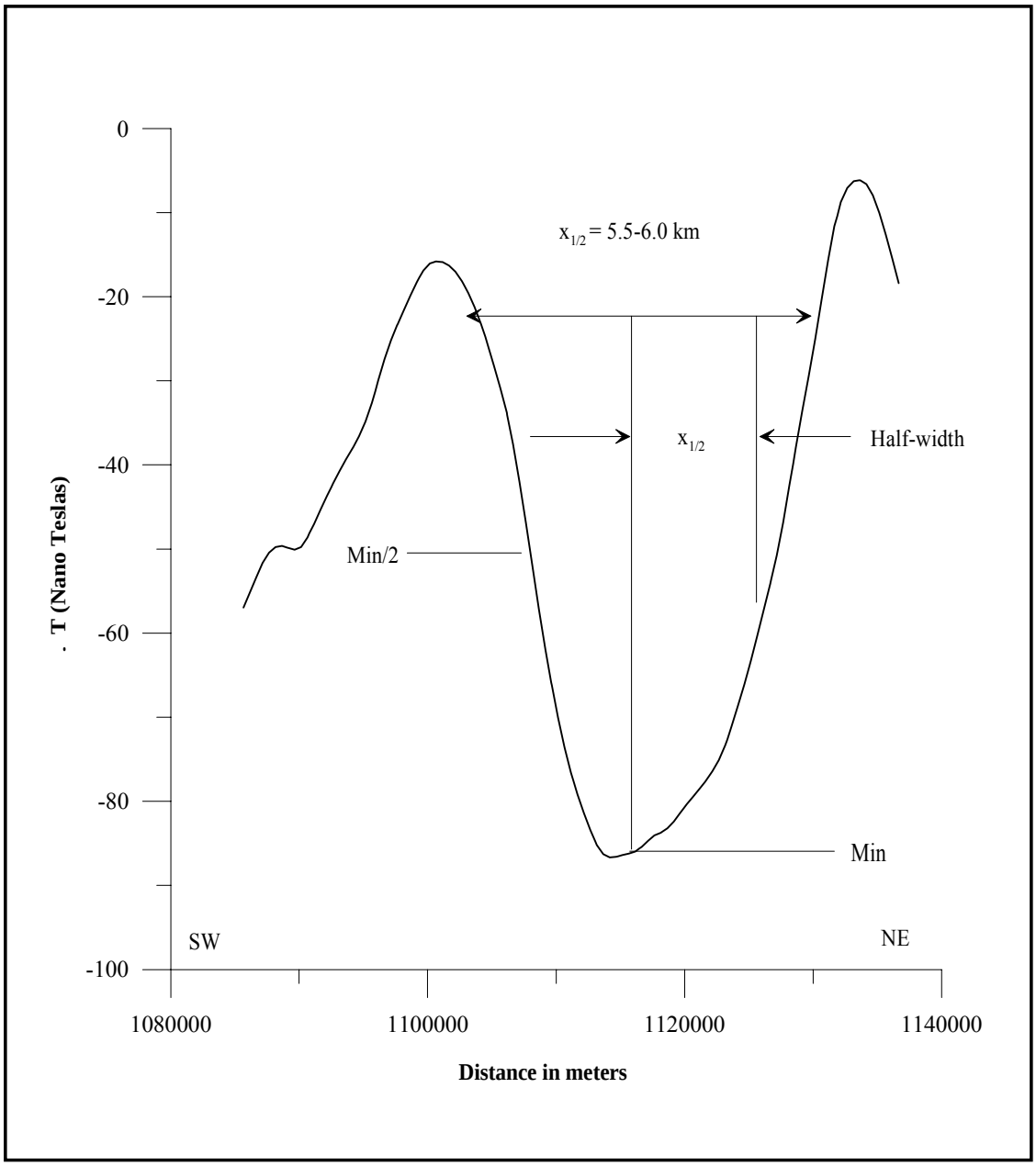

Figure 49: Total field magnetic anomaly along profile 3 in Al Azraq basin. The depth to the bedrocks beneath this profile is approximately 5.5-6.0 km.

Profile 4, Figure 50, 55 km long, is located in the north of Jordan, starting from Salt, crossing A'jlun, Jarash and ended up about 1 km south of Irbid city. One investigation oil well (A'jlun-1) was drilled in the center of this profile on A'jlun dome. The depth of these boreholes is 4200 m reached to the Salib formation.
According to half-width method, the depths to the bedrock beneath this profile are approximately 3.6-4.0 km, 3.1-3.3 km and 4.5-5.0 km beneath A'jlun dome.

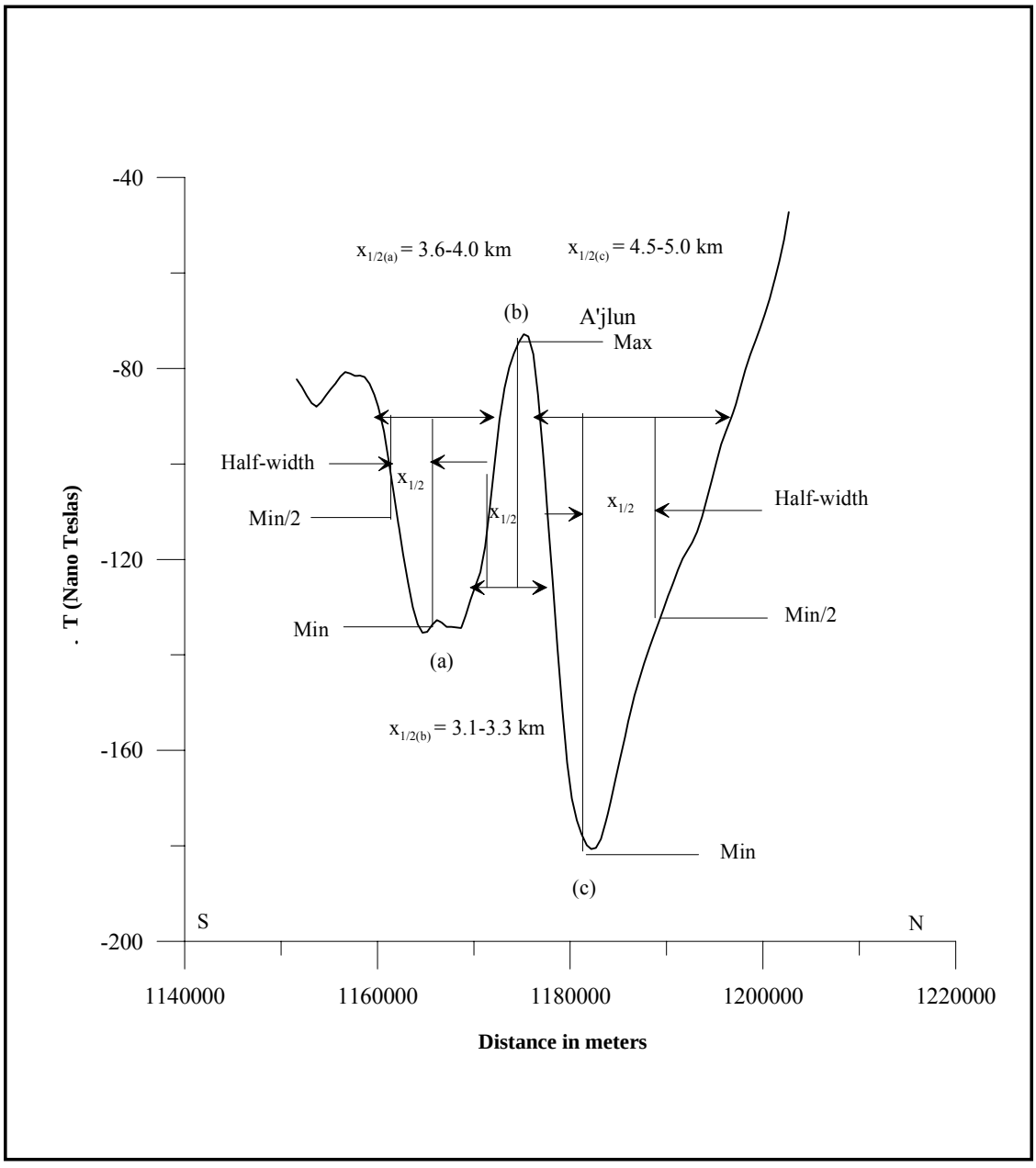

Figure 50: Total field magnetic anomaly along profile 4 in A'jlun area. The depth to the bedrocks beneath this profile is approximately 4.5-5.0 km.

Profile 5, Figure 51, 65 km long, is located in the central part of Jordan, starting about 2 km south of Al Jafr area, crossing Jabal al Mutrammel, Swaqa and ended up about 1 km north of Khan Ez Zabib area. One investigation oil well (Jafr-1) was drilled in Al Jafr area. The depth of these boreholes is 4048 m and reached the Precambrian basement. According to half-width method, the depths to the bedrock beneath this profile are approximately 3.5-4.0 km in Al Jafr area, 5.5-6.0 km in the central part of this profile, and 3.5-4.0 km beneath Swaqa and Khan Ez Zabib.

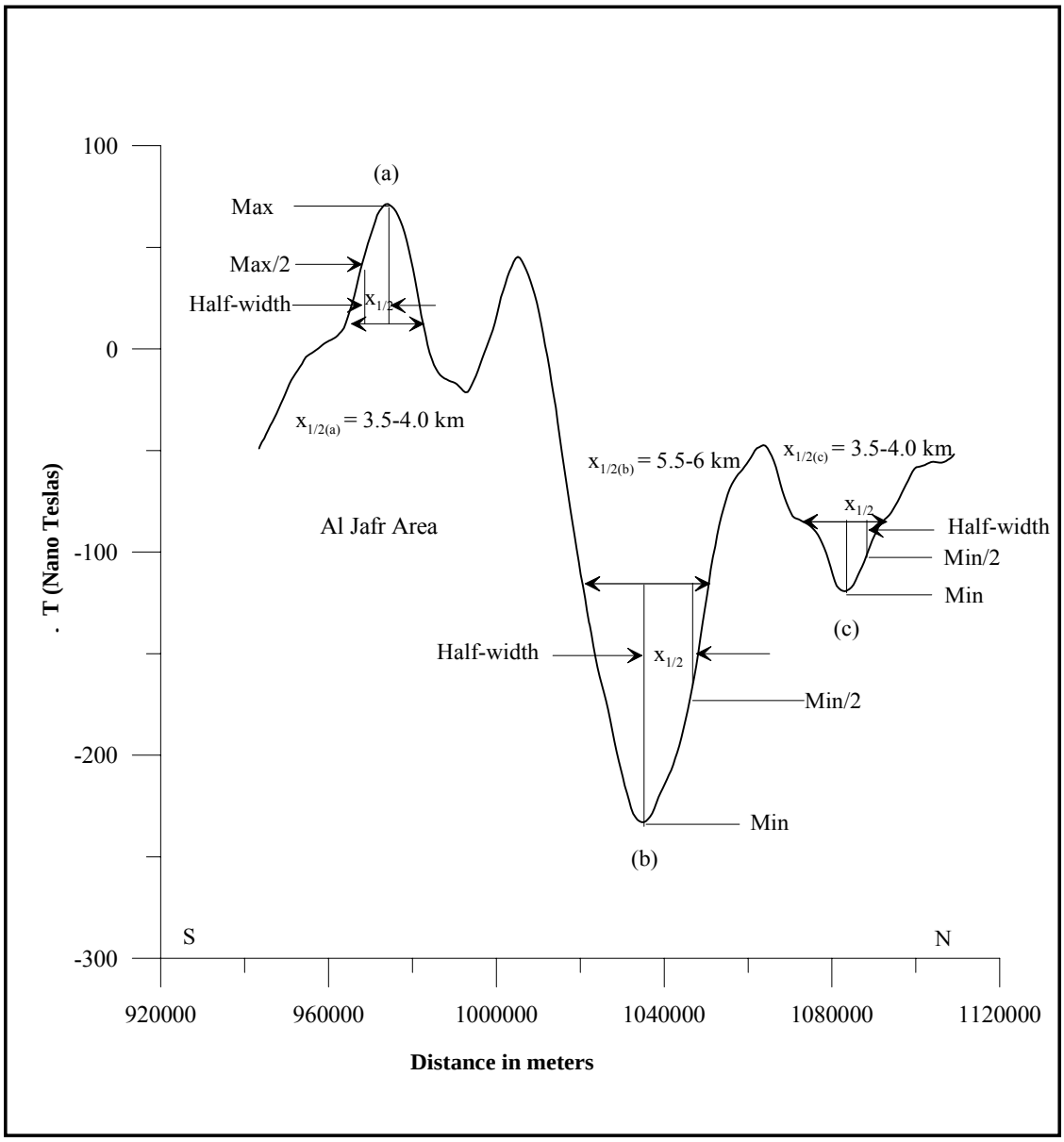

Figure 51: Total field magnetic anomaly along profile 5 in the central part of Jordan a. The depth to the bedrocks beneath this profile is approximately 3.5-4.0 km, 5.5-6.0 km and 3.5-4.0 km.

Profile 6, Figure 52, 130 km long, is located in the south east of Jordan, starting about 1 km south of Mushash Hudruj and ended up about 2 km north of Qasr Tuba. According to half-width method, the depth to the bedrock beneath this profile is approximately 4.5-5.0 km.

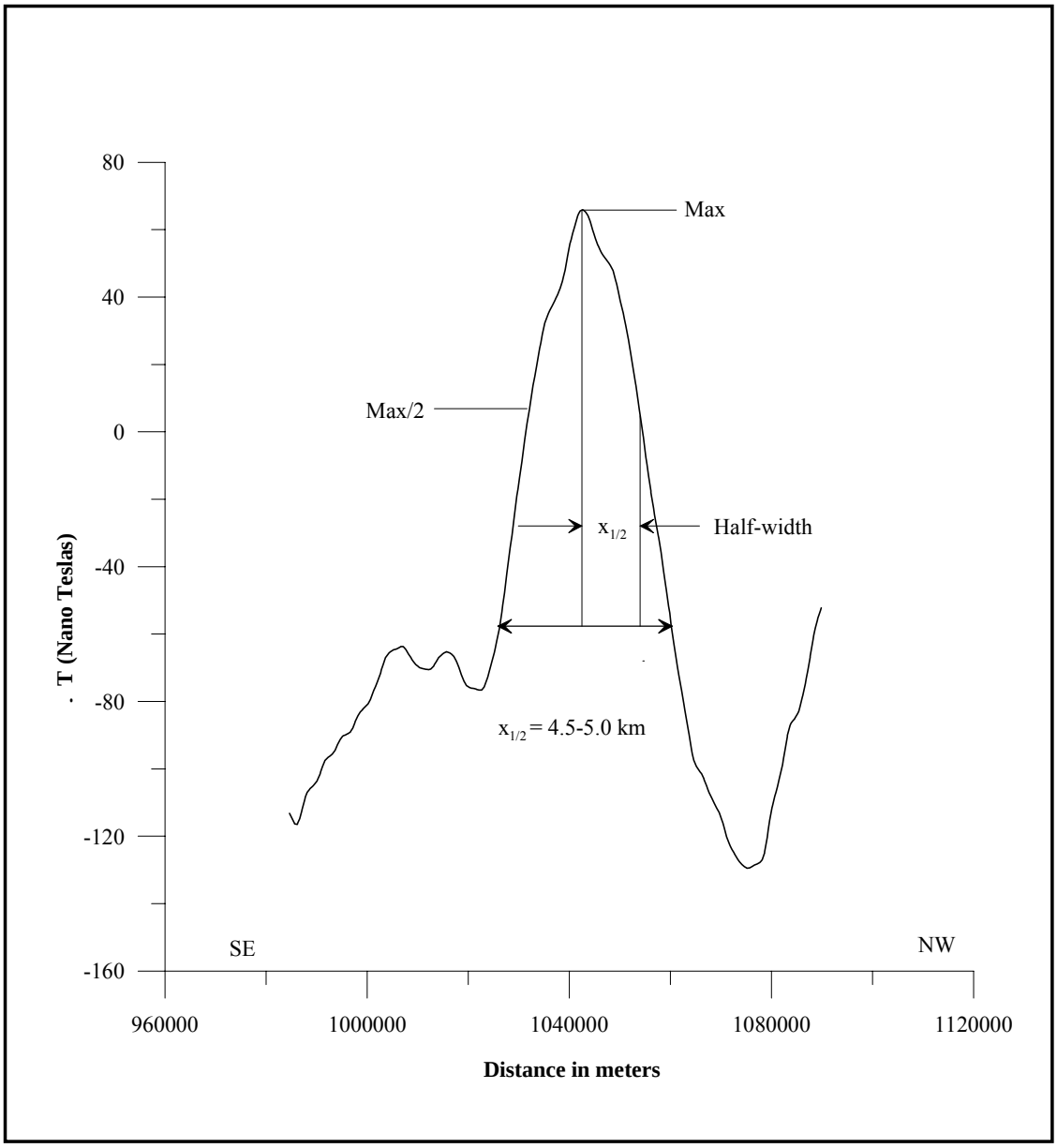

Figure 52: Total field magnetic anomaly along profile 6 in the south east of Jordan. The depth to the bedrocks beneath this profile is approximately 4.5-5.0 km.

Profile 7, Figure 53, 105 km long, is located in the south of Jordan, starting about 1.5 km west of El I'nab area and ended up about 2 km north of Wadi Hudruj area. According to half-width method, the depth to the bedrock beneath this profile is approximately 4.8-5.5 km.

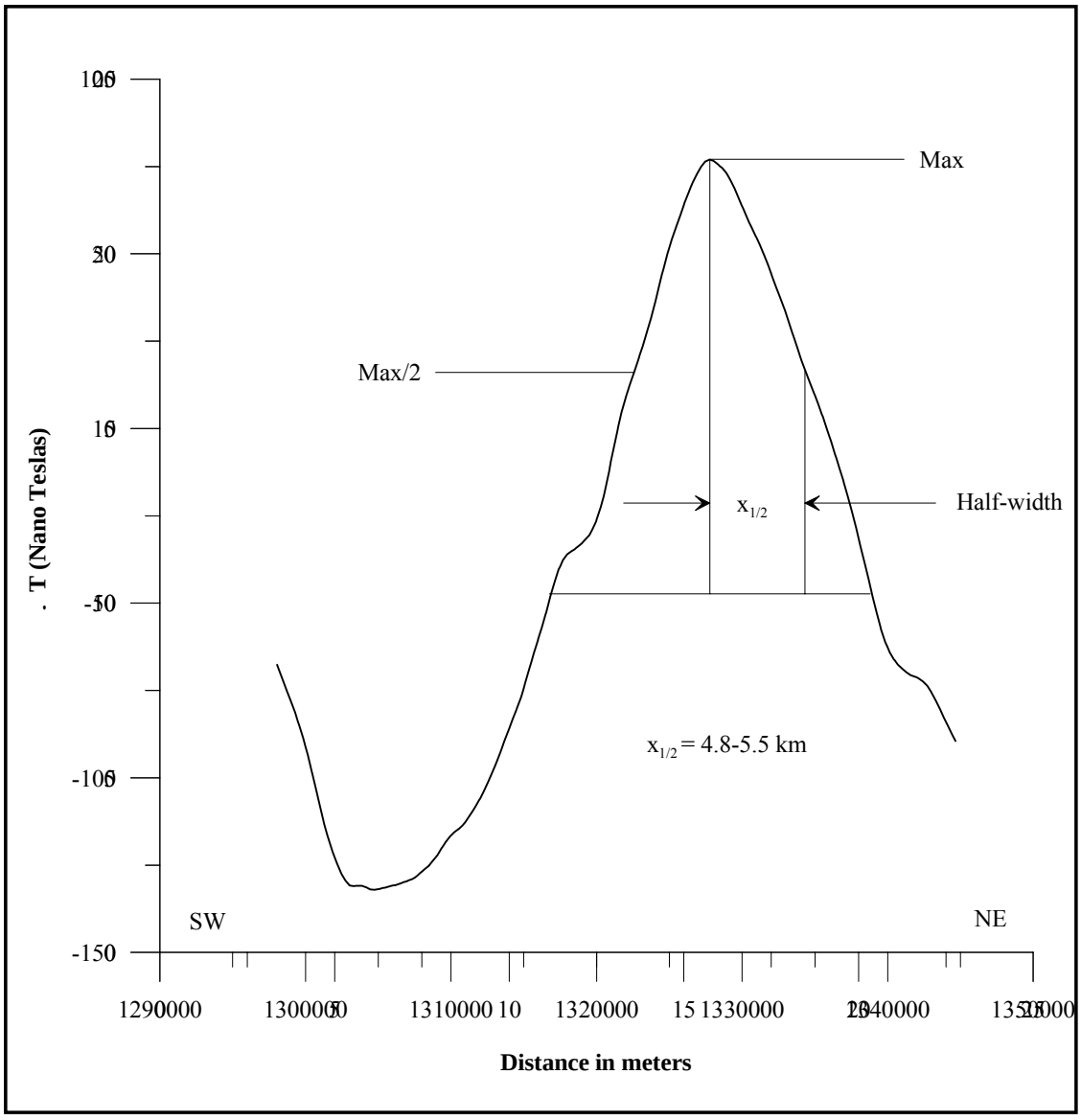

Figure 53: Total field magnetic anomaly along profile 7 in the south east of Jordan. The depth to the bedrocks beneath this profile is approximately 4.8-5.5 km.

9.3 Overview the basement depths map of Jordan

The basement depths map of Jordan (Figure 54) shows that the greatest depths to the magnetic basement are beneath the Lisan Peninsula of the Dead Sea basin, in the Risha area and in the Azraq-Wadi Sirhan basin. The total cover in the Lisan is 15,000 to 16,000 meters and in the Risha and Al Azraq basin is 7000 and 5000 meters. The basement map suggests a considerable thickness of sediments under the central part of the map and under the basalt cover in northeastern of Jordan. (5.5 to 7 thousand meters from the surface). The basement crops out in the southwest of the map and in the northernmost of the map. The basement shallows from the central part of Jordan in two directions: to the northwest and to the southwest of Jordan.

On a regional basis, this map should provide important information for oil exploration in Jordan in future because it outlines the basins and gives acceptable estimate of the total sedimentary cover in the basins.

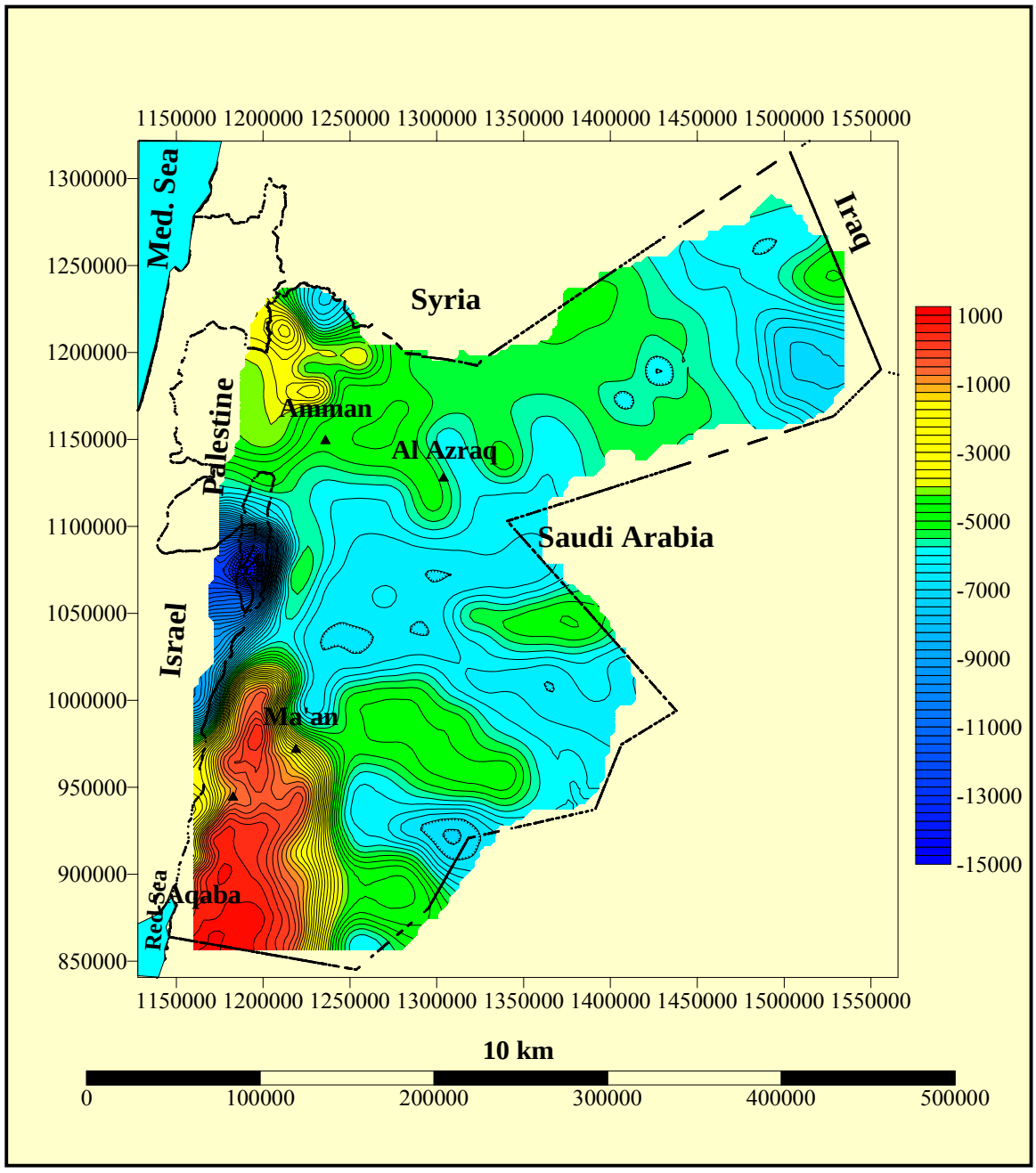

Figure 54: Preliminary basement relief map beneath Jordan from aeromagnetic, gravity and drill hole logging analysis.

10 CONCLUSIONS

Modern techniques of processing and interpretation of Bouguer gravity and aeromagnetic anomaly maps delineate the major tectonic geological structures in Jordan and reveal numerous strong negative gravity closures occupying the Rift Valley from north to south which are interpreted as shallow basins. Major fault systems are recognizable from gravity and aeromagnetic anomaly maps, north to NNE – trending faults that parallel and are adjacent to the Dead Sea Rift are prevalent in a Belt extending 100 km, north from Aqaba. Crystalline Precambrian rocks outcrop in the neighborhood of the Belt. The Araba FZ and Quweira FZ are part of this system of fractures. WNW-trending faults are also recognizable in the anomaly maps. The magnetic anomaly trends change abruptly as we move from southern to northern Jordan. The Tell Bustana FZ in the Risha area and Swaqa FZ, are included in this system of faults. Some of these faults are associated with shallow – origin negative gravity anomalies. The Finan Zukimat el Hasa FZ is probably the most prominent in these structures because of its horizontal extent and vertical displacements.

Basement depressions structures are interpreted from the gravity and aeromagnetic anomaly maps such as the Al Jafr basin, it is a rather broad basement depression flanked by the Karak Wadi al Fayha FZ. Basement relief beneath this basin is approximately 3.8-5.2 km. The Sirhan basin in the southeast corner of Jordan is apparent from the gravity and aeromagnetic anomaly maps. The Al Azraq basin, a 40 km wide depression filled with covers 1000 m of Cenozoic sediments. It is bounded to the east by the Fuluk fault which is associated with a very prominent gravity gradient. This gradient is due to the very substantial vertical throw across this fault zone.

Basement high structures also interpreted from the anomaly maps such as A'jlun high structure located in north Jordan, basement uplifts located on the up thrown side of Tell Bustana FZ, horst – like structure developed on the up thrown side of the Finan Zukeimat el Al Hasa FZ, the high structure that separates the Sahb Abyyad and Al Jafr basin, Al Hasa horst structure which is bounded to the north by the Hasa FZ, serious of horst structures in the Sirhan area, and most prominent horst structure bounded by Suwaqa fault zone, associated with major relief on the magnetic basement.

Regional E-W profiles of topography, free-air, observed gravity and Bouguer gravity anomalies across the Dead Sea transform reveal regional Bouguer anomaly under the transform valley and strong negative Bouguer anomaly under the central part of the Dead Sea basin.

The gradual decrease in the gravity from the northern and southern ends of the DSB indicates that the basin sags from the two ends toward the deepest part in the Lisan Peninsula of the DSB.

3D gravity models emphasize that the DSB is a full graben bounded by vertical faults with collapsed side blocks toward the basin. The longitudinal faults bordering the pull-apart, being continuations of the major strike-slip faults north and south of the basin. These faults are the dominant structural element along the Dead Sea transform.

The sedimentary bodies within the Dead Sea depression are marked by exceptional high rates of accumulation and great thicknesses, reaching 12-16 km beneath the

central part of the DSB, where the volume of the Lisan Diapir (salt body) is about 650 km^3. The strong negative Bouguer gravity value in the central part of the DSB is due to the presence of the salt body.

First derivative maps of the north, south, central parts of the DSB emphasize the short wavelength features of the Bouguer gravity anomaly maps.

The aeromagnetic anomaly map of Jordan, Palestine and Israel confirms the total offset along the Dead Sea wrench fault of about 105-107 km.

The greatest depths to the magnetic basement are found beneath the Lisan Peninsula of the Dead Sea basin, in the Risha area, Harrat Al Sham basaltic Plateau and in the Azraq-Wadi Sirhan basin. The results of the magnetic depth determination show that there is considerable basement topographic relief in Jordan.

This considerable thickness of sediments is very important for future oil investigations in Jordan.

11 REFERENCES

Abed, A M., 1985, Geology of Jordan. Al-Nahda Al Islamya Library. Amman-Jordan.

Abed, A M., 1985, On the supposed Pre-Cambrian pale suture along the Dead Sea Rift, Jordan. J. Geol. Soc. London, 142, 527-531.

Arbenz, J. K. , 1984, Oil potential of the Dead Sea area, Rep no. 84/111, seismic oil explor. Ltd. , Tel Aviv.

Barberi, F. , Capaldi, G. , Gasparini, P. , Marinelli, G. ,Saatracroce, R. , Scandone, R. , Tureil, M. and Varet, J. , 1979, Recent basaltic volcanism of Jordan and its implications on the geodynamic history of the Dead Sea Shear Zone, Inter. Symp. Geodynamic Evol. of the Afro-Arabian rift systems, Rome.

Basha, S., 1983, Formation and Ostracoda from Holocene sediments in the Jordanian part of the Gulf of Aqaba, Dirasat, Vol. X, PP. 109-129.

Ben-Avraham, Z., ten Brink, and Joseph Charrach, Transverse fault at the northern end of the southern basin of the Dead Sea graben, Tectonophysics, 180, (1990) 37-47.

Bender, F. , Die Sandige Schichtenfolge der Kreide in Sud-Jordanien (von F. Bender) mit der Bearbeitung einer Angiospermen-Flora aus diesen schichten (von K. Madler). Geol. Jb. Hannover: 1968.

Bender, F., Geology of Jordan, Gerbruder Borntraeger. Berlin: 1974 F. Bender. Geology of the Arabian Peninsula. U.S. Geol. Surv. Prof. Paper 560-1.

Bender, F., Geology of Jordan, 1974.

Bender, F., Geology of the Arabian Peninsula, Jordan,1975.

Bilham, R. , and G. King, 1989, The morphology of strike-slip fault: examples from the San Andreas fault, California, J. Geophys. Res. , 94, 10204-10216.

Bowin Carl, The earth's gravity field and plate tectonics, Tectonophysics, 187 (1991) 69-89.

Dubertret, L., 1932, Les formes structural de la Syrie et de la Palestine; Leur origine. C. R. Acad. Sci., Colon, Paris, T. 195.

Eckstein, Y. and G. Simmons, 1978. Measurements and interpretation of terrestrial heat flow in Israel, Geothermics, 6, 117-142.

Ellett William.J., Geologic controls on the occurrence and movement of water in the lower Cienega Creek basin. Master thesis in the graduate cooledge, University of Arizona, 1994.

Flathe, H. (1968): Geoelektrische untersuchung der grundwasserversalzung im sudlichen Jordantal. Geol. Jb. 85: 767-782, Hannover.

Folkman, R. , 1981, Magnetic and gravity investigations of the Dead Sea rift and adjacent areas in northern Israel, Geophysics, Vol. 48, pp. 34-39.

Freund, R. and Z. Garfunkel, 1976, 27 pp. , the Hebrew University, Jerusalem.

Freund, R. , 1965, A model of the structural development of Israel and adjacent areas since Upper Cretaceous times, Geol. Mag. , 102, pp. 189-205.

Freund, R. , Zak, I. and Garfunkel, Z. , 1968, Age and rate of the sinistral movement along the Dead Sea rift, Nature, Vol. 220, pp. 253-255.

Freund, R. , Garfunkel, Z. , Zak, I. , 1970, the shear along the Dead Sea rift. Phil, trans. Roy. Soc. London A 267, 107-130.

Frieslander, U. and Z. Ben Avraham, 1989, the magnetic field over the Dead Sea and its vicinity, Mar. Pet. Geol. , in Press.

Galanis, S., Sass, J., Munroe, R. and Abu-Ajamieh, M., 1986, Heat flow at Zarqa Main and Zara and a geothermal reconnaissance of Jordan, USGS open file Report 86-631, 110 P.

Garfunkel, Z. , 1981. Internal structure of the Dead Sea leaky transform (rift) in relation to plate kinematics, Tectonophysics. , 80, 81-108.

Gettings, M.E., the isostatic gravity anomaly field of southwestern Saudi Arabia and its interpretation, Technical record, USGS-TR-04-22, 1984.

Ginzburg, A., and Y. Folkman, Geophysical investigation of crystalline basement between Dead Sea rift and Mediterranean Sea, AAPG Bull., 65, 490-500, 1981.

Götze, H.-J., 1978: Ein numerisches Verfahren zur Berechnung der gravimetrischen Feldgrößen drei-dimensionaler Modellkörper. Arch. Met. Geoph. Biokl., Ser. A, 25, 195-215.

Götze, H.-J., 1984: Über den Einsatz interaktiver Computergraphik im Rahmen 3-dimensionaler Interpretationstechniken in Gravimetrie und Magnetik. Habilitations-Schrift, 121 Seiten, Technische Universität Clausthal.

Götze, H.-J. and B. Lahmeyer, 1988: Application of three-dimensional interactive modeling in gravity and magnetics, Geophysics Vol. 53, No. 8, 1096 - 1108.

Götze, H.-J. und S. Schmidt, 1998: Komplexe Interpretation zur Kohlenwasserstoff - Exploration mit 3D Dichtemodellen und GIS-Funktionen. Forschungspolitischer Dialog, Berliner Senat für Wissenschaft, Forschung und Kultur, Berlin. HTML version

Hall, J. and Neev, D., 1979, Geophysical investigations in the Dead Sea, Sed. Geol. 23, 209-238.

Ilani, S., The paleogeography of the Pleshel and Ahuzain Formations (Pliocene-Pleistocene) in the western Shomeron Foothills, Israel, J. Afr. Earth Sci., 11, 233- 242, 1990.

Joffe, S., and Z. Garfunkel, Plate kinematics of the circum Red Sea-A reevaluation, Tectonophysics, 141, 5-23, 1987.

Kashai, E. L., A review of the relations between the tectonics, sedimentation and petroleum occurrences of the Dead Sea-Jordan Rift system, in Triassic-Jurassic Rifting: Continental Breakup and the Origin of the Atlantic Ocean and Passive Margins, edited by W. Manspeizer, Dev. Geotectonics, 22, 883-909, 1988.

Kashai, E. and P. Crocker, 1987, Structural geometry and evolution of the Dead Sea-Jordan rift system as deduced from new subsurface data, Tectonophysics. , 141, 33-60.

Khalil Basem, The geology of the Ar Rabba area map sheet No. 3152 IV, Bulletin 22, Natural Resources Authority, Amman, 1992.

Knopoff. L. and J.C.Belshe, Gravity observation of the Dead SEA rift, geologic survey of Canada, pages 5-19, 1966.

Mart, Y. and Hall, J. 1984, Structural trends in the northern Red Sea. J. Geophys. Res. 89, 352-364.

Mckenzie, D., 1978, some remarks on the development of sedimentary basins, Earth Planet. Sci. J. , 40, 25-32.

Mikbel, S. and Atallah, M., 1983, Tectonics of Jordan, contribution to the structures of north Jordan, Jordania Geological Conference.

Neev, D. and Emery, K., 1967, The Dead Sea depositional processes and environments of evaporates. Geol. Survey. Israel, Bull. 41.

Nur, A. , H. Ron, and O. Scotti, Fault mechanics and the kinematics of block rotation, Geology, 14, 746-749, 1986.

Powell, J. and Khalil, B. , 1988, Structure and sedimentation of Permo-Teriassic and Triassic rocks exposed in small scale horsts and grabens of Pre-Cretaceous age, Dead Sea Margins, Jordan. 3rd Jordanian Geologists Conference.

Powell John H., 1988, the geology of Karak area, map sheet No. 3152 III, Bull 8, Natural Resources Authority (NRA), Amman.

Quennell, A., 1958, the structural and geomorphic evolution of the Dead Sea rift, Quart. J. Geol. Soc. Lond. , Vol. 114, pp. 1-24.

Rao & Murthy, Gravity and magnetic method of prospecting, 1978.

Reches, Z. and D. Hoexter, 1981, Holocene seismic and tectonic activity in the Dead Sea area, Tectonophysics. 80, 235-254.

Reches, Z. , 1987, Mechanical aspects of pull-apart basins and push-up swell with applications to the Dead Sea transform, Tectonophys. , 141, 75-88.

Rodgers, D. , 1980, Analysis of pull-apart basin development produced by en echelon strike slip faults, Spec. Publ. Int. Assoc. Sedimental. , 4, 27-41.

Ron, H., Deformation along the Yammuneh, the restraining bend of the Dead Sea Transform: paleomagnetic and kinematics implications, Tectonics, 6, 653-666, 1987.

Ron, H. , A. Aydin, and A. Nur, Strike slip faulting and block rotation in the lake Fault system, Geology, 14, 1020-1023, 1986.

Ron, H., A. Nur, and Y. Eyal, Multiple strike-slip fault sets: a case study from the Dead Sea transform, Tectonics, vol. 9, No. 6, pages 1421-1431, December 1990.

Rotstein, Y., Y. Bartov, and A. Hofstetter, Active compress ional tectonics in the Jericho area, the Dead Sea rift, Tectonophysics, 198, 239-259, 1991.

R. Stern. Najd Fault System Saudi Arabia and Egypt: a Late Precambrian Rift Related Transform System. Tectonic, Vol. 4, No.5 (1985)

Sa'ar, H., Origin and sedimentation of sandstones in graben fill formations of the Dead Sea rift valley, Rep. MM/3/86, Geol. Surv. of Isr., Jerusalem, 1985.

Schwartz Kerry, a geohydrologyic investigation of volcanic rocks using the gravity survey method: Galiuro mountains, Graham, Pinal and Cochise counties, Arizona, Master thesis in the graduate college, the University of Arizona, 1990.

Segall, P. and D. Pollard, 1980-, Mechanics of discontinuous faults, J. Geophys. Res. , 85, 4337-4350.

Steckler, M. S., and U. S. ten Brink, Lithospheric strength variations as a control on new plate boundaries: Examples from the northern Red Sea region, Earth Planet. Sci. Lett., 79, 120-132, 1986.

S.H. Mikbel. New Lights on the Major Structural Framework and Rift Tectonics of North and Central Jordan. University of Jordan: 1985

Sunna, B., 1986, the geology of salt deposits in the Lisan Peninsula, Dead Sea. Seminar on salt in the Arab World, Amman, 1-25.

Telford, W.M., Geldart, L.P., Sheriff, R.E., and Keys, D.A., 1981, Applied Geophysics: Cambridge University Press.

ten Brink, Ben-Avraham Z. , Bell R. E. , Hassouneh M., Coleman D. F. , Andreasen G. , Tibor G. , and Coakley B., Structure of the Dead Sea pull-apart basin from gravity analysis, Journal of geophysical research, Vol. 98, No. B12, pages 21,877-21,894 December 10, 1993

ten Brink and Z. Ben-Avraham, 1989, the anatomy of a pull-apart basin, seismic reflection observation of the Dead Sea basin. Tectonophysics, Vol. 8, pp. 333-350.

ten Brink, U. S. , N. Schoenberg, R. L. Kovach, and Z. Ben-Avraham, Uplift and a possible Moho offset across the Dead Sea Transform, Tectonophysics, 180, 77-92, 1990.

ten Brink, U., Rybakov, M., Al-Zoubi, A., Hassouneh, M., Batayneh, A., A., Frieslander, U., Goldschmidt, V., Daoud, M., & Rotestein, Y., 1998. Bouguer gravity anomaly map of the Dead Sea transform plate boundary in Israel and Jordan, scale 1:250,000, USGS open-file report.

ten Brink, U., Rybakov, M., Al-Zoubi, A., Hassouneh, M., Batayneh, A., A., Frieslander, U., Goldschmidt, V., Daoud, M., Rotestein, Y., & Hall, J.K. 1999.

The anatomy of the Dead Sea plate boundary: does it reflect continuous changes in plate motion? Geology, 27, 887-890.

Van Blaricom Richard, Practical geophysics II for exploration geologist, Northwest Mining Association, 1992

van Eck, T., and A. Hofstetter, Microearthquake activity in the Dead Sea region, Geophys. J. Int., 99, 605-620, 1989.

Yorri, M. and David, A., 1987, Post-Miocene rifting and diapirism in the northern Red Sea. Marine Geology, 74, pp. 173-190.

Zak, I., 1967, The geology of Mount Sedom, Ph. D. Thesis, Hebrew University, 208p.

Zak, I. , and R. Freund, Asymmetry and basin migration in the Dead Sea Rift, Tectonophysics, 80, 27-38, 1981.

APPENDICES

Appendix 1: Density depth observations in the selected oil exploration wells in Jordan.

Thickness in meters	Period	Formation
0-50	Tertiary	Sara
50-600	Cretaceous	Shueib
		Kurnub
600-1100	Triassic	Ma'in
1100-2100	Ordovician	Disi
2100-4000	Cambrian	Burj Dolomite
		Salib Arkosic Ss
4000	Precambrian	Saramuj

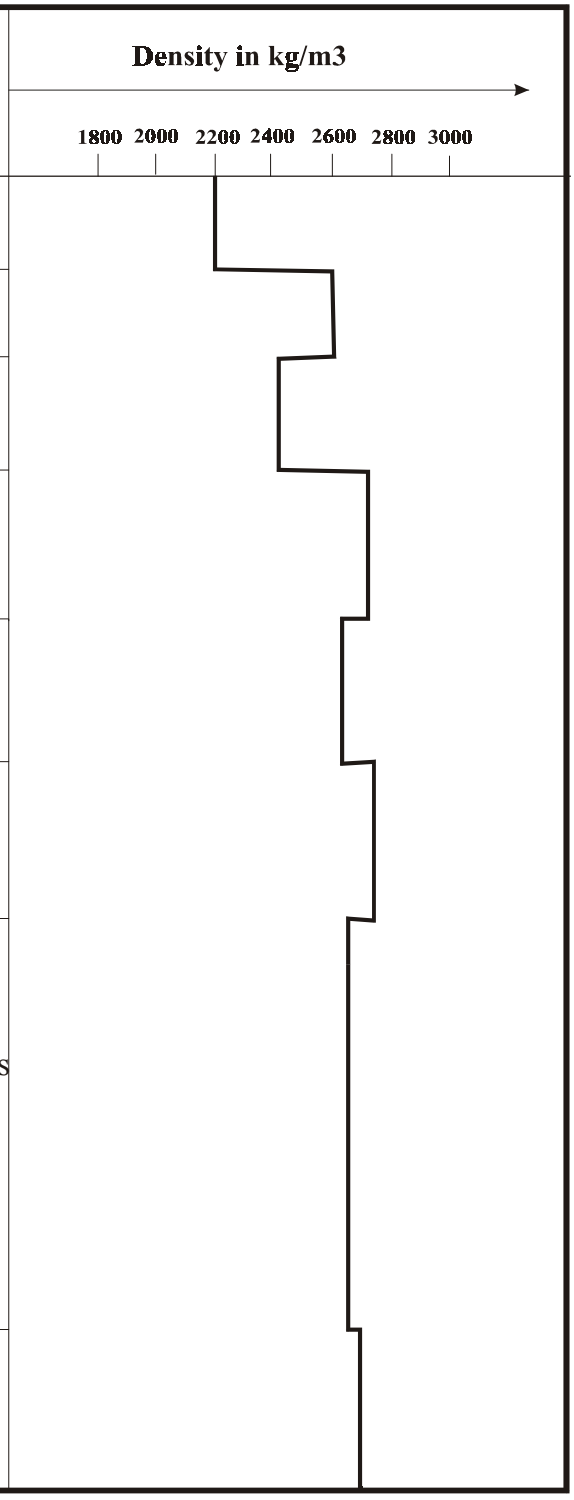

Table 2: Density depth observations in NH1 oil exploration well located near Al Mafraq area.

Thickness in meters	Period	Formation	Density in g/cm3
0-100	Tertiary	Sara	
		Taqiyeh	
100-250	Cretaceous	Ghareb	
		Wadi Essir	
		Kurnub	
250-450	Triassic	Ma'in	
450-2500	Sillurian	Khush Sha	
		Mudawwara	
2500-4000	Ordovician	Dubaydib	
		Hiswa	

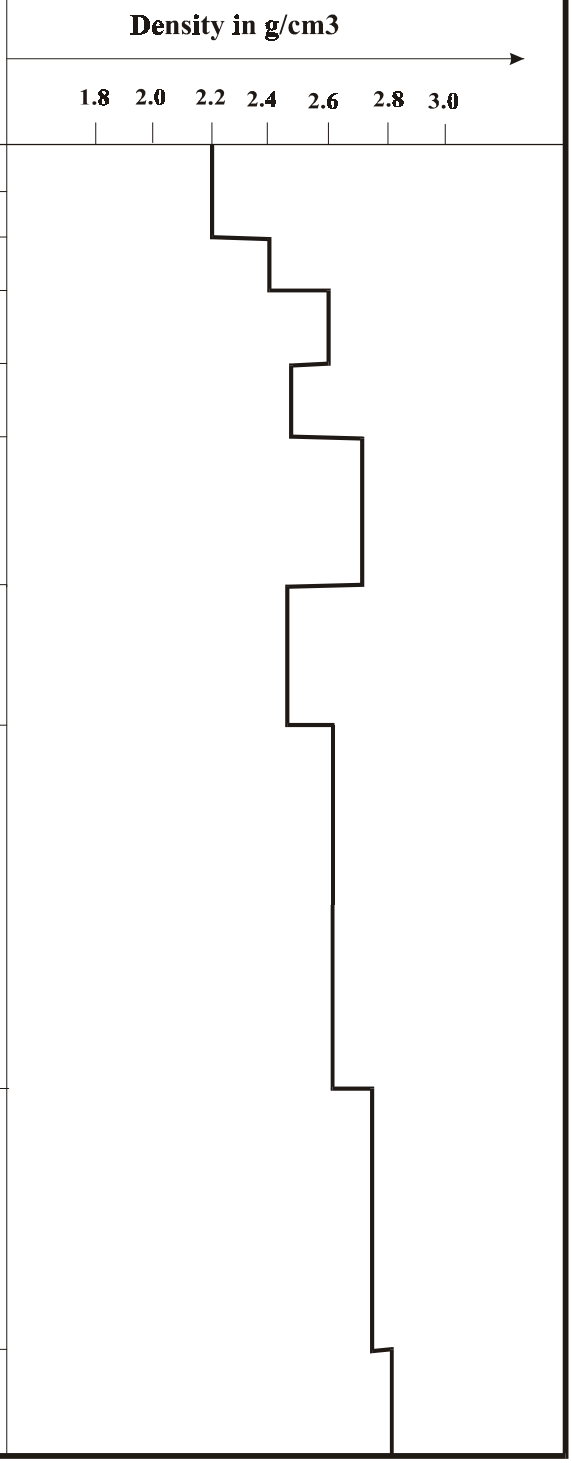

Table 3: Density depth observations in RH3 oil exploration well located in Al Risha area.

Formation	**Thickness (meters)**	**Density (kg/m^3)**	
Lisan - Marl	0-2460	2180	
Limestone	2460-2650	2620	Amman
Carbonates Anhydrate	2650-2881	2580	Wadi Es Sir
Cenomanian	2881.5-3260	2560	Carbonate +Shale
Kurnub	3260-3315	2800	sandstone

Table 4: Density depth log in I'sal1 oil exploration well drilled in the southern part of The DSB along plane Nr. 7 of the 3 D model. This borehole was drilled in 2002 by TransGlobal oil company. The calculated results from the 3D model were matched the drilling with percentage of more than 75%.

Appendix 2: Sample of model parameters for of one of the gravity planes in the study area.

```
#gmdf_ascii

unit Water
density    1.28000
unit Quaternary
density    2.15000
unit Mesozoic
density    2.55000
unit Cretaceous
density    2.41000
unit Cretaceous-Triassic
density    2.50000
unit Ordovician
density    2.70000
unit Basement
density    2.67000
reference_density    2.67000


plane   2
point        0.00000       47.00000
point      100.00000       47.00000
coordinates
    1      181.08580       -0.25974
    2      179.38921       -0.14691
    3      181.26489       -1.44149
    4      181.44659       -4.77559
    5      189.39604       -4.86693
    6      194.39285       -4.68424
    7      194.61998       -1.48717
    8      197.22031       -0.20441
    9      178.07080       -0.03408
   10       179.78650        -8.97054
   11       179.98360      -11.63779
   12       186.02631      -11.56570
   13       189.90150      -11.70988
   14       196.74040      -11.90938
   15       196.94910       -5.38777

unit Quaternary
vertices
    1   42   43   44   45   46   47   48   49   50    8    7
    6    5    4    3    2

unit Mesozoic
vertices
   54    9    1    2    3    4    5    6    7    8   18   17
   16   15   14   13   12   11   10   36

unit Cretaceous
vertices
   19   20   21   55   22   16   17   18   23   51   52   53
   24

unit Cretaceous-Triassic
vertices
   32   31   30   29    9   54   36   35   34   33

unit Ordovician
vertices
   33   34   35   36   10   37   38   39

unit Ordovician #2
vertices
   25   26   27   28   15   16   22   55   21   20

unit Basement
vertices
   39   38   37   10   11
```

Appendix 3: Computed crustal models of the Dead Sea basin.

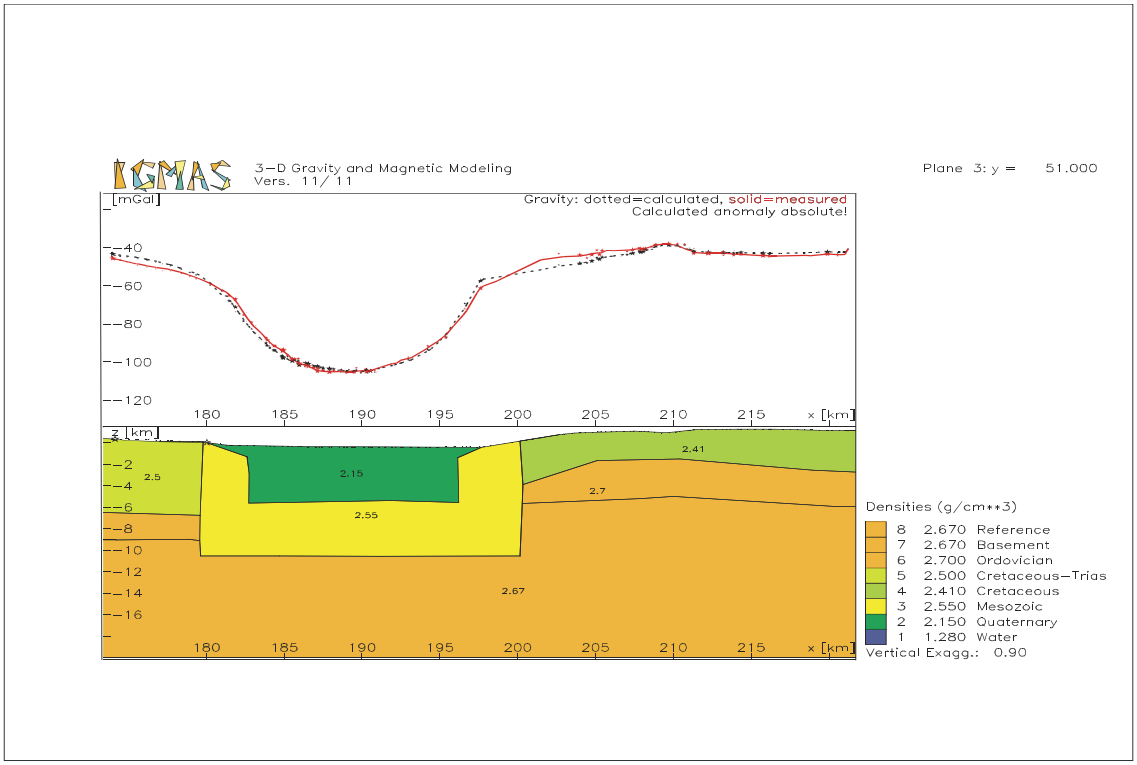

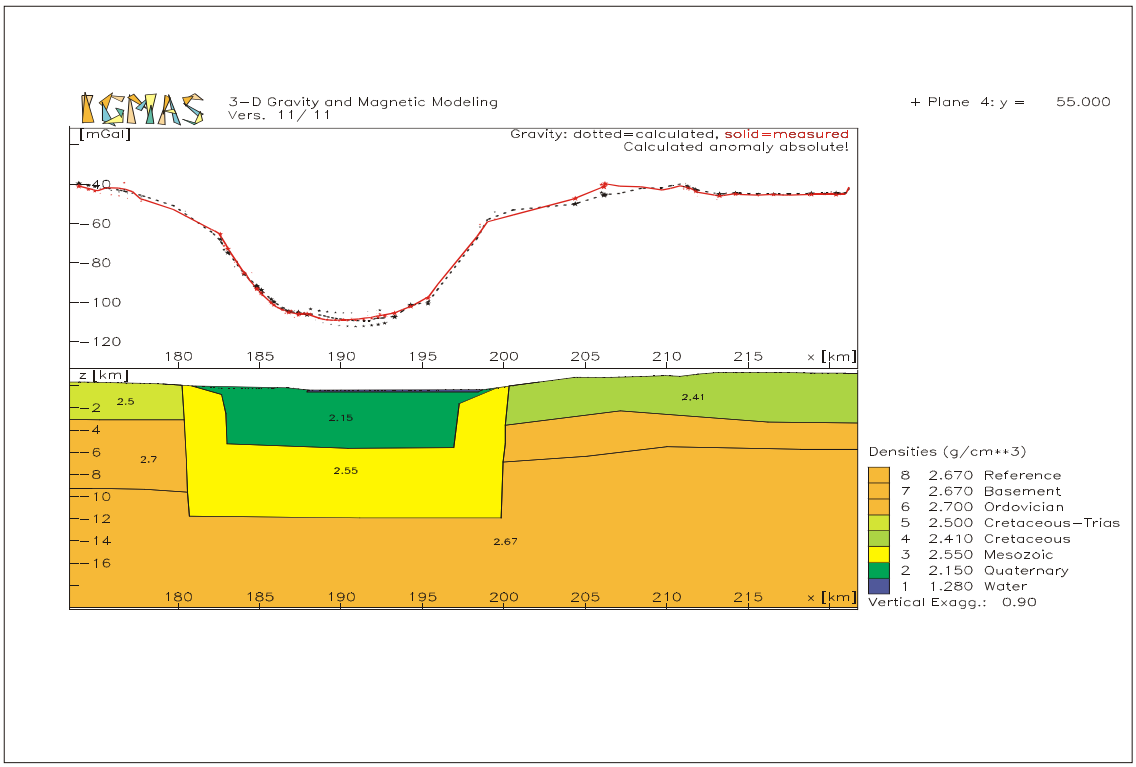

- Computed crustal models beneath plane 3 and 4 in the southern part of the Dead Sea basin.

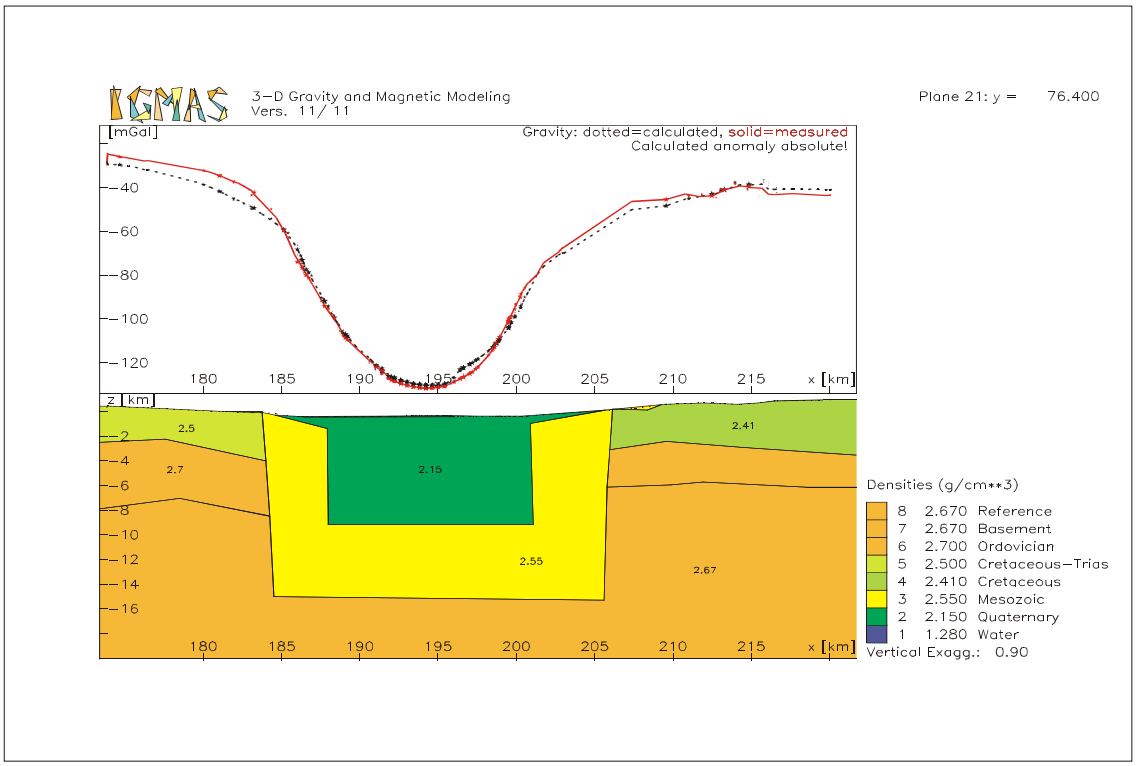

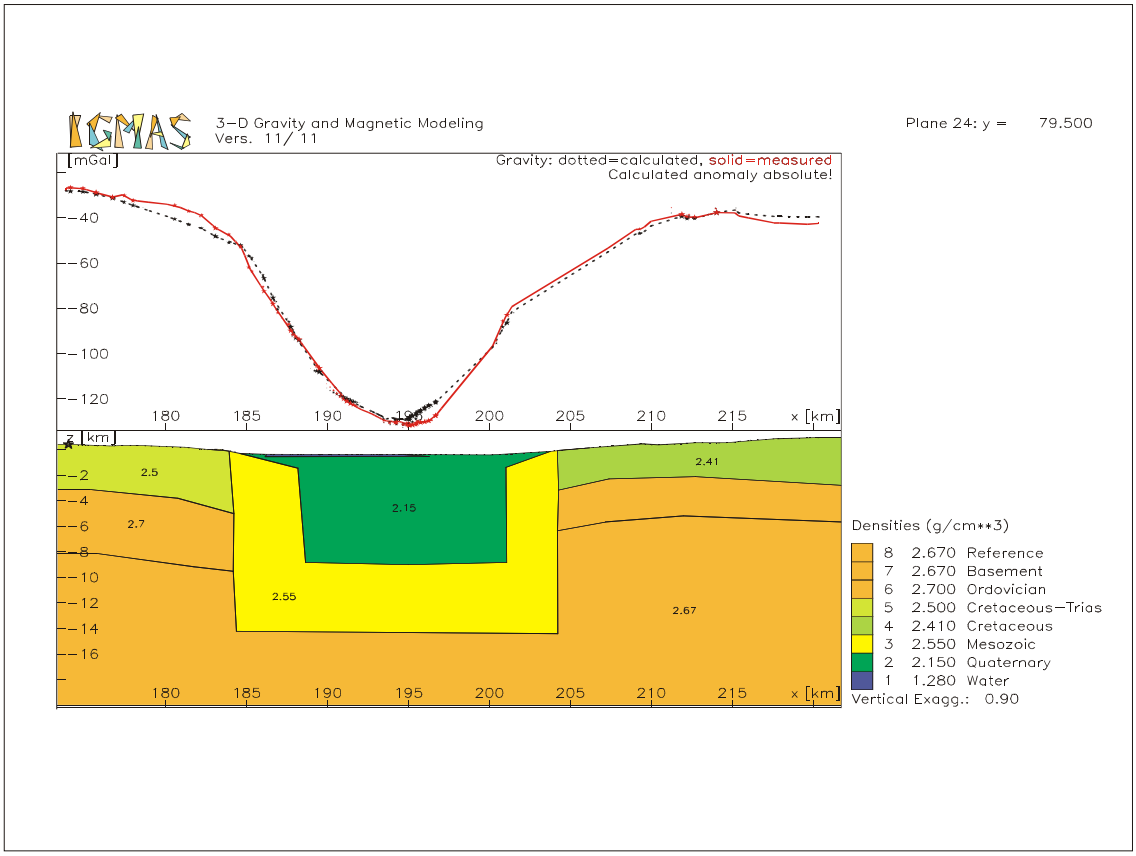

- Computed crustal models beneath plane 21 and 24 in the central part of the Dead Sea basin.

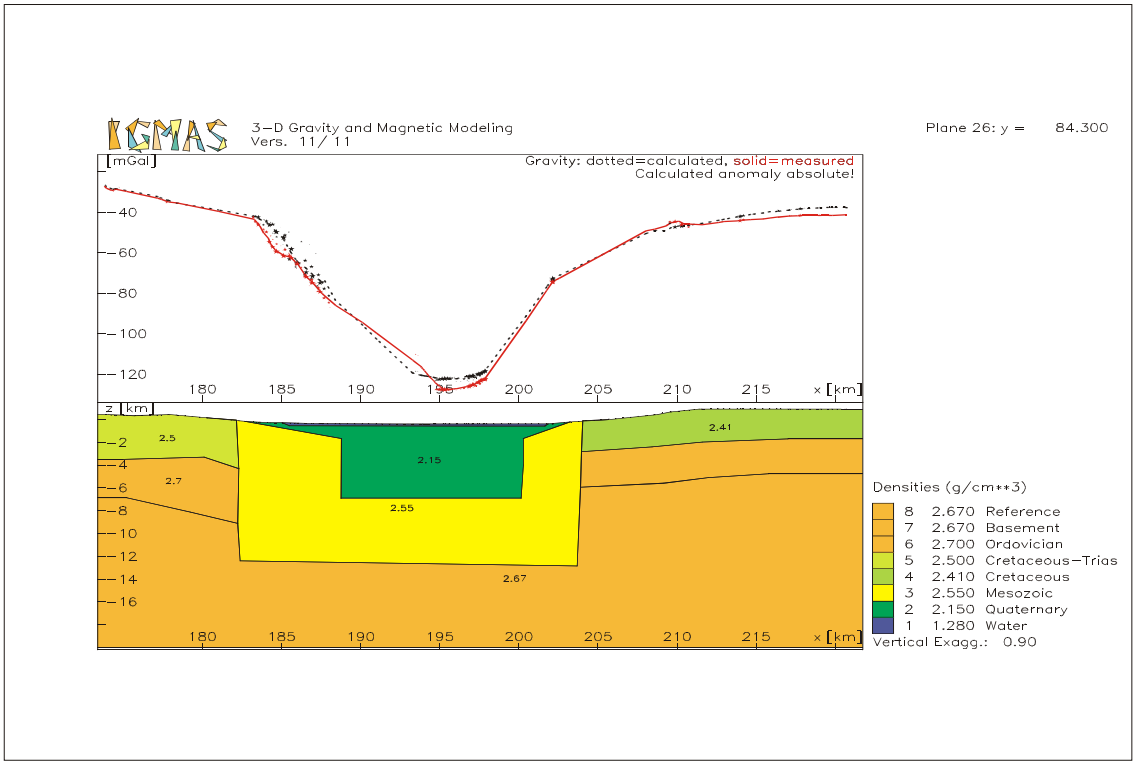

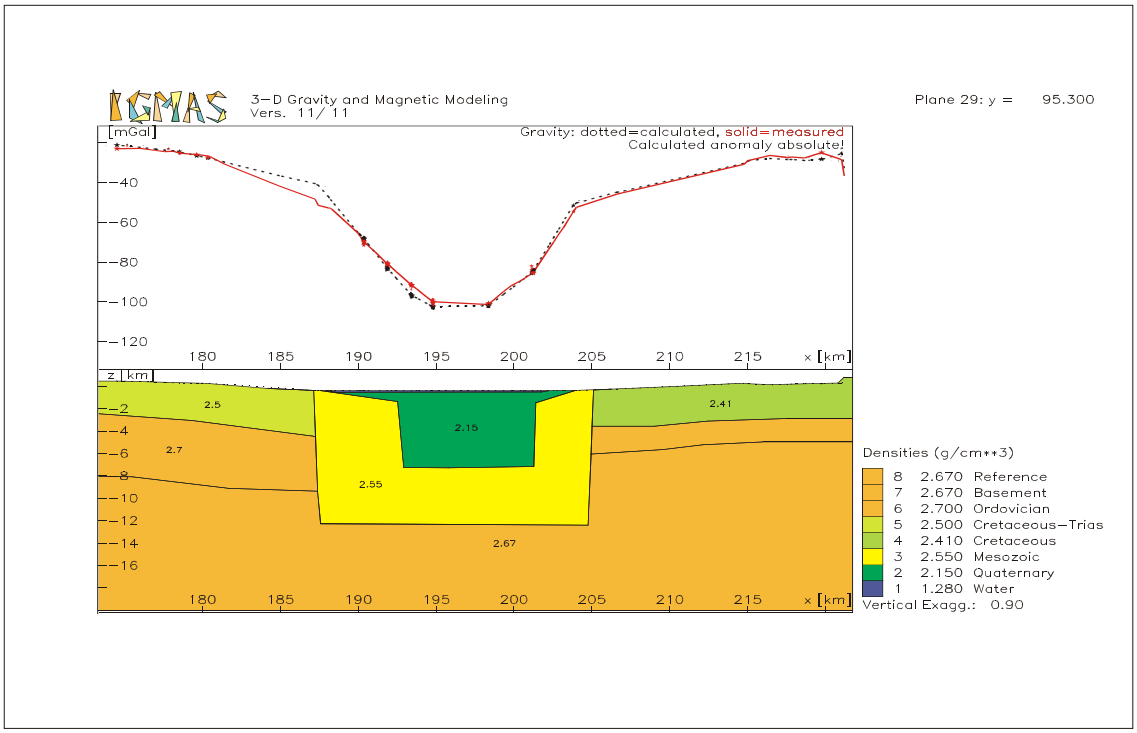

- Computed crustal models beneath plane 28 and 29 in the northern part of the Dead Sea basin.